IMAGING OF DEMYELINATION, REPAIR AND REMYELINATION IN MULTIPLE SCLEROSIS

Shahrukh Mallik

Thesis submitted to University College London (UCL)
for the degree of

Doctor of Philosophy (PhD)

April 2019

DECLARATION

I, Shahrukh Mallik, confirm that the work presented in this thesis is my own. Where information has been derived from other sources, I confirm that this has been indicated in the thesis.

Signed ……

ABSTRACT

Multiple Sclerosis (MS) is characterised pathologically by both inflammatory demyelination and neurodegenerative neuroaxonal loss, occurring in varying degrees in the white matter (WM) and in the grey matter (GM). Studies of MS commonly use imaging surrogates of inflammation (e.g. MRI lesions) and neurodegeneration (e.g. atrophy) as outcome measures to assess potential neuroprotective effects. As trials of potentially remyelinating agents become more important in the spectrum of MS research, imaging outcomes sensitive to myelin, such are magnetisation transfer ratio (MTR), are required to adequately assess any such agents.

With the above in mind, for this thesis, I performed 4 studies:

1. MTR and atrophy localisation in the GM using voxel-based morphometry - MRI measures of GM MTR and volume were used to assess the regional localisation of reduced MTR (in part reflecting demyelination) and atrophy (in part reflecting neuro-axonal loss) in 98 patients with MS, as well as 29 controls. Subgroups of MS patients were compared with controls, adjusting for age and gender. Overall, whilst some regionally consistent reductions in MTR and atrophy were seen in GM, this study found that these mostly do not co-localise. The differing location and extent of regional MTR and volumetric abnormalities in MS subgroups argues against a single mechanism for demyelination and neuronal loss in the GM of MS patients.

2. MRI substudy of Dronabinol (Δ^9-THC) vs placebo – 273 patients with secondary progressive MS (SPMS) received either Dronabinol or placebo (in a ratio of 2:1), with the aim of assessing the potential neuroprotective effects of Dronobinol. T2-weighed (T2w) and T1-weighted (T1w) lesions, and percentage brain volume change (PBVC) were assessed over 3 years. Over the course of the entire study, the occurrence of new or enlarging T2w or T1w lesions, or PBVC was not affected by Dronabinol.

3. Individual lesion area MTR analysis of autologous mesenchymal stem cells (AMSC) in patients with SPMS – A proof-of-concept individual lesion area MTR analysis pathway was developed and used *post-hoc* on 10 patients with SPMS and optic nerve disease from the MSCIMS study, which investigated the potential reparative effects of AMSC. For T2w lesion areas, a significant difference in rate of change of MTR was noted after infusion; this was not seen with T1w lesion areas.

4. Individual lesion MTR analysis in a crossover study of AMSC in patients with active MS – the proof-of-concept work above was refined for use in STREAMS, a crossover study of AMSC. 12 patients with active MS received either AMSC or placebo for 24 weeks, and then crossover to the other arm for a further 24 weeks. MTR was measured at week 0, 12, 24, 26, and 48 in both old and newly appearing lesions. There was not noted to be any significant effect of AMSC on the MTR of either old or newly appearing lesions.

IMPACT STATEMENT

The work in this thesis makes important contributions in the field of understanding basic MS pathology, specifically a novel look at the interrelation between inflammatory demyelinating and neurodegenerative pathology in the grey matter, and how they differ in various MS disease subtypes.

Understanding these differences might help in informing the design of future studies, specifically in choosing the appropriate patient cohorts and outcome measures to investigate interventions with various putative effects.

In addition, this thesis describes a novel analysis method of measuring MTR over time, which is a practical and feasible outcome measure to detect remyelination. As studies of potentially remyelinating and reparative agents in MS become more common, this analysis method might be an important measure to utilise.

PUBLICATIONS AND CONFERENCE ABSTRACTS RELATED TO THIS THESIS

Publications

- Zajicek, J. et al. (2013) 'Effect of dronabinol on progression in progressive multiple sclerosis (CUPID): a randomised, placebo-controlled trial.', Lancet neurology. Elsevier Ltd, 4422(13) 857-865–9. doi: 10.1016/S1474-4422(13)70159-5.
- Mallik, S., Samson, R. S., *et al.* (2014) 'Imaging outcomes for trials of remyelination in multiple sclerosis.', *Journal of neurology, neurosurgery, and psychiatry*, 85(12), pp. 1396–1404. doi: 10.1136/jnnp-2014-307650.
- Mallik, S., Muhlert, N., *et al.* (2015) 'Regional patterns of grey matter atrophy and magnetisation transfer ratio abnormalities in multiple sclerosis clinical subgroups: A voxel-based analysis study.', *Multiple sclerosis (Houndmills, Basingstoke, England)*, 21(4), pp. 423-432. doi: 10.1177/1352458514546513.]

Conference Abstracts

- Mallik S, Muhlert N, Samson RS, Sethi V, Wheeler-Kingshott CAM, Miller DH, Chard DT. **Localisation of Grey Matter Atrophy and Magnetisation Transfer Ratio Abnormalities in Multiple Sclerosis subgroups**. Poster discussion session presented at: 2013 Association of American Neurologists Meeting; 2013 Mar 21; San Diego, CA, USA.

- Mallik S, Muhlert N, Samson RS, Sethi V, Wheeler-Kingshott CAM, Miller DH, Chard DT. **Regional patterns of grey matter atrophy and magnetisation transfer ratio abnormalities in multiple sclerosis clinical subgroups**. Poster session presented at: 2013 Association of British Neurologists Annual Meeting; 2013 May 23; Glasgow, UK.
- Mallik S, Ball S, Dalton C, Macmanus D, Tozer D, Miller DH, Zajicek K. **Cannabinoid Use in Progressive Inflammatory brain Disease (CUPID) MRI sub-study**. Poster session presented at: 2013 Association of British Neurologists Annual Meeting; 2013 May 23; Glasgow, UK.
- Mallik S, Tozer DJ, Altmann DR, Miller DH, Connick P, Kolappan M, Chandran S. **Serial individual lesion MTR follow-up for studies of potentially remyelinating therapies in MS**. Poster session presented at: 2014 Joint ACTRIMS-ECTRIMS Meeting; 2014 Sep 10-13; Boston, MA, USA.
- Ali R, Nicholas R, Marley S, Mallik S, Palanicawandar R, Zamarreno B, Dazzi F, Miller DH, Muraro P. **Preliminary results of a phase 2 trial of autologous mesenchymal cell therapy in MS (STREAMS).** Poster session presented at 2015 ECTRIMS Meeting; 2013 October 7-10; Barcelona, Spain.

ACKNOWLEDGEMENTS

The work contained in this thesis was performed at the department of Neuroinflammation and the Queen Square Multiple Sclerosis Centre, at the Institute of Neurology, Queen Square, London. I am indebted to the MS Society of Great Britain and Northern Ireland and the UK Stem Cell Foundation for funding and supporting my work. I would like to thank Professor David H Miller (DHM) for his guidance and support during his role as my supervisor, as well as Professor Claudia Wheeler-Kingshott (CW-K), and Dr Declan Chard (DC) for their considerable support, and in their supervising roles. I would also like to thank my family, who supported me during my work, as well as the participants of the various studies.

INDIVIDUAL CHAPTER ACKNOWLEDGEMENTS

Chapter 2: MTR VBA Study

The patient scan data was collected by multiple previous clinical fellows. Dr Nils Muhlert (NM) helped to support me with the work, including troubleshooting with the SPM software.

Chapter 3: CUPID MTR substudy

This substudy, from the larger CUPID trial, was made possible through the work of Prof John Zajicek's team at Peninsula medical school, who designed the study, as well as the various study centres who were responsible for collecting the MRI data (Appendix 12). Mr David MacManus (DM) and his team received the scan data from each site, and performed the initial image processing, prior to further analysis. Dr Catherine Dalton (CD) and Dr Daniel Tozer (DT) helped with the Quality Assurance (QA) of the Brain Extraction Tool (BET) and lesion marking processes. David H Miller

(DHM), DM, CD, and DT were all involved with the decision-making process on data exclusion criteria.

Chapter 4: MSCIMS Individual Lesion Area Substudy

The participant scans were acquired by Dr Madhan Kolappan, for the original MCSCIMS study. DT helped develop the scan registration pathway, as well as the individual lesion area analysis pathway. He was also integral, along with DHM, in the QA process for registration and lesion marking. Dr Daniel Altmann (DA) helped with the statistical analysis

Chapter 5: STREAMS Individual Lesion MTR study

This study, a part of the larger MESEMS worldwide collaboration (under the overall auspices of Professor Antonio Uccelli of Genoa, Italy) was a collaboration with Imperial College and UCL Institute of Neurology. I am grateful to Dr Rehiana Ali (RA) and Professor Paulo Muraro (PM), both from Imperial, as they were responsible for the recruitment of participants into the study, as well as bone marrow aspiration, stem cell culture preparation, and subsequent infusion into participants. Randomisation into the parallel group arms was also performed at the Imperial site. Dr Marios Yiannakas (MY) helped develop the MRI protocols. Dr Ferran Prados Carrasco (FPC) helped to develop a new, improved, registration pathway, as well as a lesion splitting method which preserved lesions as a whole over contiguous slices. DHM was involved in the QA of registration and lesion marking. DA helped with the statistical analysis of the data.

CONTENTS

LIST OF FIGURES AND TABLES

Figures

Tables

ABBREVIATIONS

3T	3-Tesla
AAL	Automated Anatomical Labelling
AD	Alzheimer's Disease
AHSCT	Autologous Haematopoietic Stem Cell Transplant
AMSC	Autologous Mesenchymal Stem Cells
BBB	Blood-Brain Barrier
BET	Brain Extraction Tool
BH	Black Holes
CBD	Cannabidiol
CI	Confidence Interval
CIS	Clinically Isolated Syndrome
CNS	Central Nervous System
CSF	Cerebrospinal Fluid
DIS	Dissemination in Space
DIT	Dissemination in Time
DMD	Disease Modifying Drug
DT	Diffusion Tensor
DTI	Diffusion Tensor Imaging
DW	Diffusion Weighted
DWI	Diffusion Weighted Imaging
EAE	Experimental Autoimmune Encephalitis
EDSS	Expanded Disability Status Score
FA	Fractional Anisotropy

FFE	Fast Field Echo
FSE	Fast Spin Echo
FWE	Family Wise Error
FWHM	Full Width Half Maximum
GCIP	Ganglion Cell and Inner Plexiform
Gd	Gadolinium
GEL	Gadolinium-enhancing lesion
GE	Gradient Echo
GM	Grey Matter
GMf	Grey Matter fraction
HARDI	High-Angular-Resolution Diffusion Imaging
HLA	Human Leukocyte Antigen
HSC	Haematopoietic Stem Cells
ICV	Intracranial Volumes
LPC	Lysolecithin
mcDESPOT	multi-component Driven Equilibrium Single Pulse Observation of T1&T2
MCR	Multi-component relaxometry
MD	Mean Diffusivity
ml	millilitres
MNI	Montral Neurological Institute
MR	Magnetic Resonance
MRI	Magnetic Resonance Imaging
MS	Multiple Sclerosis
MSC	Mesenchymal Stem Cells

MSE	Multi Spin Echo
MSIS-29	Multiple Sclerosis Impact Scale-29
MT	Magnetisaton Transfer
MTR	Magnetisaton Transfer Ratio
MWF	Myelin Water Fraction
NAWM	Normal Appearing White Matter
NBV	Normalised Brain Volume
NODDI	Neurite Orientation Dispersion and Density Imaging
OCB	Oligoclonal bands
OCT	Optical Coherence Tomography
ODI	Orientation Dispersion Index
ON	Optic Neuritis
OPC	Oligodendrocyte Precursor Cell
OR	Odds Ratio
PBH	Persistent Black Holes
PBVC	Percentage Brain Volume Change
pcu	percent units
PDTW2	Proton Density T2-Weighted
PET	Positron Emission Tomography
PIB	Pittsburgh Compound B
PPMS	Primary Progressive Multiple Sclerosis
QA	Quality Assurance
qMT	Quantitative Magnetisation Transfer
RNFL	Retinal Nerve Fiber Layer

ROI	Region of Interest
RRMS	Relapsing Remitting Multiple Sclerosis
RXR-γ	Retinoid X receptor-γ
SD	Standard Deviation
SE	Spin Echo
SIENA	Structural Image Evaluation using Normalisation of Atrophy
SIENAX	SIENA Cross-sectional
SPGR	Spoiled Gradient Echo
SPMS	Secondary Progressive Multiple Sclerosis
STIR	Short-tau Inversion Recovery
T1w	T1-weighted
T2w	T2-weighted
TE	Echo Time
THC	Tetrahydrocannabinol
TR	Repetition Time
TSE	Turbo Spin Echo
UK	United Kingdom
unc	uncorrected
VBA	Voxel-Based Analysis
VBM	Voxel-Based Morphometry
VEP	Visual Evoked Potential
WM	White Matter

INTRODUCTION

Multiple Sclerosis (MS) has long been considered a predominantly inflammatory condition of the central nervous system (CNS), with a particular predilection for white matter (WM), driven by an underlying autoimmune mechanism (Thompson, Baranzini, *et al.*, 2018). It is however becoming increasingly apparent that grey matter (GM) involvement is common and important (Hulst and Geurts, 2011), and that, in addition to an autoimmune-derived inflammatory process, there is also a significant neurodegenerative component, manifesting histopathologically as neuroaxonal loss (Chard and Miller, 2009). The exact relationships between these pathological processes (demyelination and neuroaxonal loss), in both the GM and WM, is not well understood, however.

A key area of focus in MS therapeutic research in the last few decades has been to understand and potentially slow the neurodegenerative component of the disease, which is the pathology thought to underly progression and long-term disability (Bjartmar and Trapp, 2003; Stys, 2004). However, there has also been long-standing interest in the possibility of promoting remyelination in areas of the brain affected by demyelination, as a more potentially more reparative process. Ultimately, a fundamental component to the potential utility of such research studies is the ability to measure and quantify neuroaxonal loss and demyelination *in vivo*.

Within this thesis, I aim to:

1. Explore the pathological relationships between neuroaxonal loss and demyelination in the GM of different MS subtypes.
2. Utilise currently established imaging measures of neuroprotection within the context of a placebo-controlled clinical trial.
3. Explore the concept and practicality of imaging myelin *in vivo*
4. Develop a novel method of measuring the myelination of individual MS lesions, and apply these methods, as proof-of-concepts, to trials utilising a putative remyelinating therapy – autologous mesenchymal stem cells (AMSC) – in patients with MS.

However, prior to looking at these areas in detail, I will describe a few key aspects of MS as a disease entity, including some basic epidemiology, pathology, predominant clinical manifestations, radiological measures, and the main available treatment options. As these areas are not the main focus of the thesis, they will be briefly summarised in the sections below.

1.1 EPIDEMIOLOGY

In the United Kingdom (UK), there are estimated to be approximately 100,000 to 125,000 people with MS, with an overall incidence of between 3 and 9 per 100,000 per year, and an overall prevalence of between 150 to 200 per 100,000 population (Mackenzie *et al.*, 2014). There is significant variation with geographical location, and rates demonstrably increase with increasing latitude (Simpson *et al.*, 2011).

Scotland has the highest incidence and prevalence of MS in the British Isles, with the Orkney Islands demonstrating the highest rates in the world (Visser *et al.*, 2012).

MS is significantly more common in females than in males. In the UK, incidence rates for women are more than double that for men (11 per 100,000 per year vs 5 per 100,000 per year, respectively), a pattern also seen in prevalence rates (285 per 100,000 vs 113 per 100,000, respectively). Overall, females accounted for more than 70% of both incident and prevalent cases (Mackenzie *et al.*, 2014).

1.2 AETIOLOGY

The underlying pathogenesis of MS is poorly understood, and although there are a number of plausible theories under consideration, it is likely that the underlying pathology is dependent on the co-existence of one or more overlapping factors, including diet, smoking status, vitamin D deficiency, genetics, to name a few (Thompson, Baranzini, *et al.*, 2018).

Vitamin D deficiency

The co-association of increasing latitude with increasing levels of MS (Simpson *et al.*, 2011), as well as increasing levels of vitamin D deficiency (Hyppönen and Power, 2007), have led to speculation on the role of vitamin D in the pathogenesis of MS. A few studies have shown that patients with lower levels of serum 25-hydroxyvitamin

D had a higher risk of developing MS (Munger *et al.*, 2004, 2006), and that month of birth, as a possible reflection of maternal sun exposure during pregnancy, also affected risk of MS development (Dobson, Giovannoni and Ramagopalan, 2013). There is also evidence suggesting that higher levels of serum 25-hydroxyvitamin D can lead to lower rates of relapse (Simpson *et al.*, 2010). It is not clear whether vitamin D deficiency has a direct effect on the pathogenesis of MS, or whether the two are related to an as yet unknown third factor.

Genetics

Several studies implicate genetic susceptibility in the pathogenesis of MS. Concordance rates are higher in monozygotic than dizygotic twins, while non-twin siblings and other first degree relatives show comparatively lower risks, but still have higher rates than in the general population (Willer *et al.*, 2003). A number of human leukocyte antigen (HLA) and non-HLA genetic risk factors have been linked with MS (Gourraud *et al.*, 2012).

Other factors

A number of other factors have been implicated as being possibly causative links with MS, many of which are environmental (Thompson, Baranzini, *et al.*, 2018). It is likely that the pathogenesis of MS depends on certain environmental factors in individuals who demonstrate genetic susceptibility.

1.3 BASIC PATHOLOGY

The pathology of MS affects the CNS, which includes predominantly the brain and spinal cord, but also the optic nerves. Each of these can broadly be divided into 2 main tissue compartments, namely the Grey Matter (GM), and the White Matter (WM). GM can be cortical or deep.

The pathological processes of MS in the CNS can include both inflammatory demyelination, and neurodegenerative neuroaxonal loss, each seen in varying amounts. Both processes can be seen in the WM and GM.

Demyelination

The fundamental pathological process is the inflammatory demyelinating lesion. Demyelination, which is the loss of myelin sheath surrounding the axons, is a major contributor to impaired neurological function and disability through impaired saltatory conduction and conduction block (Redford, Kapoor and Smith, 1997). In the WM, it is likely that demyelination occurs secondary to an inflammatory T-cell mediated insult to myelin and/or oligodendrocytes, although B-cell mediated effects, as well as oligodendrocyte apoptosis have also been implicated (Barnett and Prineas, 2004). New demyelinating lesions are associated with varying degrees of inflammation, oedema, gliosis, and breakdown of the blood-brain barrier (BBB) (Lucchinetti *et al.*, 2000). Demyelination in the GM may also occur secondary to a similar immune pathology, although inflammatory changes and BBB breakdown tend to occur less often than in the WM (Bø *et al.*, 2003). There is also evidence

that meningeal inflammation is prominent, and may play an important role in cortical demyelination, especially in progressive disease and in the subpial region (Howell *et al.*, 2011).

Neurodegeneration and Neuroaxonal loss

In addition to demyelination, neuronal and axonal loss occurs to varying extents within WM lesions (Trapp *et al.*, 1998), normal appearing white matter (NAWM) (Bjartmar, Wujek and Trapp, 2003), and GM (Geurts *et al.*, 2012; Klaver *et al.*, 2013). Neuroaxonal loss and neurodegeneration is thought to be the major pathological substrate for of irreversible neurological disability (Bjartmar and Trapp, 2003; Stys, 2004).

Grey Matter Pathology

Cortical grey matter pathology includes demyelinating lesions (Calabrese *et al.*, 2007), and cortical atrophy (Calabrese *et al.*, 2009), and these correlate with cognitive impairment and clinical disability (Fisniku *et al.*, 2008; Calabrese *et al.*, 2009; Rudick *et al.*, 2009). Lesions and atrophy are also seen in the deep GM in MS, although the nature of these is less well studied than cortical pathology in MS (Vercellino *et al.*, 2005, 2009; Gilmore *et al.*, 2009). This will be discussed in more detail in Chapter 3.

1.4 CLINICAL FEATURES

At diagnosis, the majority (approximately 80-85%) of patients will have a relapsing-remitting form of the disease (RRMS), whereby they will experience multiple episodes of neurological dysfunction (relapses) followed by periods of remission, in which there is variable improvement towards normal function (Compston, 2005). Relapses are episodes of neurological disturbance affecting one or more sites that last from between 24 hours to 1 month, which reflect areas of new inflammatory demyelination in the brain or spinal cord. Conventionally, the diagnosis MS is not usually considered unless there have been at least 2 episodes consistent with a clinical relapse; a single episode is referred to as a clinically isolated syndrome (CIS). However, the McDonald criteria for the diagnosis of MS (see below) does allow for a diagnosis of MS after a CIS, and practice is changing to reflect this. Between 30-70% of patients experiencing a CIS will go on to formally develop MS, the exact risk depending on a number of prognostic indicators (Miller *et al.*, 2005).

The typical symptoms patients may experience as part of a relapse include weakness, sensory disturbance (such as numbness and paraesthesia), reduced coordination, vertigo, double vision, or monocular visual impairment (Compston, 2005). Optic neuritis (ON) is the first episode in approximately 20% of cases, and will occur at some point during the course of the illness in 50% (Balcer, 2006). Some patients may experience worsening of symptoms with heat (Uhthoff phenomenon), or electric-shock like sensations on forward flexion at the neck (Lhermitte's phenomenon). Other symptoms that may include stiffness, neuropathic pain,

sphincter disturbance, cognitive dysfunction, and fatigue (Compston and Coles, 2008).

The natural history of RRMS is for eventual progression to the secondary progressive phase (SPMS). The likelihood of progression increases with duration of disease, such that between 10-15 years after onset, approximately 60% will have progressed; after 20 years, the rate is 80% (Clarke *et al.*, 2016). In a few patients (approximately 15-20%) MS starts in the primary progressive form (PPMS). The progressive groups demonstrate insidious accrual of disability and gradual decline in function without prominent relapses or periods of remission.

The diagnosis of MS is suggested on clinical grounds, supported by imaging, and is made according to the McDonald Criteria, most recently updated in 2017 (Thompson, Banwell, *et al.*, 2018).

1.5 CLINICAL IMAGING

Magnetic Resonance (MR) imaging allows *in vivo* assessment of MS pathology, and has become a core component of MS clinical and research work. MR imaging can be made sensitive to different tissues, based upon the behaviour of protons when exposed to a magnetic field. Magnetising protons disrupts their normal, randomised alignment, and they return to their normal alignment through various relaxation processes. T1-weighted (T1w), and T2-weighted (T2w) sequences are characterised by the relaxation times of protons in various tissues.

Standard Clinical Imaging Measures

T2w sequences are sensitive in detecting the WM lesions of MS, but lack the specificity to differentiate between the pathological substrates of MS, such as inflammation, oedema, axonal damage, demyelination, remyelination and gliosis (Filippi M De Stefano N, et al, 2011), and are very insensitive to GM lesions (Geurts *et al.*, 2005).

On T1w imaging, WM lesions appear hypointense, and these are often referred to as Black Holes (BH). A proportion of these lesions will remain persistently hypointense on T1w scans after the period of active inflammation (between 25-40%) (Riva *et al.*, 2009), and are called Persistent Black Holes (PBH), indicative of varying amounts of axonal loss and demyelination (van Walderveen *et al.*, 1998).

In the acute phase of lesion formation, there is breakdown of the BBB, which shows gradual and variable recovery over the following 6-8 weeks. The administration of gadolinium chelate (Gd) contrast agent (which normally does not cross the BBB) is thus useful in demonstrating acute or active lesions; a Gd enhancing lesion (GEL) generally suggests the lesion is less than 2 months old (Ciccarelli and Miller, 2002).

The characteristic radiological features of MS are lesions disseminated in time (DIT) and space (DIS). DIT may be demonstrated by either performing MR imaging at two different time points and demonstrating new T_2w lesions, or demonstrating the presence of GEL and non-GEL in the same scan. DIS is determined by the presence

of 1 or more asymptomatic lesion on T_2w imaging in 2 out of the 4 following characterisic areas: juxtacortical, periventricular, infratentorial, spinal cord. The diagnosis of PPMS requires the demonstration of at least 1 year of clinical progression, as well as 2 of the following 3 features: 1 or more T_2w lesions in at least 1 characteristic brain area (juxtacortical, periventricular, infratentorial), 2 or more T_2w lesions in the spinal cord, or the presence of unmatched oligoclonal bands (OCB) in the CSF (Thompson, Banwell, *et al.*, 2018).

Neuro-axonal loss can be detected as atrophy on MR imaging, and MS patients demonstrate accelerated brain atrophy compared to the general population. In MS, the average reported rate is between 0.5% - 1% per year, compared to between 0.1%-0.3% per year in non-MS patients (Barkhof *et al.*, 2009).

1.6 IMAGING ATROPHY AND NEUROAXONAL LOSS

Imaging Brain Atrophy

The primary radiological marker of neurodegeneration and pathological neuroaxonal loss in the brain is atrophy, which is detectable in the earliest stages of all forms of MS, but is especially associated with progressive MS, and correlates with disability (Popescu *et al.*, 2013). This has been a key focus of a number of explorative studies and clinical trials in the last few decades.

Measures of atrophy can take into account both the whole brain, or certain compartments (such as WM or GM), or focus on lesional measures. Whole-brain

atrophy can be measured using longitudinal and cross-sectional techniques. Structural Image Evaluation using Normalisation of Atrophy (SIENA) (Smith *et al.*, 2001) compares longitudinally acquired images and measures changes in whole brain volume over time, with low error rates (0.15%) (S.M. Smith, Y. Zhang, M. Jenkinson, J. Chen, P.M. Matthews, A. Federico, 2002). SIENAX is the cross-sectional counterpart to SIENA, and provides tissue specific volume estimates, but using serial cross-sectional measurements to assess change overtime is less precise (upto 1% error) (S.M. Smith, Y. Zhang, M. Jenkinson, J. Chen, P.M. Matthews, A. Federico, 2002). To account for this, normalised brain volume (NBV) is often calculated using SIENAX, and then SIENA is used to estimate percentage brain volume change (PBVC) over time. SIENAX and SIENA are commonly used as primary imaging outcomes in trials of potentially neuroprotective agents (Lublin *et al.*, 2016; Montalban *et al.*, 2017). Lesional measures are more variable, and thus less reliable, and are mainly based on noted statistical correlations between T1w lesion appearance and local neuro-axonal loss (Walderveen *et al.*, 1998; Chard *et al.*, 2002).

<u>Imaging Neuroaxonal loss for studies of potentially neuroprotective agents</u>

As well as whole-brain atrophy measures, regional atrophy (such as cortical volume, and GM fraction), normal appearing WM (NAWM) and GM (NAGM) measures, and lesional (T2w and T1w) metrics can also be assessed in studies of potentially neuroprotective agents. In addition, spinal cord lesions and atrophy, and anterior visual pathway assessments (clinical, paraclincal, and imaging meaures) have all been utilised to assess neurodegenerative change. These methods are well established (Barkhof *et al.*, 2009; Moccia, de Stefano and Barkhof, 2017), and are

not the main focus of this thesis, so they will not be described in any further detail here. In chapter 3, I will utilise a combination of lesional and whole brain atrophy measurements to assess the potential neuroprotective effect of cannabinoids in MS.

1.7 IMAGING MYELIN AND REMYELINATION

Remyelination refers to the process of restoring the myelin sheath around demyelinated axons. It can result in recovered function through improved conduction, as well as providing a degree of axonal protection (Irvine and Blakemore, 2008). It is thought that endogenous remyelination in the CNS occurs through the action of oligodendrocyte precursor cells (OPCs) generating new oligodendrocytes, which encourage the production of myelin in demyelinated areas (Franklin and Ffrench-Constant, 2008). In MS, remyelination can occur in variable amounts; when it occurs, and by how much, is poorly understood. Unlike toxin-induced demyelination, where post-insult remyelination often occurs in a complete fashion (Woodruff and Franklin, 1999), in MS the continued presence of auto-reactive T cells may create a hostile environment for optimal oligodendrocyte function, and may thus inhibit complete remyelination. Despite this, however, some patients may demonstrate complete or near complete remyelination in a number of lesions (Patrikios *et al.*, 2006), especially in early MS (Prineas *et al.*, 1993). It is likely that constitutional factors such as sex, age, stage of disease, and genetic make-up influence the efficiency of remyelination (Bieber, Ure and Rodriguez, 2005; Li *et al.*, 2006; Goldschmidt *et al.*, 2009). Some potentially

remyelinating pharmacological therapies of recent or current interest are mentioned in table 1.1.

Table1.1: Remyelinating agents recently or currently under investigation	
Retinoid X receptor-γ (RXR-γ) agonists	RXR-γ is significantly up-regulated in oligodendrocyte-derived cells in remyelinating lesions in experimental lysolecithin (LPC) models, and in the CNS in humans. Administration of an RXR-γ agonist (9-*cis*-retinoic acid) upregulated endogenous OPC differentiation, and increased myelination in demyelinated cerebellar slice cultures, suggesting that RXR-γ is a feasible target for CNS remyelinating therapy (Huang *et al.*, 2011).
Anti-LINGO-1 monoclonal antibody (Opicinumab)	LINGO-1 is a transmembrane signal-transducing molecule that is expressed on oligodendrocytes and neurones in the CNS (Rudick, Mi and Sandrock, 2008), which inhibits oligodendrocyte differentiation, and may be a potentially important cause of remyelination failure in MS (Mi *et al.*, 2005). Anti-LINGO-1 monoclonal antibody enhanced oligodendrocyte differentiation and myelination, and promoted functional recovery in EAE models, which correlated with radiological and electron microscopy metrics showing increased remyelination and axonal integrity in the spinal cord (Mi *et al.*, 2007). The Phase IIb SYNERGY study of Opicinumab was not noted to improve disability in SPMS (Mellion *et al.*, 2017).
Olexosime	Olexosime, which has a number of potentially neuroprotective and neuroregenerative properties (Bordet *et al.*, 2007), accelerated maturation of oligodendrocytes and promoted remyelination in vitro and in vivo in LPC and cuprizone mouse models of demyelination (Magalon *et al.*, 2012).
Mesenchymal Stem Cells	Autologous mesenchymal stem cells are multipotent bone marrow derived stromal cells that may have potential to promote myelin repair, in addition to other potentially complementary effects, in MS (Uccelli, Laroni and Freedman, 2011). A Phase 2 trial of autologous mesenchymal stem cells in secondary progressive MS patients with visual pathway disease (MSCIMS) demonstrated significant improvement in visual acuity, Visual Evoked Potential (VEP) latency, and optic nerve area (Connick *et al.*, 2012).
Wnt signalling pathway modifiers	The Wnt signalling pathway, which is an important aetiology in a number of neoplastic conditions, also down-regulates differentiation of OPCs (Fancy *et al.*, 2009). In experimental models, inhibiting the activity of tankyrase (a polymerase enzyme) can reduce activity in the Wnt signalling pathway, enhancing remyelination (Franklin *et al.*, 2012).
Other agents	Progesterone (Schumacher *et al.*, 2012), and Fingolimod (Miron *et al.*, 2010) may also promote remyelination in experimental models.

<u>Investigating Remyelination in MS</u>

In investigating potentially remyelinating pharmacological therapies in patients with MS, there is a need for outcome measures that are sensitive and specific to

myelination, with the added requirement of being quantitative and reproducible. Ultimately, such measures should also reflect and predict a clinically meaningful outcome.

Acute lesions that correspond to acute clinical episodes (relapses) pathologically demonstrate the presence of demyelination, inflammation, and oedema to varying extents (Dousset *et al.*, 1998). Improvement in clinical symptoms reflects varying degrees of resolution of inflammation and oedema as well as remyelination; no clinical markers are specific to myelin content alone.

Although histopathological assessment through biopsy is possible and suited to experimental models or post mortem MS studies, it is an unrealistic outcome measure in patient studies. Certain electrophysiological investigations may infer myelination status for specific functions, such as visual evoked potentials (VEP) for the optic nerve. As a whole, however, imaging markers offer the most direct and practical potential means for detecting remyelination *in vivo*.

Imaging Remyelination in the Brain

Conventional Magnetic Resonance (MR) imaging sequences

As noted in chapter 1, while conventional T2w MR imaging is very sensitive in identifying brain WM lesions of MS, it lacks the specificity to differentiate between

the pathological substrates of MS, such as inflammation, oedema, axonal damage, demyelination, remyelination and gliosis (Filippi M De Stefano N, et al, 2011).

On T1w imaging, active lesions (those showing gadolinium-enhancement) appear hypointense on T1w images, and these are often referred to as Black Holes (BH). Following the evolution of BHs post-resolution of active inflammation may be a useful outcome measure in trials of neuroprotection (van den Elskamp *et al.*, 2008). A longitudinal change in lesion signal intensity from hypointense to isointense on T1w images (the disappearance of BHs) after the period of active inflammation may be indicative of remyelination (Bitsch *et al.*, 2001), but also reduction in oedema. Given that T1w lesions show poor specificity for myelin *per se*, and are predominantly influenced by axonal pathology (van Walderveen *et al.*, 1998), they are likely to be of only indirect value in studies of remyelination.

Magnetisation Transfer Ratio

Magnetisation Transfer (MT) imaging is a semi-quantitative technique based on the premise that protons in biological tissue exist in two 'pools', a free ('liquid') pool, in which protons are highly mobile, and a restricted ('semi-solid') pool consisting of protons attached to macromolecules, which are therefore relatively immobile. Exchange of magnetisation takes place between the two pools, and this can have important effects on the relaxation properties of tissue. The bulk of the observable signal in conventional MR images originates from the free proton pool, since the restricted proton pool has a very short T2 relaxation time (~10-20μs) and therefore

its signal decays very rapidly, rendering this compartment 'invisible'. MT imaging provides access to the restricted protons, which are located in biologically interesting tissue compartments.

The Magnetisation Transfer Ratio (MTR) is a widely used measurement of the amount of MT exchange taking place between the two proton compartments, obtained from two images acquired with and without MT-weighting (through the application of a dedicated radiofrequency pulse) so that a ratio can be estimated from the signal intensities. Most commercial scanners have the ability to acquire MTR sequences, and whole brain acquisition times are short enough to be feasible for most study protocols.

MTR is affected by myelin, but may also be influenced by water content and inflammation (Vavasour *et al.*, 2011), and axonal density (Schmierer *et al.*, 2004). In MS brain white matter lesions (figure 1), the MTR is lower than in the normal appearing white matter (NAWM), although NAWM also shows decreased MTR in MS compared with healthy controls (Filippi *et al.*, 1995). Lesion MTR is lower in the presence of demyelination, with significantly higher MTR observed in remyelinated lesions (Schmierer *et al.*, 2004), although this is still lower than in NAWM, which may be due to incomplete remyelination, morphological differences in the newly formed myelin, and a degree of axonal loss.

Quantitative MT (qMT): The restricted proton fraction, f

Although MTR protocols are readily available on clinical scanners they have the drawback of being 'semi-quantitative', in that the MTR value depends on the MT pulse properties, the type of acquisition sequence (e.g. gradient echo/spin echo), excitation pulse flip angle and echo time (TE), repetition time (TR) and spoiling characteristics. This could potentially lead to issues with changes in scanners over time, or in studies involving multiple scanners. Mathematical models of the MT effect in biological tissues have been proposed in order to measure more fundamental quantitative parameters related to tissue structure, such as the restricted proton fraction, f (Cercignani *et al.*, 2005). These quantitative parameters are more robust and are greatly influenced by the myelin content in the brain or spinal cord (since restricted protons are known to be attached to macromolecules such as myelin), and have been demonstrated to be reliable and reproducible (Levesque, Sled, *et al.*, 2010). The restricted proton fraction, f, has also been shown to correlate mainly with myelin content and to a lesser extent, axonal count in the brain (Schmierer, Tozer, *et al.*, 2007; Schmierer *et al.*, 2008). Results of animal studies have also supported the hypothesis that f is an imaging biomarker of demyelination (Ou *et al.*, 2009).

Performing qMT measurements is challenging, because it requires several images to be sampled (rather than just two) with different MT-weighting in order to fit the model to the data and estimate the fundamental qMT parameters. This can result in long scan times, and the model of the MT effect is not unique as the tissue structure is complex.

Multi-component T_2 relaxometry: the Myelin Water Fraction (MWF)

Complicated biological systems are likely to be characterized by many different compartments. Multi-component relaxometry (MCR) probes these different environments using their different relaxation characteristics. It is possible to distinguish between different components via their T_2 relaxation times (MacKay *et al.*, 1994):

- A short T_2 component with T_2 between 10 and 55ms (approximately 20ms), attributed to water trapped within myelin bilayers (myelin water)
- A medium T_2 component with T_2 between 70 and 95ms (approximately 80ms), thought to be intracellular and extracellular water.
- A long T_2 component with T_2 of more than 100ms, which reflects CSF.

In particular, the ratio of myelin water signal to total water signal, termed the myelin water fraction (MWF) (MacKay *et al.*, 1994), has been shown to correlate with histological measures of myelin content (Laule *et al.*, 2008). It has also been shown to be independent of other pathological processes such as axonal degeneration and inflammation (Gareau *et al.*, 2000). Decreased MWF reflects demyelination, and increase is thought to reflect remyelination (Laule *et al.*, 2007; Vavasour *et al.*, 2009). Levesque *et al* performed single slice qMT and MWF measurements longitudinally over the course of a year in five relapsing-remitting MS patients and five healthy controls (Levesque, Giacomini, *et al.*, 2010). They found that parameters obtained from qMT were able to track the degree and timing of partial recovery in enhancing MS lesions, attributed to quick resolution of

inflammation, followed by slower partial remyelination. However, measurements obtained from multi-component relaxometry were much more variable, which may have been partly caused by the large voxel sizes resulting in errors due to partial volume effects, in addition to the small number of participants studied.

The major limitation to this technique is limited brain coverage with traditional multi-component T_2 relaxometry using 2D multi spin echo (MSE) sequences. These 2D sequences are additionally at risk of magnetisation transfer effects (Vavasour *et al.*, 2000). In order to prevent this, 3D sequences should be acquired, which can increase acquisition time. These limitations would most likely make using standard 2D/3D MSE T_2 relaxometry derived MWF unfeasible for most clinical trials of potential remyelinating agents.

Multi-component driven equilibrium single pulse observation of T1 and T2 (mcDESPOT) is a MCR technique that utilizes rapid gradient acquisition steady-state imaging (i.e., spoiled gradient echo [SPGR] and balanced steady-state free precession [bSSFP]) over a range of flip angles, giving a more clinically feasible sequence (acquisition times ~16-30 minutes), enabling whole brain coverage (Deoni *et al.*, 2008; Kolind and Deoni, 2011; Kolind *et al.*, 2012). This method can be used to measure the myelin water fraction (a measure of the amount of water trapped within myelin layers) in the brain and spinal cord. The myelin water fraction has previously been shown to relate to estimates of myelin content measured from histological staining (Laule *et al.*, 2008), and is also independent of concomitant pathological processes such as axonal degeneration, and is insensitive to

inflammation (Gareau *et al.*, 2000). In a study of 2 patients with PPMS compared to healthy controls, mcDESPOT demonstrated decreased MWF in areas corresponding to WM lesions (Deoni *et al.*, 2008). It should be noted, however, that one recent study performed propagation-of-error analysis of mcDESPOT data, and demonstrated an inability of mcDESPOT signals to precisely estimate parameters of a two-pool model with exchange (Lankford and Does, 2013). Therefore further investigation may be required in order to interpret the quantitative parameters obtained from mcDESPOT.

Other sequences, such as T2prep 3D SPIRAL (Nguyen *et al.*, 2012), and 3D-GRASE (Prasloski *et al.*, 2012), allow whole brain coverage with acquisition speeds that are faster than traditional 2D MSE T_2 relaxometry, and demonstrate similar MWF in brain tissues.

Diffusion Tensor Imaging

Diffusion-weighted (DW) MRI provides quantitative information about the diffusion behaviour of water molecules *in vivo*, which is altered in pathology as a consequence of microstructural changes (Pierpaoli *et al.*, 2001). By modelling the signal behaviour of water in tissue when sensitised to water molecule diffusion using diffusion tensor (DT) imaging, it is possible to derive several parameters that provide sensitive biomarkers for characterising tissue microstructural abnormalities. These include the fractional anisotropy (FA), mean diffusivity (MD), axial diffusivity ($\lambda_{\parallel}$), and radial diffusivity ($\lambda_{\perp}$) (figure 2).

FA has been shown to correlate both with axonal counts (Schmierer, Wheeler-Kingshott, *et al.*, 2007; Gouw *et al.*, 2008), and myelin content (Schmierer, Wheeler-Kingshott, *et al.*, 2007). In healthy tissue and in the presence of a main fibre bundle with a well-defined direction, radial diffusivity ($\lambda_\perp$) reflects movement of water molecules perpendicular to the axon and is thought to reflect myelin content (Song *et al.*, 2005). In contrast, axial diffusivity ($\lambda_\parallel$) reflects movement of water molecules parallel with the axon, and is potentially sensitive to axonal pathology (Song *et al.*, 2002). Loss of myelin has been associated with increased radial diffusivity ($\lambda_\perp$) in experimental models (Song *et al.*, 2002, 2005), but not with axial diffusivity ($\lambda_\parallel$) (Song *et al.*, 2002). The main limitation of these indices is that the DT and its eigenvalues are a mathematical model based on the assumption of Gaussian water diffusion behaviour, which is not true in tissue where restriction and hindrance take place. Therefore, indices like $\lambda_\perp$ and $\lambda_\parallel$ depend on the ability of the DT to detect the correct fibre-tract orientation per voxel. Complex tissue microstructure or tissue disrupted by pathology can affect the ability to detect myelin content via measurement of the radial diffusivity (Laule *et al.*, 2007; Wheeler-Kingshott and Cercignani, 2009). It is essential that when analysing radial diffusivity as a measure of demyelination care is taken to understand how the DT has been fitted to the signal and examine its eigenvectors as well as its eigenvalues (Wheeler-kingshott *et al.*, 2012).

Fox *et al* imaged 21 patients with MS starting natalizumab serially for 12 months (Fox *et al.*, 2011). They followed gadolinium-enhancing lesions and 20 regions of interest from normal-appearing white and grey matter longitudinally and observed

increased FA and decreased radial diffusivity ($\lambda_{\perp}$) of the lesions during the first two months, which they attributed to partial remyelination, supporting the use of DTI as a measure of integrity for studies of potentially reparative therapies.

Neurite Orientation Dispersion and Density Imaging

Neurite Orientation Dispersion and Density Imaging (NODDI) is a promising new diffusion imaging technique that quantifies microstructural indices of neurites *in vivo* using a multi-compartment model. It provides two key parameters, the neurite density (υ_{IC}) (the intra-cellular volume fraction), and the orientation dispersion index (ODI), which characterises the orientation dispersion of the axonal and/or dendritic projections. These parameters have been shown to disentangle the source of diffusion anisotropy, providing more specific measures of brain tissue microstructure than the standard parameters derived from the DT eigenvalues (Zhang *et al.*, 2012).

A three-compartment tissue model is fitted to high-angular-resolution diffusion imaging (HARDI) acquired with two different DW (i.e. one shell with low and one shall with high b-value), optimised for clinical feasibility.

A strong correlation of neurite density with the intensity of myelin stain under light microscopy has previously been demonstrated, indicating that neurite density may be a useful marker for demyelinating disorders such as MS (Jespersen *et al.*, 2010).

Positron Emission Tomography

Positron Emission Tomography (PET) imaging uses various radio-labelled isotopes to target specific tissue substrates and as such has a range of clinic uses in various medical conditions. Thioflavin T derivative [methyl-^{11}C]-2-(4'-methylaminophenyl)-6-hydroxybenzothiazole ([^{11}C]PIB, a carbon-labelled version of Pittsburgh Compound B) has been shown to be a useful biomarker for PET imaging in Alzheimer's Disease (AD). Previous Congo Red derivatives that showed affinity for amyloid plaques in AD were also shown to bind to myelin in the CNS (Stankoff *et al.*, 2006).

Stankoff and colleagues have demonstrated via in-vitro studies that PIB binds to myelinated tracts in the cerebellar WM and corpus callosum of mice, as well as in human WM tracts. In MS brains, PIB demonstrated lack of staining within demyelinated lesions, and the ability to differentiate between NAWM, partially demyelinated WM, and fully demyelinated WM. In addition, after systemic injection in-vivo into mice, PIB was found to stain WM areas, and the level of staining varied with myelin content (Stankoff *et al.*, 2011).

As PIB shows binding affinity to CNS myelin, [^{11}C]PIB can be seen as a potential biomarker for in vivo PET imaging of myelin in MS. Stankoff and colleagues looked at PET imaging with [^{11}C]PIB in baboons, showing selective labelling of WM, especially in the subcortical areas. In a proof of concept study of 2 patients with Relapsing-Remitting MS (RRMS), PET imaging with [^{11}C]PIB labelled NAWM effectively, with reduced uptake in lesions seen on MR imaging. Reduced PIB

uptake was of a lesser degree in gadolinium-enhancing lesions, suggesting that levels of myelination differ between newer and older lesions, with newer lesions showing incomplete demyelination (Stankoff *et al.*, 2011).

While further in-vivo studies are required, these findings are encouraging and suggest [^{11}C]PIB PET could be a potential future imaging outcome in trials of remyelination and repair in MS.

Sample Size Calculations for trials using Lesion MTR

In this section, I consider the sample sizes required for proof-of-concept trials of potentially remyelination agents using lesion MTR as an outcome measure. The simplest analysis approach involves measuring *average lesion MTR* per participant per time point, and observing change longitudinally. MTR lesions would need to be correlated with either T2w lesions (acute and/or chronic) or gadolinium enhancing lesions (acute).

A recent paper used data from *in vivo* and *ex vivo* studies to estimate required sample sizes for remyelination trials in MS using mean MTR change of lesions detected at baseline on T2w images (Altmann *et al.*, 2013). As these lesions are likely to be chronic, the assumption is that any spontaneous remyelination has already taken place, and thus MTR would remain more-or-less stable over time. The *ex vivo* study, which included 12 patients with progressive MS who had died, showed that remyelinated lesion MTR lay approximately halfway between NAWM

and demyelinated lesions (Schmierer, Tozer, *et al.*, 2007). The *in vivo* data was derived from 18 patients with RRMS of short duration (less than 3 years) and low disability (EDSS less than 3) (Davies *et al.*, 2005). Patients had two scans separated by a year interval. Power calculations on this data were performed on the basis that remyelinated MTR values were roughly halfway between lesion and NAWM MTR. Sample sizes for both in vivo and ex vivo data are summarised in table 2.

Other factors which could complicate the assumption of a direct correlation between lesion MTR increase and extent of remyelination include the presence of significant inflammation and oedema, variability in the extent and quality of remyelination in different lesions, and technical factors, such as scanner differences in multi-centre studies (Altmann *et al.*, 2013).

In contrast to chronic lesions, acute lesions typically have an early MTR nadir consistent with demyelination followed by partial recovery that is thought, at least partly, to reflect spontaneous remyelination (Richert *et al.*, 2001). Taking this into account, trials of potentially remyelinating agents focusing on acute lesions (as detected by gadolinium-enhancement, for instance) using mean lesion MTR as an outcome measure, will need to be able to measure levels of residual (final) MTR in recovered acute lesions, in comparison to NAWM, as the main treatment effect. Power calculations for studies using mean MTR of gadolinium-enhancing (acute) lesions were performed using data from 32 RRMS patients, assuming a mean number of six gadolinium-enhancing lesions per patient, and a mild variance in treatment response between patients, and are summarised in table 2 (van den Elskamp *et al.*, 2010).

Another approach to analysing lesion MTR involves calculating the *MTR for individual lesions*, per patient per time point, and following these longitudinally. The simplest method is to follow every lesion detected at baseline over the therapeutic time course, which allows for longitudinal assessment of MTR of individual chronic lesions. This method could also be used for lesions not seen at baseline, but appearing at subsequent time points, effectively allowing longitudinal assessment of MTR of individual acute lesions.

A more novel technique for studying MTR in individual acute lesions has recently been described based on data from a study on autologous haematopoietic stem cell transplantation (AHSCT) in 10 patients with aggressive MS (Brown, Narayanan and Arnold, 2013). Patients had three MRI scans pre-AHSCT, and a number of follow-up scans post-AHSCT. The paper described a measure of cumulative change in MTR (ΔMTR), which is the difference between MTR at a time point compared to the first time point, and defined significant changes in ΔMTR according to a method described by Chen at al.(Chen *et al.*, 2008) Voxels were identified as 'increasing' (ΔMTR > 99^{th} percentile of NAWM ΔMTR), 'decreasing' (ΔMTR < 1^{st} percentile of NAWM ΔMTR), or 'stable' (neither 'increasing' nor 'decreasing'), and this detection method was applied to the entire brain parenchyma. Only groups of 5 or more changing ('increasing' or 'decreasing') voxels that overlapped with T_2w lesions that were not changing at the previous time point were included, thereby producing a map of newly changing lesions. Newly increasing lesions corresponding to lesions at previous time points with MTR decreases were discarded to avoid accounting for the same lesion multiple times.

The paper also defined two metrics, $MTR_{Recovered}$, which is the relatively stable MTR value after the recovery phase following the nadir, and MTR_{Drop}, which is the difference in MTR pre-lesion (i.e. at baseline) and post-lesion (i.e. at follow-up). Both were applied to ΔMTR lesions, as well as gadolinium-enhancing lesions. Approximately a third of gadolinium-enhancing voxels did not correspond to ΔMTR voxels, and ΔMTR voxels were also identified that did not show gadolinium enhancement. Patients demonstrating clinical improvement post-ASCT showed significantly improved MTR recovery, whereas those who remained stable clinically showed significantly poorer MTR recovery. Power calculations on this data are summarised in table 1.2.

Table 1.2: Sample sizes per arm for a placebo-controlled trial using *in vivo* lesion MTR recovery as primary surrogate outcome marker of remyelination (80% power)

Effect size	**Mean lesion MTR**		**Individual lesion MTR**			
	T_2w lesions	Gd lesions	Gd lesions		ΔMTR lesions	
			$MTR_{Recovered}$	MTR_{Drop}	$MTR_{Recovered}$	MTR_{Drop}
30%	38	68	22	12	19	21
40%	21	38	-	-	-	-
50%	14	24	10	6	8	8
60%	10	18	-	-	-	-
70%	-	14	6	6	5	5

Gd lesions: Gadolinium-enhancing lesions

It is evident in Table 1.2 that the required sample sizes for acute gadolinium-enhancing lesions are larger than that of all T_2w lesions, probably because there is spontaneous partial MTR recovery of the former whereas the latter are assumed to have an unchanged MTR without active treatment. However, the acute and post-acute lesions may be more biologically amenable to remyelination (Goldschmidt *et al.*, 2009). In addition, the $MTR_{Recovered}$ and MTR_{Drop} metrics appear to have

potentially greater statistical power for detecting treatment effects, and correlate with clinical outcomes.

So far, I have considered only brain measures of myelination. Spinal Cord and Optic Nerve involvement is also very common and measuring remyelination in these regions will be discussed in the sections that follow.

Imaging Remyelination in the Spinal Cord

Involvement of the spinal cord is common in MS, and often leads to substantial motor, sensory and sphincter dysfunction. Demyelinating lesions are commonly seen on MRI, especially in the cervical spine (Grossman, Barkhof and Filippi, 2000). However clinical, especially motor, disability appears from post mortem studies to be less associated with lesion numbers and more so with axonal loss in the cord (Lovas *et al.*, 2000; DeLuca *et al.*, 2006).

Quantitative measurements in the spinal cord though are more challenging than in the brain (Wheeler-Kingshott *et al.*, 2013); nevertheless there is a great potential in studying this part of the central nervous system as its contribution to disability is substantial.

MTR

MTR is reduced in the spinal cord in MS, both in vivo (Filippi *et al.*, 2000; Hickman, Hadjiprocopis, *et al.*, 2004), and post-mortem (Mottershead *et al.*, 2003), and correlates with myelin content (Mottershead *et al.*, 2003), and clinical disability (Zackowski *et al.*, 2009). MTR measurement is often performed using a SPGR sequence, which is time-consuming, and may be susceptible to motion artefact. MTR normalised to CSF signal intensity on an MT-weighted scan (MTCSF) is a measure that can be useful where conventional MT imaging is not feasible due to motion degradation or low SNR (Smith *et al.*, 2005). However, discriminating myelination and inflammation may be difficult as MTCSF is also sensitive to CSF flow and tissue relaxation times.

DTI

In MS, radial diffusivity ($\lambda_{\perp}$) reflects demyelination in ex vivo spinal cords (Klawiter *et al.*, 2011). FA and radial diffusivity ($\lambda_{\perp}$) in the corticospinal tracts and posterior columns are correlated with clinical outcomes such as the Expanded Disability Status Scale (EDSS), the timed 25-Foot Walk, and the 9-Hole Peg Test (Naismith *et al.*, 2013).

However, specificity of DTI metrics to myelin in the spinal cord is unclear. Compared to the brain, DTI metrics should theoretically be easier to measure in the spinal cord, given that fibre-tract orientation in white matter columns is essentially unidirectional. However the small size of the spinal cord, physiological noise, signal

contamination from CSF and poor homogeneity due to the presence of tissue/bone interface make DW measurements in the spinal cord more difficult than in the brain (Grossman, Barkhof and Filippi, 2000).

NODDI

The feasibility of this sequence in studying the spinal cord of healthy volunteers and MS patients has recently been shown (Grussu *et al.*, 2013). The potential clinical value of NODDI in the spinal cord in MS needs further investigation to evaluate its sensitivity towards the effects of disease when an optimised protocol has been implemented.

PET

[^{11}C]MeDAS is a radiolabelled substrate that, in experimental models, crosses the BBB and selectively labels WM regions in the brain and spinal cord, and is highly sensitive and specific to myelin content (Wu *et al.*, 2010, 2013). Serial PET imaging with [^{11}C]MeDAS in LPC rat models showed low spinal cord uptake at the peak of demyelination on day 7 post-injection, and demonstrated gradual increased uptake on days 14 and 21, reflecting remyelination. Similar changes in uptake in the spinal cord reflecting myelination was also seen in the experimental allergic encephalitis (EAE) model (Wu *et al.*, 2013). At present, there have been no human studies of [^{11}C]MeDAS-PET.

Imaging Remyelination in the Optic Nerves

The optic nerve forms part of the anterior afferent visual pathway, a discrete WM tract, and is often affected in patients with MS. Optic Neuritis (ON) may be the initial clinical presentation in 20% of cases of MS (The Optic Neuritis Study Group, 2008), and may occur during the disease course in 50% of MS cases (Balcer, 2006). Subclinical involvement of the optic nerves is also common (Toussaint *et al.*, 1983), as is involvement of the optic radiation (Hornabrook *et al.*, 1992; Plant *et al.*, 1992). The main pathology in the optic nerves is the demyelinating lesion, although similarly to the brain and spinal cord, inflammation, gliosis, oedema, and axonal loss are also present (Youl *et al.*, 1991; Breij *et al.*, 2008). The optic nerve thus represents an important area of investigation, when considering possible remyelinating agents in MS.

Visual Evoked Potential (VEP), which records evoked potentials following the administration of visual stimuli in the central 30° of the visual field (P100), can suggest demyelination in the optic nerves as increased latency, and axonal loss as decreased amplitude (conduction block due to demyelination can also reduce amplitude). In the MSCIMS trial, patients with secondary progressive MS, who received autologous mesenchymal stem cells, demonstrated significantly reduced VEP latencies ($p=0.02$), increased optic nerve area ($p=0.006$), increased LogMAR visual acuity overall (0.003), as well as a trend suggesting increasing mean T_1w lesion MTR ($p=0.097$) (Connick *et al.*, 2012).

Optical Coherence Tomography (OCT) is a non-invasive imaging technique that allows quantifiable measurement of retinal structures (Frohman *et al.*, 2008). Retinal nerve fibre layer (RNFL) thickness is a measure of axon integrity of the optic nerve, and many MS patients, even without a clinical episode of ON, will have demonstrable RFNL thickness reduction on OCT (Fisher *et al.*, 2006; Petzold *et al.*, 2010). Ganglion cell and inner plexiform (GCIP) layer thickness is also reduced in MS, and may correlate better with clinical vision measures than RNFL thickness (Saidha *et al.*, 2011). These retinal measures are representative of axonal integrity in the anterior visual pathways.

It has been reported that delayed latency on VEP correlates with RNFL thinning in MS patients with ON (Henderson *et al.*, 2011), as well as without ON (Klistorner *et al.*, 2013), suggesting the clinical and subclinical demyelination may be associated with increased axonal vulnerability. This also supports the concept that remyelination may be neuroprotective. Thus, while OCT outcomes are not themselves intrinsically representative of myelin content, they may be useful adjuncts in trials of potentially remyelinating agents to measure possible secondary neuroprotective effects.

Imaging the optic nerves (figure 3) can be technically more difficult than imaging the brain and cord, as the optic nerves are small in diameter, and are especially susceptible to motion artefact. In addition, orbital fat and CSF in the optic nerve sheath may contaminate optic nerve signal, making interpretation difficult. These limitations need to be taken into account when considering the feasibility of any imaging modality in the optic nerves (Barker, 2000).

Conventional MR sequences

The lesions of optic neuritis can be seen as signal hyperintensities on conventional T_2w images, but surrounding fat also generates high signal, making identification of lesions difficult. The use of fat suppression sequences, such as short-tau inversion recovery (STIR) (Johnson *et al.*, 1987), can help, but can result in high signal from the surrounding CSF, obscuring signal from the optic nerve. In addition, these sequences lack the ability to differentiate between demyelination, oedema, gliosis, inflammation and axonal loss.

MTR

MTR (figure 4) is reduced in optic nerves affected by ON, compared to both unaffected and control nerves, and correlates inversely with VEP latencies (Thorpe *et al.*, 1995; Trip *et al.*, 2007). This correlation may be greater when assessing lesion, rather than whole-nerve, MTR.(Trip *et al.*, 2007) While MTR reduction often occurs rapidly in new brain lesions (Dousset *et al.*, 1998; Richert *et al.*, 2001), one study noted that reduction was not marked in the acute phase of the symptomatic ON lesion, and nadir was not reached for many months after the initial clinical episode (Hickman, Toosy, *et al.*, 2004). Recovery of lesion MTR is often seen within the first few months, and can continue up to 1 year post appearance.

Patients with incomplete recovery and poorer visual outcomes following ON demonstrate lower affected optic nerve MTR compared with the unaffected nerve

(Trip *et al.*, 2007), as well as the affected nerve of patients showing good recovery (Inglese *et al.*, 2002) .

While good inverse correlation with VEP latencies in ON suggests that MTR is sensitive to demyelination, axonal loss has also been shown to be an important factor, and one study suggests that it may even exert greater influence than demyelination on MTR values (Klistorner *et al.*, 2011).

DTI

In one study of acute ON, significantly decreased $\lambda_{||}$ at baseline was associated with worse visual outcomes, smaller VEP amplitude, prolonged VEP latency and thinner RNFL at six months (Naismith *et al.*, 2012). In a study more than six months following an episode of ON, $\lambda_{\perp}$ was highly correlated with visual outcomes, VEP latency, VEP amplitude and RNFL thickness (Naismith *et al.*, 2010). It is at present unclear whether diffusion measurements reflect changes in myelin or axonal integrity (Trip *et al.*, 2006), although a recent study in patients with MS demonstrated reduction of FA and increase in $\lambda_{\perp}$, with no difference of MD and $\lambda_{||}$, suggestive of demyelination (Samson *et al.*, 2013).

Applying DTI imaging to the optic nerves may be technically challenging. Signal contamination from fat and CSF (Barker, 2001), and motion artefacts (Xu *et al.*, 2008), can occur. A fat and CSF suppressed zonal oblique multi-slice echo planar imaging (ZOOM-EPI) sequence can improve resolution and reliability, and reduce

artefacts to a minimum (Wheeler-kingshott *et al.*, 2002), but this, and other selective excitation sequences, are not readily available on all scanners, and may require long scan times in order to acquire anisotropy indices such as FA (Hickman *et al.*, 2005).

Summary

Trials of potentially remyelinating agents are becoming more important in the overall spectrum of MS research, and should be designed in order to maximise their sensitivity to true treatment effects. In addition to selecting patient groups with the most potential to show a response, and generating sound sample size calculations that give a trial sufficient power to detect a true effect on the chosen primary outcome measure, imaging outcomes are needed that are feasible from a time and practicality point of view, as well as being sensitive and specific to myelin, whilst also being reproducible, and clinically meaningful.

There are a number of potential outcome measures available for use in such trials (table 1.3). Some, such as MTR, DTI, and MWF have shown excellent sensitivity to detecting changes in myelin in vivo. However, it is difficult to ascribe the influence of a specific biophysical phenomenon on the MR signal, and this is complicated by the typical coupling of different pathological features, such as inflammation, oedema, axonal loss and demyelination.

Given that no one measure demonstrates uniformly high specificity, reproducibility, and correlation with clinical features, it may be useful to employ more than one imaging outcome sensitive to remyelination in future trials, and results from these must be correlated with other measures, especially with functionally relevant clinical outcome measures, in order to better understand their potential to detect myelination and reflect clinically meaningful effects. At present, in addition to the standard T_1w, T_2w and gadolinium- enhanced sequences, MTR and a DTI metric such as radial diffusivity ($\lambda_\perp$) would appear to represent realistic and feasible options to be considered as imaging outcomes in the brain and spinal cord. Clear multi-centre study designs (including both acquisition and analysis procedures) are essential for evaluating the sensitivity and reproducibility needed for detecting changes modulated by treatment response. [^{11}C]PIB PET in the brain and [^{11}C]MeDAS in the spinal cord represent promising future imaging modalities, but radiation accumulation will limit the number of repeat studies possible, and further investigation and validation is required to determine their utility, especially in human MS studies. In addition, the optic nerves are frequently affected in MS, and demyelination is commonly seen, corresponding well with clinical and paraclinical measures. The afferent visual pathway thus represents an important WM system for studying demyelination and remyelination. VEP can infer demyelination and, although quantitative imaging of the optic nerve is technically challenging, should be correlated when possible with an imaging outcome (such as optic nerve MTR), potentially adding support for the sensitivity of these outcomes to myelination. Although OCT reflects axonal pathology, it should be considered as an adjunct to more intrinsic measures of myelin, as it may demonstrate potential neuroprotective effects secondary to remyelination.

Table 1.3: Summary of Imaging outcomes for remyelination and repair in MS					
Modality	*Myelin Sensitivity*	*Myelin Specificity*	*Clinical Correlation*	*Acquisition Time**	*Comments*
T_2 lesion evolution	Excellent	Poor	Moderate	Short	Confounded by inflammation, axonal loss and oedema
T_1 lesion evolution	Moderate	Poor	Unknown	Short	BH evolution may be useful in neuroprotection trials
MTR	Excellent	Good	Good	Short	Semi-Quantitative
qMT	Excellent	Good	Unknown	Moderate/ Long	Modelling the MT effect in tissue is complex
MWF	Excellent	Good	Unknown	Long	Limited brain coverage
• *mcDESPOT*	*Excellent*	*Good*	*Unknown*	*Moderate*	*Accuracy questioned*
• *T2prep 3D SPIRAL*	*Excellent*	*Good*	*Unknown*	*Moderate*	*Limited evidence in patient groups*
• *3D-GRASE*	*Excellent*	*Good*	*Unknown*	*Short*	*Limited evidence in patient groups*
DTI	Excellent	Moderate	Unknown	Moderate	Low resolution and SNR, motion artefact susceptibility
PET	Excellent	Excellent	Unknown	Moderate/Long	Further in-vivo studies required
OCT	Moderate	Poor	Excellent	Short	Useful to detect secondary neuroprotective effects
*Acquisition Times: Short <15 mins, Moderate = 15-30mins, Long >30 mins. These will vary somewhat by operator and scanner					

1.8 CLINICAL MANAGEMENT

Patients with MS may experience a number of symptoms, and clinical management of the condition is multi-faceted, and is important for potentially reducing rates of relapse, improving recovery from an active relapse, and managing ongoing symptoms.

- Disease Modification

  Several drugs have been licensed for use in reducing the rates of relapse in patients with RRMS. These vary in their effectiveness and side-effect profiles, and have various indications for use, dependent on patients' clinical and imaging features and the licensing regulations in respective countries (Thompson, Baranzini, *et al.*, 2018).

- Acute Relapse Management

  Patients demonstrating evidence of an acute and disabling relapse may be treated with intravenous or oral steroids. This can help speed recovery time, but has no demonstrable long-term prognostic benefit.

- Symptomatic treatment

  Symptoms such as pain, spasticity, and bladder dysfunction can be managed with pharmacological therapy, as well as non-pharmacological therapy, such as physiotherapy, occupational therapy, and psychological and psychiatric support.

2. REGIONAL PATTERNS OF GM ATROPHY AND MTR ABNORMALITIES IN MS CLINICAL SUBGROUPS: A VOXEL-BASED ANALYSIS

2.1 BACKGROUND

In MS, GM demyelination and neuronal loss are all recognised histopathological features (Geurts and Barkhof, 2008). Cortical demyelination can be seen in the earliest clinical stages of MS (Lucchinetti *et al.*, 2011), and may be extensive in progressive forms of the disease (Kutzelnigg *et al.*, 2005; Popescu and Lucchinetti, 2012). Similarly, GM neuronal loss, especially in the deep GM structures, can be seen early in MS (Vercellino *et al.*, 2009), and is evident in the cortex later in the course of the disease (Wegner, Esiri and Chance, 2006; Magliozzi *et al.*, 2010; Choi *et al.*, 2012).

It is not known how closely GM demyelination and neuronal atrophy and loss are related. One histopathological study using material from 22 people with MS (clinical sub-types were not specified) found no clear association between local cortical demyelination and cortical thickness, although neuronal densities were reduced in leukocortical lesions (Wegner, Esiri and Chance, 2006). More recently, evidence has emerged that meningeal inflammation is linked with both cortical demyelination (Magliozzi *et al.*, 2007; Howell *et al.*, 2011; Choi *et al.*, 2012), and neuronal loss (Magliozzi *et al.*, 2010). Such meningeal inflammation appears to be particularly apparent in SPMS and PPMS subgroups (Magliozzi *et al.*, 2007; Howell *et al.*, 2011; Choi *et al.*, 2012). In spite of these observations, it is uncertain to what extent GM

demyelination and neuronal loss are spatially co-localised, and whether or not they are caused by a common pathological process, such as meningeal inflammation. It is also not known if links (if present) between local demyelination and neuronal loss occur in all MS subtypes.

Brain GM atrophy, which is associated with neuronal and axonal loss (Miller *et al.*, 2002), can be detected using MR imaging, and appears to have a greater impact on clinical disability in the long-term than WM lesion accrual (Fisher *et al.*, 2008; Fisniku *et al.*, 2008; Bonati *et al.*, 2011). However, GM atrophy does not appear to be uniform throughout the brain, with some regions more frequently affected than others (Audoin *et al.*, 2006, 2010). and this may vary between different MS phenotypes (Ceccarelli *et al.*, 2008).

Magnetisation transfer (MT) imaging provides insight into intrinsic structural tissue abnormalities. In WM, the MT ratio (MTR) is reduced in the presence of demyelination, and to a lesser degree axonal loss (Schmierer *et al.*, 2004), and in the cortex has also been shown to reflect predominantly demyelination (Chen *et al.*, 2012). Abnormal GM MTR has been shown even in the earliest stages of MS, correlating with disease duration (Dehmeshki *et al.*, 2003), clinical disability (Ranjeva *et al.*, 2005), and cognitive impairment (Rovaris and Filippi, 2000). MTR will be discussed in further detail in Chapter 4.

Voxel-Based Analysis (VBA) is a fully automated technique which allows whole-brain comparisons to be made between patient groups on a voxel-wise basis, via spatial transformation of images to a normalised template. This method differs from region of interest (ROI) and histogram based methods in that it allows unbiased assessment of whole brain areas, leading to greater sensitivity to detect region specific changes between patient groups (Audoin *et al.*, 2004; Giuliani *et al.*, 2005). VBA methods allow the detection of consistent effects within a group, by demonstrating regions where the majority of participants in the group show significant change. Voxel-Based Morphometry (VBM) specifically allows the volume and concentration of GM to be compared between patient groups at a voxel-by-voxel level, and is used to quantify atrophy (Ashburner and Friston, 2000). Previous voxel-based studies have demonstrated consistent regional MTR reductions in some areas in RRMS (insula and lenticular nuclei bilaterally, as well as the left posterior cingulate cortex, and the right orbitofrontal cortex)(Audoin *et al.*, 2007). In one study of people with PPMS, MTR changes were found to co-localise with atrophy in small GM regions (Khaleeli *et al.*, 2007), but MTR reductions were also seen in areas without GM atrophy, and in the majority of cases co-localisation in GM was not observed.

To date, no studies have systematically assessed regional GM atrophy and MTR abnormalities across RRMS, PPMS, and SPMS.

2.2 AIMS

In this study I undertook VBA of brain GM atrophy and MTR in a relatively large cohort of people with MS including all three subgroups. Using VBA to identify regions of the brain that are consistently affected in each group, I sought to answer the following questions:

1. Which GM regions show consistent atrophy, suggesting neuro-axonal loss, in each clinical subgroup of MS?
2. Which GM regions show consistent MTR reduction, suggesting demyelination, in each clinical subgroup of MS?
3. What is the location and extent of co-localisation of GM MTR abnormalities and atrophy, and does this differ amongst MS clinical subgroups?

2.3 METHODS

Participants

People with clinically definite MS (Polman *et al.*, 2011), who had not experienced a relapse or received corticosteroids in the four weeks prior, were recruited into the study. Healthy controls with no history of neurological or psychiatric disorders were also recruited. All participants gave informed consent before taking part in this study. This study was approved by the local institutional research ethics committee (The National Hospital for Neurology and Neurosurgery & Institute of Neurology Joint REC reference number 09/H0716/77, 2009). All participants had a clinical assessment to confirm the clinical subtype of MS, disease duration, and disability as measured using the Expanded Disability Status Scale (EDSS).

MRI acquisition

Images were acquired using a 3T Philips Achieva scanner (Philips Healthcare, Best, The Netherlands) with a 32-channel head coil and multi-transmit technology. T1w volumetric and MT images were obtained sagittally, with a field-of view of 256x256x180mm^3 and 1mm isotropic resolution with the following parameters: T1w volumes, using a 3D inversion-prepared (TI=824ms) gradient echo (FFE) sequence (TR/TE=6.9/3.1ms); flip angle (α)=8°; MTR data, using a 3D slab selective spoiled gradient echo (FFE) sequence with 2 echoes (TR=6.4ms, TE1/TE2=2.7/4.3ms, α=9°) with and without Sinc-Gaussian shaped MT saturating pulses of nominal α=360°, offset frequency 1kHz, duration 16ms applied prior to the excitation pulse.

Image Analysis

NiftyReg (Modat, 2010) was used to affine register the MT-on and MT-off images to the T1w volume. MTR maps were calculated using the equation [MTR = (MT-off – MT-on)/ MT-off]. White matter lesion-filled T1w images (Chard *et al.*, 2010) were segmented using the "New Segment" function in SPM8 (UCL Wellcome Trust Centre for Neuroimaging, London). The resulting GM tissue probability maps were all checked for accuracy and then used in two ways. First, they were binarised using a conservative 90% threshold, and overlaid on the MTR map to define GM regions to be included in the subsequent VBM analysis. The binarised GM volumes for each individual patient were divided by their respective intracranial volumes (ICV), calculated by summing the GM, WM and CSF volumes, to calculate the GM fraction (GMf).

Second, the probability maps were used to create a custom diffeomorphic anatomical registration using exponentiated Lie algebra (DARTEL) template using SPM8 (Ashburner, 2007). Each participant's GM probability map was registered to this template using a non-linear transformation, and then affine transformed into Montreal Neurological Institute (MNI) space with sinc interpolation, before being smoothed with an 8mm full width half maximum (FWHM) Gaussian smoothing kernel. Each participant's segmented GM MTR map was then transformed to MNI space via the DARTEL template using the same transformations in a single step with sinc interpolations. The MTR maps were then smoothed using an 8mm FWHM Gaussian smoothing kernel. The global mean GM MTR value for the segmented MTR maps was calculated using the 'fslstats' command from the FSL suite (FMRIB Software Library, Oxford) (Jenkinson *et al.*, 2012).

Statistical analysis

Age, demographic and clinical data were compared between groups using independent samples t-tests in PASW statistics (IBM SPSS Statistics, version 18.0). Volumetric and MTR VBA was performed using SPM8. Areas of abnormality were considered statistically significant at an alpha threshold of p=0.05, corrected for multiple comparisons using Gaussian random field theory (family wise error [FWE]) at voxel level. Age and gender were included as covariates in the general linear models. Analysis was also performed at p=0.001 uncorrected, for comparison.

Identification and quantification of consistently affected regions and voxels

When comparing each of the 3 MS clinical subgroups with controls, and comparing the clinical subgroups with each other, MRIcron (Rorden, Karnath and Bonilha, 2007) was used to:

- label regions of consistent MTR reduction
- label regions of consistent atrophy
- label regions where MTR reduction and atrophy co-localised
- count the number of voxels affected by each pathological process in each region.

This was done by overlaying the images of significant clusters from SPM8 onto the Automated Anatomical Labelling (AAL) atlas (Tzourio-Mazoyer *et al.*, 2002).

2.4 RESULTS

Participant Characteristics

A total of 98 patients and 29 healthy controls were included in the study. Of the patients, 51 had RRMS, 28 had SPMS, and 19 had PPMS. Participant characteristics are summarized in Table 2.1.

Table 2.1: Participant characteristics

	RR	SP	PP	Controls
N (males)	51 (19)	28 (7)	19 (8)	29 (13)
Mean Age (years)	42.35	53.43	52.05	36.97
SD	9.84	7.73	9.48	12.04
Range	21-64	36-65	27-65	22-63
Mean Duration (years)	11.85	22.73	13.53	-
SD	*9.09*	*11.16*	*7.97*	-
Range	*0.5 – 45.0*	*7.5 – 47.83*	*2.5 – 27.25*	-
Median EDSS	2.0	6.5	6.0	-
Range	1.0 – 7.0	4.0 – 8.5	1.5 – 6.5	-
Use of DMT	40	13	3	-
Current Use	29	7	1	-
Previous Use	11	6	2	-
Mean GMf	0.474	0.472	0.468	0.478
SD	0.012	0.010	0.014	0.013
Mean GM MTR	30.74	29.78	30.23	31.86
SD	1.211	1.141	1.498	0.566

RR: Relapsing-Remitting; PP: Primary Progressive; SP: Secondary Progressive; EDSS: Expanded Disability Status Score; SD: Standard Deviation; GMf: Grey Matter fraction; MTR: Magnetisation Transfer Ratio; DMD: Disease Modifying Drug

Overall, those with MS were older than controls ($p<0.001$). People with RRMS were significantly younger than both SPMS ($p<0.001$) and PPMS ($p<0.001$). There was no significant difference in age between the SPMS and PPMS groups ($p=0.83$). The age ranges included in the control and MS groups were similar. The SPMS group had a significantly longer mean disease duration than either PPMS ($p=0.004$), or RRMS

(p<0.001). There was no significant difference in mean duration between RRMS and PPMS (p=0.49). There was a significant difference in the global GM MTR between RRMS and SPMS (P<0.001), but no significant difference between RRMS and PPMS (p=0.13), and PPMS and SPMS (p=0.25).

Clinical subgroups compared to controls

A summary of results can be seen in table 2.2, showing voxel counts for MTR reduction, atrophy and co-localisation of MTR reduction and atrophy, in the total GM, in the cortex, in the deep GM, and in the thalamus, for the different clinical subgroups in MS compared with healthy controls.

Table 2.2: VBA significant voxel counts (compared with controls) by clinical subgroup and location (FWE 0.05)

	Overall MTR Reduction			Overall Atrophy			MTR reduction and Atrophy		
	RR	SP	PP	RR	SP	PP	RR	SP	PP
Total	3615	13109	318	5026	1538	0	2157	610	0
Cortex	399	9320	318	206	117	0	21	109	0
(% total)	(11.04%)	(71.10%)	(100%)	(4.10%)	(7.61%)	(0.00%)	(0.97%)	(17.87%)	(0.00%)
Deep GM	3216	3789	0	4820	1421	0	2136	501	0
(% total)	(89.96%)	(28.90%)	(0.00%)	(95.90%)	(92.39%)	(0.00%)	(99.03%)	(82.13%)	(0.00%)
Thalamus	3042	2325	0	4747	1421	0	2136	501	0
(% deep GM)	(94.59%)	(61.36%)	(0.00%)	(98.49%)	(100%)	(0.00%)	(100%)	(100%)	(0.00%)
(% total)	(84.15%)	(17.74%)	(0.00%)	(94.45%)	(92.39%)	(0.00%)	(99.03%)	(82.13%)	(0.00%)

RR: Relapsing Remitting; SP: Secondary Progressive; PP: Primary Progressive; MTR: Magnetisation Transfer Ratio; VBA: Voxel Based Analysis; FWE: Family Wise Error; GM: Grey Matter

MTR reduction: Overall whole GM MTR (table 2.1) was reduced in all groups compared to controls (RRMS vs controls, p value =0.00002; SPMS vs controls, p value <0.00001; PPMS vs controls, p value <0.00001), and in SPMS compared to RRMS (p value = 0.0009). Consistent regional MTR reductions were seen in the GM

of all clinical subgroups compared to controls, but were more extensive in SPMS (13109 voxels) than in RRMS (3615 voxels) and PPMS (3825 voxels). MTR reduction was more extensively seen in the cortex than in the deep GM in PPMS (100% of the voxels that showed MTR reduction in this subgroup were located in the cortex) and SPMS (71%), while in RRMS deep GM regions were most extensively affected (90%). Thalamic MTR reduction was seen in RRMS and SPMS compared to controls, and accounted for 95% of all deep GM involvement in RRMS, and 61% of deep GM involvement in SPMS. The precise regions of cortical and deep GM MTR reduction for each clinical subgroup, compared to controls, are summarised in Appendices 1 and 2.

Atrophy: Compared to controls, consistent regional atrophy was seen more extensively in RRMS (5026 voxels) and SPMS (1538 voxels) than in the PPMS group (no significant regional atrophy compared to controls). Deep GM atrophy accounted for most of the regional atrophy seen in RRMS (96%) and SPMS (93%). The areas of consistent cortical and deep GM atrophy for each clinical subgroup, compared to controls, are summarised in Appendices 3 and 4. Thalamic atrophy accounted for 98% of deep GM atrophy in RRMS and 100% of deep GM atrophy in SPMS groups.

Co-localisation of MTR reduction and Atrophy: Co-localised MTR reduction and atrophy was seen in both RRMS (2157 voxels) and SPMS (610 voxels), mainly affecting the thalami (as a proportion of the total GM, thalamic MTR reduction and atrophy co-localisation was seen in 99% and 82% respectively). The areas of cortical

and deep GM MTR and atrophy co-localisation for each clinical subgroup, compared to controls, in order of voxels, are summarised in Appendices 5 and 6.

Subgroup comparison

At FWE 0.05, only a small area of difference in MTR reduction was detected in the SPMS versus RRMS subgroup comparison (left precentral region, 124 voxels); no significant differences were detected in the other inter-subgroup comparisons for MTR reduction or atrophy alone, or co-localisation of both.

Controls compared to all patients and clinical subtypes

Controls did not show any areas of consistent MTR reduction, atrophy, or co-localisation in GM compared to all patients, or to PPMS, SPMS and RRMS subgroups.

Reanalysis without FWE

Given the small effect sizes obtained using FWE 0.05, the analysis was rerun without FWE, using an alpha level of 0.001, uncorrected. The intention for this additional analysis was to further explore whether, by reducing certain statistical stringencies, similar patterns were seen, albeit with great effect sizes, or if entirely different patterns started to become visible. The results are shown in Table 2.3, and are grossly similar pattern to the previous analysis. Figure 2.1 illustrates the areas affected by MTR reduction, atrophy, and both MTR reduction and atrophy, in all subgroups compared to controls, without FWE, using an alpha level of 0.001,

uncorrected. the subgroup comparisons were also rerun without FWE, using an alpha level of 0.001 uncorrected, and the summary of the findings are shown in Table 2.4.

Table 2.3: VBA significant voxel counts (compared with controls) by clinical subgroup and location (0.001, uncorrected)

	Overall MTR Reduction			Overall Atrophy			MTR reduction and Atrophy		
	RR	SP	PP	RR	SP	PP	RR	SP	PP
Total	53672	97707	24615	27903	30153	1857	14649	18867	875
Cortex (% total)	38049 (70.89%)	80051 (81.93%)	20917 (84.98%)	9562 (34.27%)	17647 (58.52%)	712 (38.34%)	4770 (32.56%)	11985 (63.52%)	703 (80.34%)
Deep GM (% total)	15623 (29.11%)	17656 (18.07%)	3698 (15.02%)	18341 (65.73%)	12506 (41.48%)	1145 (61.66%)	9879 (67.44%)	6882 (36.48%)	172 (19.66%)
Thalamus (% deep GM) (% total)	6503 (41.62%) (12.17%)	5481 (31.04%) (5.61%)	853 (23.07%) (3.47%)	6094 (33.23%) (21.84%)	3853 (30.81%) (12.78%)	122 (10.66%) (6.57%)	5119 (51.82%) (39.94%)	3087 (44.86%) (16.36%)	82 (47.67%) (9.37%)

RR: Relapsing Remitting; SP: Secondary Progressive; PP: Primary Progressive; MTR: Magnetisation Transfer Ratio; VBA: Voxel Based Analysis; FWE: Family Wise Error; GM: Grey Matter

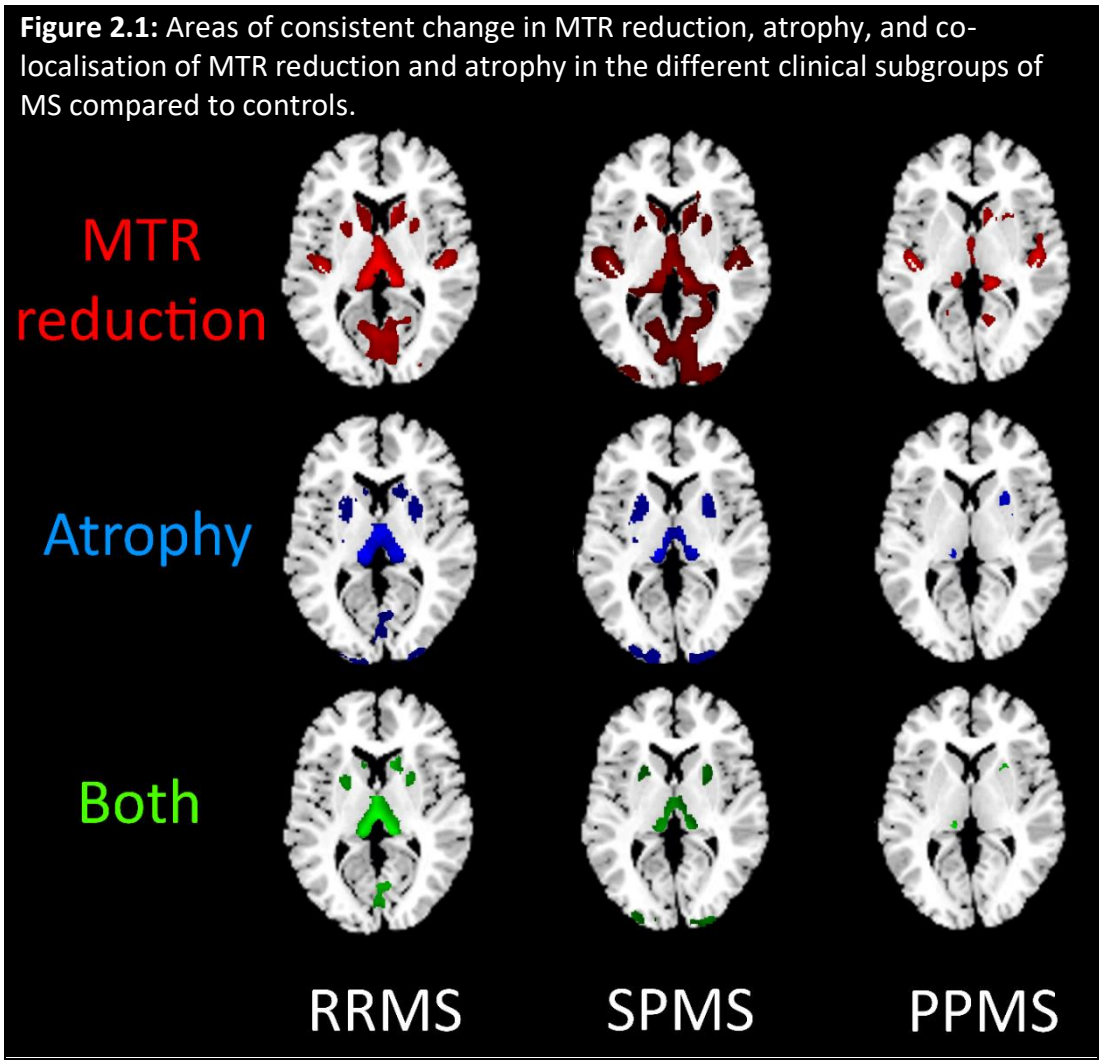

Figure 2.1: Areas of consistent change in MTR reduction, atrophy, and co-localisation of MTR reduction and atrophy in the different clinical subgroups of MS compared to controls.

Table 2.4: VBA significant voxel counts of clinical subgroup comparisons by location (0.001, uncorrected)

	Overall MTR Reduction						Overall Atrophy					
	RR vs PP	RR vs SP	SP vs PP	SP vs RR	PP vs SP	PP vs RR	RR vs PP	RR vs SP	SP vs PP	SP vs RR	PP vs SP	PP vs RR
Total	**4581**	**4808**	**8150**	**15976**	**431**	**430**	**367**	**0**	**3886**	**939**	**0**	**0**
Cortex	**4580**	**4808**	**7321**	**15951**	**431**	**430**	**329**	**0**	**3886**	**939**	**0**	**0**
(% total)	(99.98%)	(100%)	(89.83%)	(99.84%)	(100%)	(100%)	(89.65%)		(100%)	(100%)		
Deep GM	**1**	**0**	**829**	**25**	**0**	**0**	**38**	**0**	**0**	**0**	**0**	**0**
(% total)	(0.02%)	(0%)	(10.17%)	(0.16%)	(0%)	(0%)	(10.35%)		(0%)	(0%)		

RR: Relapsing Remitting; SP: Secondary Progressive; PP: Primary Progressive; MTR: Magnetisation Transfer Ratio; VBA: Voxel Based Analysis; FWE: Family Wise Error; GM: Grey Matter

This suggests that in PPMS, there is considerably more MTR reduction than atrophy (24615 voxels vs 1857 voxels respectively), and that the former is seen predominantly in the cortex (85%). SPMS shows the most widespread MTR reduction (97707) and atrophy (30153) of all the subgroups, the former being most extensive in the cortex (71%), while the latter is seen in both the cortex and deep GM, with slightly more in the cortex (59%). The largest difference seen compared to the analysis with FWE correction (p=0.05) is in RRMS, which revealed a higher volume of MTR reduction than atrophy (53672 voxels vs 27903 voxels), the former mainly in the cortex (71%), while the latter is seen more in the deep GM (66%).

Comparing subgroups (without FWE, using and alpha level of 0.001, uncorrected) reveals overall small differences in regions of MTR reduction and atrophy, with no differences seen in co-localisation, and support the findings from comparison with controls. Greater cortical MTR reduction and atrophy is seen in RRMS compared to PPMS, although PPMS patients do also show MTR reduction in some cortical regions not seen in the RRMS subgroup. SPMS and RRMS comparisons reveal overall greater areas of MTR reduction and atrophy in the former, mainly in the cortex, although there are regions of MTR reduction and atrophy in RRMS not seen in the SPMS group. Similarly, when comparing SPMS and PPMS, while the latter does demonstrate greater MTR reduction in a few regions, overall SPMS patients showed more MTR reduction and atrophy.

2.5 DISCUSSION

In this study, the results reveal small but important differences in the spatial patterns of MTR reduction and atrophy in different clinical subgroups and may help improve our understanding of the pathophysiological basis of GM pathology in MS. The most striking observations are the differences in extent and location of consistent MTR reduction and atrophy in the cortex and deep GM of the different clinical subgroups of MS compared with controls. The PPMS subgroup showed more extensive MTR change compared to atrophy, and limited involvement of the deep GM. The RRMS subgroup showed more extensive atrophy than reduced MTR, mainly affecting the deep GM, with minimal cortical involvement. The SPMS subgroup showed both MTR reduction and atrophy, involving both GM compartments, with more extensive MTR reduction in the cortex, and more extensive atrophy in the deep GM, and especially the thalamus.

MTR reduction is thought to reflect demyelination, as shown by histopathological work in cortical GM (Chen *et al.*, 2012), as well as WM (Schmierer *et al.*, 2004), and atrophy is predominantly secondary to neuronal loss (Miller *et al.*, 2002). Co-localisation of MTR reduction and atrophy would therefore suggest a direct link between demyelination and neuronal loss, and that there could be a common cause for both. The presence of atrophy alone suggests neuronal loss without demyelination, and this might occur as a result of the distant effect of axonal transection and degeneration occurring in inflammatory-demyelinating WM lesions. The presence of MTR reduction alone without significant atrophy co-

localisation is suggestive of demyelination without significant neuronal loss, which may indicate a less destructive pathological process predominantly affecting myelin and sparing neurons.

With the above in mind, these results support the concept that significant cortical demyelination occurs in the SPMS and PPMS subgroups, which is agreement with histopathological work (Kutzelnigg *et al.*, 2005; Vercellino *et al.*, 2005). Further, this appears to be relatively greater in SP compared with PPMS; cortical demyelination has recently been linked with meningeal inflammation, and in turn this is more evident in SPMS than PPMS (Magliozzi *et al.*, 2007; Choi *et al.*, 2012).

Co-localisation of MTR reduction and atrophy occurred in a minority of regions, but did so most often in deep GM (principally the thalamus), in RRMS and SPMS. This is consistent with a recent MRI study (Minagar *et al.*, 2013), and is supported by previous histopathological work demonstrating that demyelination and neuronal loss frequently occur in the deep GM of relapse-onset MS, particularly the thalamus, and that neuronal density is lower in demyelinated compared with non-demyelinated regions (Vercellino *et al.*, 2009). This would suggest a contributory role for local demyelination as a cause of neuronal atrophy or loss in the thalamus in RRMS and SPMS. Notwithstanding, a recent combined MRI and histopathology study demonstrated a link between cortical thickness, thalamo-cortical white matter tract myelination, and thalamic nucleus cell density, supporting this concept that tract-mediated changes distant to the site of the initiating pathological event

may also contribute to thalamic neuronal loss and hence atrophy (Kolasinski *et al.*, 2012).

The patterns of atrophy differed between RRMS, SPMS and PPMS. In RRMS, it was mostly localized to the deep GM, but less so in the other subgroups. In PPMS only minimal co-localisation of atrophy with MTR reduction was seen, while it was more extensive in the RRMS and SPMS. A previous VBM study of atrophy in the GM of early PPMS patients (within 5 years of symptom onset) demonstrated a shift in the pattern of atrophy as the disease progresses, with deep GM atrophy seen early on and greater involvement of the cortex later (Sepulcre *et al.*, 2006). The present PPMS cohort has a longer disease duration than in that study, and so suggests that this trend to greater cortical involvement continues. In addition, when we consider the RRMS and SPMS subgroups as a single relapse-onset cohort, we see a similar difference in the regional emphasis of atrophy with the longer disease duration SPMS group exhibiting involvement of more cortical areas.

Although significant inflammation is usually seen in cortical demyelinating lesions in early MS, this is usually not so in MS of a longer duration (Bø *et al.*, 2003; Brink *et al.*, 2005; van Horssen *et al.*, 2007). As atrophy may occur secondary to local inflammatory demyelination, our results (minimal co-localisation of MTR reduction and atrophy in the cortex of PPMS, but increasing degrees of co-localisation in RRMS and SPMS respectively) suggest that inflammatory demyelination plays a relatively limited direct role in cortical atrophy and is more likely secondary to the

downstream effects of WM inflammatory pathology without associated demyelination (Geurts and Barkhof, 2008).

These results need to be interpreted with respect to the methodology used. This was a cross-sectional study with a modest sample size, which may affect the generalizability of the findings. The use of FWE (p=0.05) produced results with small effect sizes, and this is likely a reflection of the conservative nature of the VBA analysis (which detects consistent group level changes rather than any voxel that is abnormal in any individual patient). For the MTR analysis a threshold of 90% was used for GM extraction, to limit partial volume effects. However, given that a substantial proportion of cortical GM demyelination occurs in the subpial layers (Kutzelnigg *et al.*, 2005; Magliozzi *et al.*, 2007), this may also have reduced the sensitivity to cortical demyelination. This study also used a tissue segmentation pipeline optimised for MS, with lesion-filling prior to processing by SPM8, and custom built DARTEL templates, which have been shown to reduce artefactual changes in MS studies (Ceccarelli *et al.*, 2012), but may also further reduce effect size. Using an uncorrected statistical threshold (p=0.001), results of the comparisons with controls were broadly consistent with those from the more stringent FWE (p=0.05) analysis, but with greater effect sizes, confirming that the choice of threshold does not substantially alter our main conclusions. Comparison between subgroups without FWE correction also overall agreed with this pattern of results.

Overall, whilst some regionally consistent reductions in MTR and atrophy were seen in GM, this study finds that these mostly do not co-localise. In so far as a reduction in MTR reflects demyelination in GM, and atrophy reflects neuro-axonal loss, these observations suggest that local GM demyelination is most often not associated with co-localised atrophy, and that neuro-axonal loss or atrophy is either mainly the result of an independent process occurring within the affected GM or a remote tract-mediated effect of demyelination elsewhere in the central nervous system. The differing location and extent of regional MTR and volumetric abnormalities in MS subgroups argues against a single mechanism for demyelination and neuronal loss in the GM of MS patients.

3. CUPID MRI SUBSTUDY

3.1 BACKGROUND

Therapies targeting progressive MS and neuroaxonal loss

Progression and accrual of disability is thought to be due mainly to neurodegeneration and axonal loss (Reynolds *et al.*, 2011; Lassmann, Van Horssen and Mahad, 2012), and there have been a number of putative neuroprotective strategies under investigation, specifically targeting the axons (Villoslada, 2016). While a number of potentially neuroprotective therapies have been tested in progressive forms of MS, until recently most had not shown any significant objective evidence of clinically or radiologically slowing progression (Kapoor *et al.*, 2010; La Mantia *et al.*, 2013; Correale *et al.*, 2017). A recent phase IIb trial of high dose Simvastatin (MS-STAT) showed some effect in slowing radiological progression in secondary progressive MS (Chataway *et al.*, 2012), and a larger study (MS-STAT2) is now underway (Chataway, 2017).

Disease modifying drugs (DMD) can reduce the rate of relapse in MS, and potentially slow the rate of disability accrual from relapses. Recently published work has suggested that DMDs can have also an impact on delaying onset of secondary progression in patients with the RRMS (Brown *et al.*, 2019). Recent studies have demonstrated slowing of progression with Ocrelizumab in PPMS (Montalban *et al.*, 2017), and Siponimod in SPMS (Kappos *et al.*, 2018).

Cannabinoids as a potential neuroprotective agent

Cannabinoids are a class of chemicals that act on cannabinoid receptors. There are several types of cannabinoid compound, the most notable of which are Tetrahydrocannabinol (THC), which is known for being the psychoactive component of cannabis, and Cannabidiol (CBD), which is non-psychotropic (Lafaye *et al.*, 2017). The effects of THC are mediated through 2 main receptors: a) CB1, found throughout the CNS, and b) CB2, found mainly on immune cells (Pertwee *et al.*, 2010). Activation of CB1 receptors mainly leads to inhibition of neurotransmitter release. In *in vitro* studies, cannabinoids have been shown to reduce glutamate release and calcium flux, and also have notable anti-oxidant effects. These actions are thought to be of importance for the potential neuroprotective effect of THC, as it has been suggested that excess excitatory neurotransmitter release, increased calcium flux, and free radical damage may have some role in promoting neuronal death (Pertwee *et al.*, 2010). CBD, in contrast, has little affinity for CB1 or CB2 receptors (Zou and Kumar, 2018).Cannabinoids, in the form of Nabiximols (which contains both THC and CBD), have been shown to be useful in the symptomatic management of MS, especially with respect to spasticity (Zajicek *et al.*, 2005). There has also been experimental evidence to suggest that THC, but not whole cannabis extract, may also have an anti-inflammatory, and possibly neuroprotective, effect (Pryce *et al.*, 2003; Zajicek *et al.*, 2005; Zajicek and Apostu, 2011). The CUPID study was thus designed to formally assess whether THC had any effect on clinical or radiological progression in SPMS.

3.2 AIMS

This chapter will report on the MRI substudy results from the CUPID (Cannabinoid Use in Progressive Inflammatory brain Disease) study.(Zajicek *et al.*, 2013) The main study looked mainly at the effects of oral Dronabinol (Δ^9-THC) on clinical markers of disease progression: time to EDSS (Kurtzke, 1983) progression, and change in patient-reported MS impact scale: MSIS-29 (Zajicek *et al.*, 2013). The MRI substudy aimed to examine whether Dronabinol is better than placebo at reducing the rates of new T2w hyperintense lesions, new T1w hypointense lesions, and brain atrophy in patients with progressive MS.

3.3 METHODS

Study Design

The CUPID study was a double-blind, randomised, placebo-controlled, parallel group, multi-centre trial, with patients prospectively enrolled from 27 UK sites (Appendix 12). The MRI substudy was formed from a subset of patients from 13 of the 27 participating sites (Appendix 12).

Duration and Follow Up

Patients were followed up for an initial 3 years (including 1-month titration). Those demonstrating EDSS progression at 3 years, were followed up for an additional 6 months.

Participants

The criteria for inclusion and exclusion are listed in table 3.1 and table 3.2.

Table 3.1: CUPID Inclusion Criteria (all of the following)

1. Primary or secondary progressive MS, according the McDonald 2001 criteria (Mcdonald *et al.*, 2001).
2. Aged 18-65 years.
3. EDSS 4.0 to 6.5 (inclusive)
4. Disease progression in the preceding year, as defined by an increase in physical disability, not due to a major relapse.
5. Willing and able to comply with study visits according to protocol for the full study period.
6. Willing to abstain from cannabis use (excluding study medication) for three years.

Table 3.2: CUPID Exclusion Criteria (one or more)

1. Any immunosuppressive or immunomodulatory therapy received in the previous 12 months.
2. Corticosteroids in the previous 3 months.
3. Significant MS relapse, likely to have had an effect on EDSS, occurring in the previous 6 months.
4. Predominantly relapsing-remitting disease over the previous 12 months.
5. Other serious illness or medical condition likely to interfere with study assessment, including ischaemic heart disease, neoplasia or evidence of chronic infection from any source, including pressure sores.
6. Previous history of psychotic illness.
7. Severe cognitive impairment such that the patient is unable to provide informed consent.
8. Pregnant or breast-feeding women, or patient/partner planning a pregnancy within the next 3 years.
9. Cannabinoids taken in previous four weeks.
10. Serum creatinine, ALT or bilirubin 2.6 times upper limit of normal.
11. Participation in another investigational medicinal product study within the last three months.
12. Any other factor that might interfere with long-term study compliance in the opinion of the local research team.
13. Any factor contraindicated for MRI, e.g. cardiac pacemaker, metallic implants, claustrophobia or movement disorder sufficient to prevent high quality imaging.

Randomisation

After eligibility was confirmed and informed consent signed, patients were allocated a unique study number by the central trial coordinator. A computer-based randomisation procedure was used to assign participants into either active or placebo groups in a 2:1 ratio, balanced according to EDSS, centre, and disease type by minimisation. This was carried out by the pharmacy coordinator, at a separate site to the coordinating centre, to maintain blinding amongst the trial coordinating team.

Drug administration details

Medication was prescribed by investigators, with an initial 1-month titration phase, relative to body weight and adverse effects. Dronabinol was prescribed in the form of 3.5mg capsules. Patients were advised to increase their dose by one capsule twice daily at weekly intervals during the four-week titration period up to a maximum weight-related dose. The maximum dose was 28mg per day.

MRI protocol

Patients participating in the MRI substudy had MRI scans at 4 timepoints:

- Baseline (BL)
- End of Year 1 (Yr1)
- End of Year 2 (Yr2)
- End of Year 3 (Yr3)

The baseline scans were performed after the screening visit, and prior to the prescription of medication. All participating sites were required to perform a pre-enrolment qualifying scan, prior to starting patient recruitment.

MRI sequences included axial dual echo, fast (turbo) spin echo (FSE/TSE) proton density and T2w scans, as well as a conventional T1w spin echo (SE) scan. Images were orientated in a plane parallel to a line connecting the anterior and posterior commissures in a similar axial plane. 46 contiguous 3mm thick axial slices were performed for each acquisition. Scans underwent local radiology review and reporting in accordance with local departmental policy. Image data was archived to disk and sent for processing to the NMR Research Unit Trials Centre at the Institute of Neurology, UCL (University College London). Individual sites retained hard copies of each scan, stored according to local policy.

<u>New T2w lesions and T1w Black holes</u>

Image analysis was carried out using JIM 6.0 software (Xinapse Systems, UK; http://www.xinapse.com) on a SUN workstation running CentOS operating system. Scans from each time point were compared with the immediate preceding scan.

New T2w lesions and new T1w hypointense lesions were marked by me using the semi-automated regions of interest (ROI) marking tool. ROI markings for 20 scans were assessed and compared visually by Dr Catherine Dalton (CD) and Dr Daniel

Tozer (DT). If a scan had been missed at a certain timepoint, comparison was made with the last scanned timepoint.

Normalised brain volume (NBV) at Baseline using SIENAX

Brain tissue volume, normalised for patient head size, was estimated with SIENAX (Smith *et al.*, 2001, 2002), part of FSL (Smith *et al.*, 2004). SIENAX utilises the brain extraction tool (BET) to extract brain and skull images from the single whole-head input data (Smith, 2002). The outputs of the BET were reviewed visually by myself and CD, and manually edited using Jim 6.0 to further remove non-brain tissue (such as eyes and optic nerve). A co-efficient of variation was calculated to be 0.24% between the 2 assessors using an initial 20 BET outputs.

Percentage brain volume change (PBVC) using SIENA

Two-timepoint percentage brain volume change (PBCV) was estimated with SIENA (Smith *et al.*, 2001, 2002), part of FSL (Smith *et al.*, 2004). PBVC is a measure for rate of brain atrophy. Using this method, we calculated the PBVC from 3 separate "timepoint-pairs":

- Baseline to Year 1 (BL-Yr1)
- Year 1 to Year 2 (Yr1-Yr2)
- Year 2 to Year 3 (Yr2-Yr3)

Any individual cases where PBVC was more than +/- 1.96 standard deviations from the mean were considered outliers and examined specifically to determine their

inclusion in statistical calculations. This included visual assessment by myself and CD, and discussion with DT and Prof David H Miller (DHM) about their inclusion.

Statistical analysis (including dealing with early withdrawals and missing data)

Statistical Analysis was performed by Susan Ball (Peninsula Clinical Trials Unit, Plymouth University Peninsula Schools of Medicine and Dentistry, Plymouth, UK). A multi-level model was used to analyse PBVC (transformed to cumulative and relative PBCV on the $\log_{10}$ scale). Logistic Regression models were used to examine the effect of treatment on new T1w hypointense lesions, and new or enlarging T2w hyperintense lesions during follow-up. Final models were identified using a forward selection procedure, and included main effects and interactions significant at the 5% level, as well as the main effect of treatment.

3.4 RESULTS

Patients

In total, 273 patients were enrolled in the MRI substudy, from 13 of the 27 participating centres (Table 3.3). Of these, 182 (67%) were on active treatment, and 91 (33%) on placebo. Of these, 45 patients missed one or more scans (see table 2.4).

Table 3.3: Baseline characteristics of patients in CUPID MRI substudy			
	Active (N=182)	Placebo (N=91)	All (N=273)
Age in years at registration, mean (SD)	52.4 (7.3)	52.2 (8.1)	52.3 (7.6)
Men, n (%)	80 (44.0)	31 (34.1)	111 (40.7)
Women, n (%)	102 (56.0)	60 (65.9)	162 (59.3)
PPMS, n (%)	60 (33.0)	38 (41.8)	98 (35.9)
SPMS, n (%)	122 (67.0)	53 (58.2)	175 (64.1)
Baseline mean EDSS	6.0	6.0	6.0

Table 3.4: CUPID Missing scan points					
Missed Scans	Year1 Year 2 Year 3	 Year 2 Year 3	 Year 3	Year 1 Year 3	Year 1 Year 2
Number	25	9	9	1	1

Data was excluded from further analysis if there were missing critical data points, or if there was significant cause for concern that the data was either unreliable (e.g. due to scanner changes), or was uncharacteristically different from other participant data; including an exaggerated result, even if true, might skew the analysis away from a true representation of mean change within the whole group.

Those that only had the baseline scan were excluded from all further analyses. 32 patients were also excluded from the PBVC analysis (24 active, 8 placebo) as they had no NBV measurement at baseline, precluding any calculation of PBVC. There were 30 outliers according to the +/- 1.96 SD criteria (see above). From the 30 outliers, 13 were due to scanner changes between timepoints, so were excluded. 1 was included because there did appear to be true dramatic ventricular and cortical atrophy. 1 was excluded because new periventricular lesions were included in SIENA CSF mask (aberrant segmentation). Thus from the 30 outliers, there were 29 timepoint exclusions. In addition, 24 patients without outlying results also had a scanner change between timepoints, and the relevant timepoints were excluded.

Figures 3.1 and 3.2 show the patient's flow-charts through the MRI substudy.

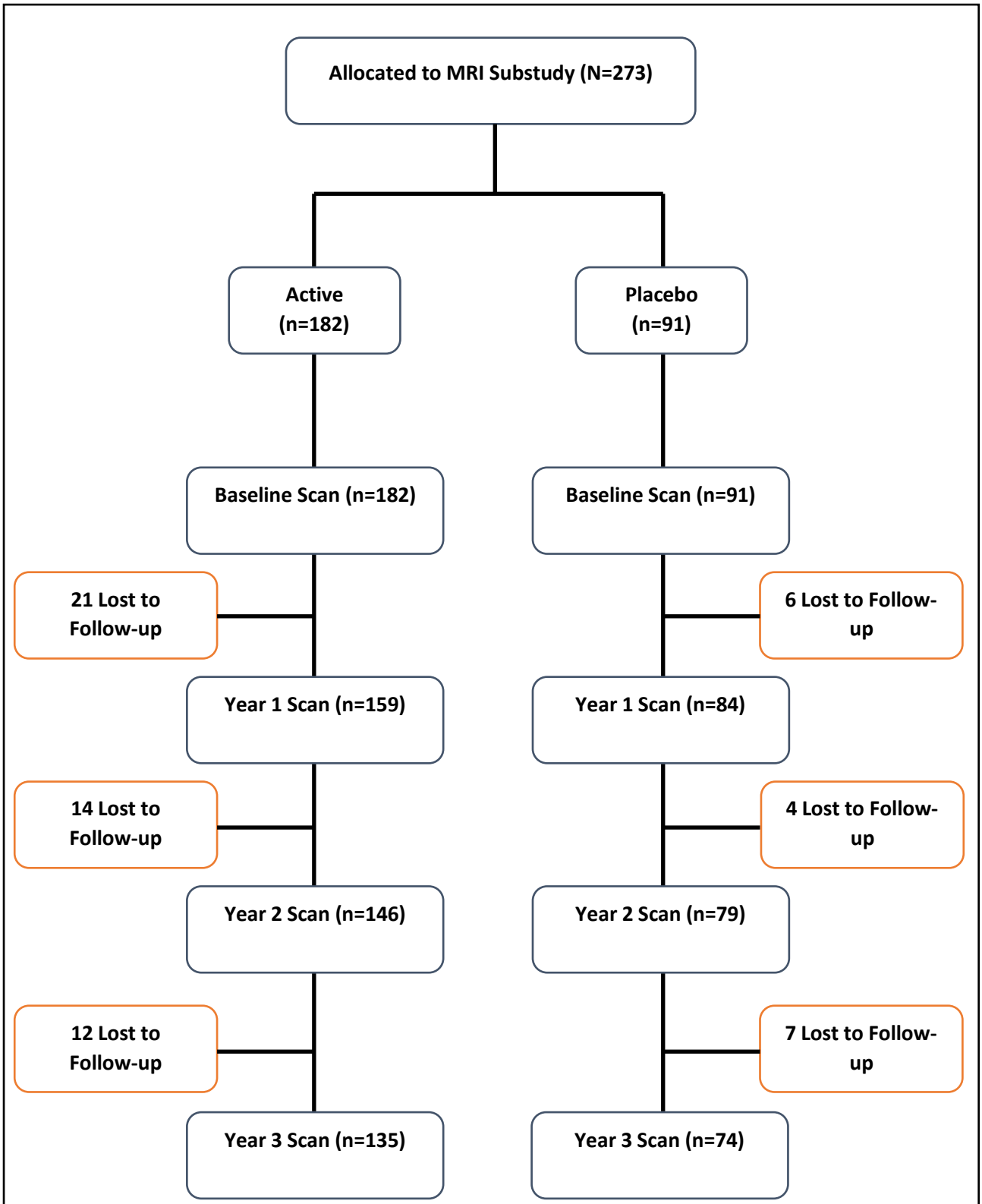

Figure 3.1: Flow-chart of participants through the CUPID MRI substudy

Figure 3.2: Flow-chart of participants for NBV (Normalised Brain Volume) and PBVC (Percentage Brain Volume Change) analysis

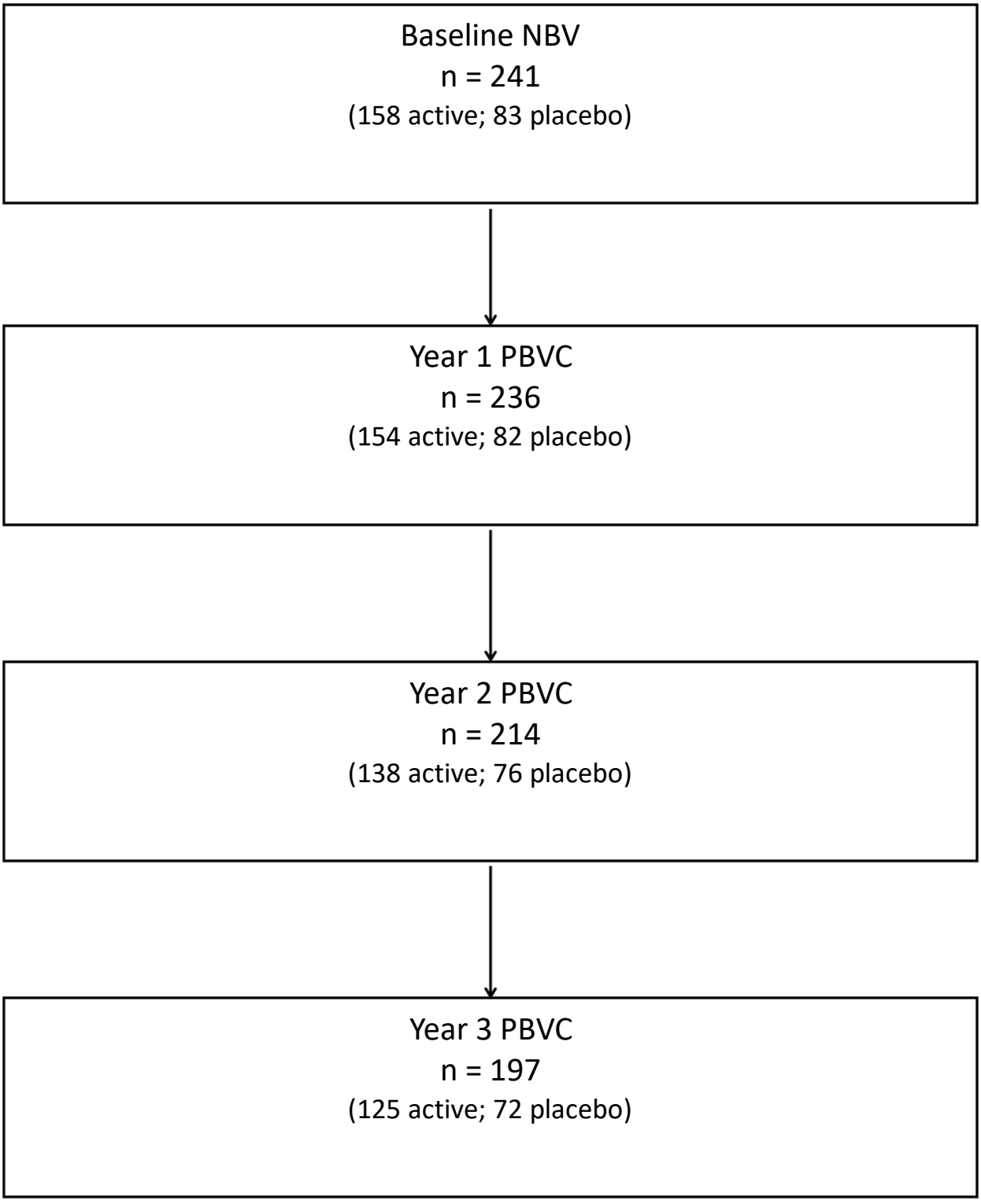

Baseline NBV

Table 3.5 summarises the baseline NBV results. The mean NBV was 1420 ml overall. A t-test comparing mean NBV across both groups demonstrated no significant difference between active and placebo.

Table 3.5: Normalised Brain Volume (ml) at Baseline

Group	Number	Missing/Excluded	Min	Max	Mean	SD	P value
Active	158	24	1153	1634	1422	91.05	0.70
Placebo	83	8	1176	1582	1417	85.14	
Total	241	32	1153	1634	1420	88.91	

PBVC (Yearly)

Table 3.6 summarises the yearly PBVC. There was no significant difference in mean PBVC between active and placebo arms, using two-sample t-test. The mean annual change was -0.68 (SD 0.95) in the active group, and -0.66 (SD 0.98) in the placebo group; estimated treatment effect -0.01, 95% CI -0.26-0.24; p=0.94.

Table 3.6: Yearly Percentage Brain Volume Change (%)

Year	Group	No.	Missing/Excluded	Min	Max	Mean	SD	P value
BL-Yr1	Active	154	28	-2.60	2.22	-0.59	0.95	0.93
	Placebo	82	9	-2.96	1.26	-0.60	0.95	
Yr1-Yr2	Active	138	44	-2.78	2.21	-0.61	0.91	0.98
	Placebo	76	15	-2.69	2.24	-0.65	0.95	
Yr2-Yr3	Active	125	57	-2.93	1.83	-0.89	0.87	0.53
	Placebo	72	19	-2.79	2.53	-0.76	1.04	

PBVC (Cumulative)

Figure 3.3 summarises the cumulative relative PBVC (%). There was no significant difference in PBVC between groups (two-sample t-test).

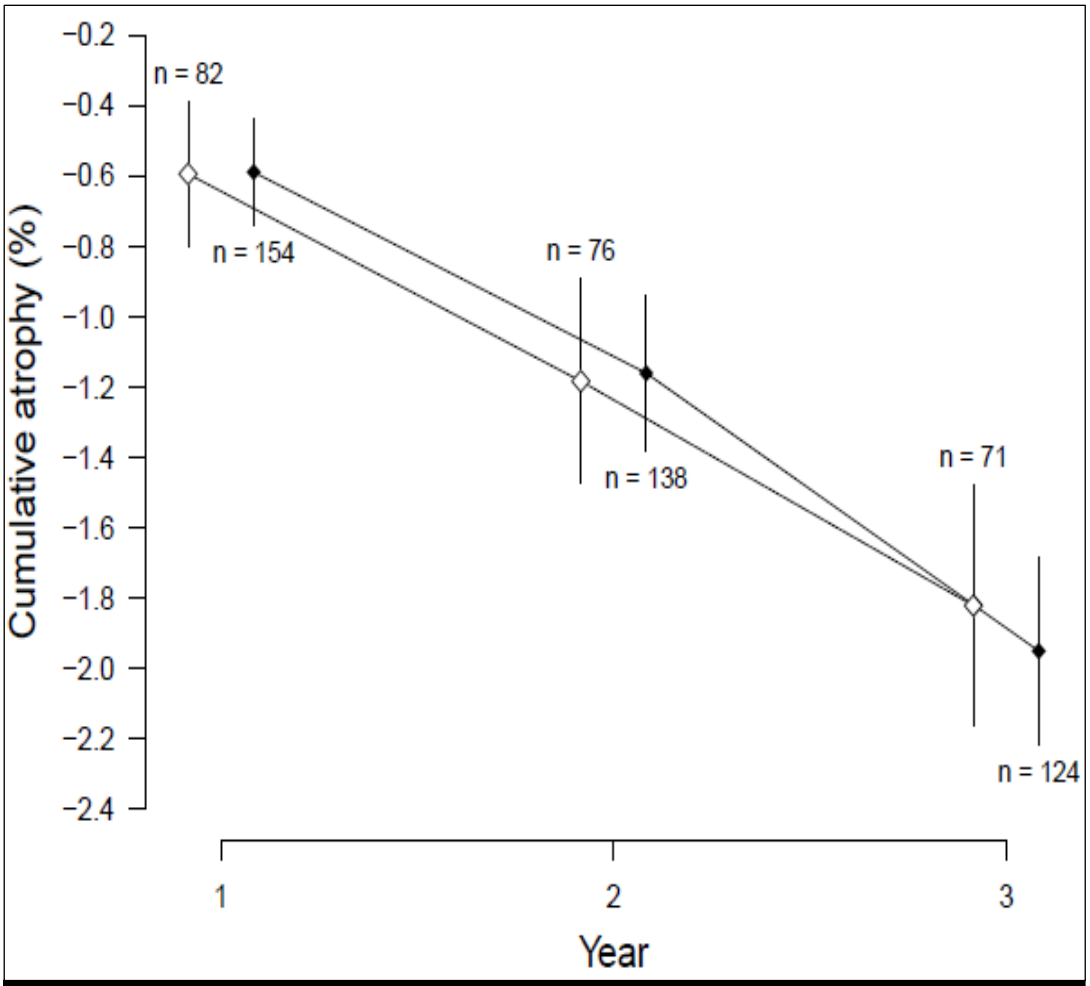

Figure 3.3: Estimated mean cumulative PBVC (%) and 95% CI, by treatment group, measured at yearly MRI visits; Black diamonds, active treatment; White diamonds, placebo. n=number of patients with cumulative PBVC calculated at each visit.

New or enlarging T2w Hyperintense Lesions

Over the course of the entire study, the occurrence of new or enlarging T2 hyperintense lesions was not affected by Dronabinol; estimated Odds Ratio (OR)

1.05, 95% CI 0.59-1.88; p=0.87. Table 3.7 further compares groups by number of new lesions at different timepoints.

Table 3.7: New or newly enlarging T2w hyperintense lesions, n (%); p-value calculated using Fisher's exact test.

	Year 1		Year 2		Year 3	
New Lesions	Active	Placebo	Active	Placebo	Active	Placebo
0	118 (74.2)	56 (66.7)	111 (76.0)	71 (89.9)	113 (83.7)	61 (82.4)
1	20 (12.6)	15 (17.9)	23 (15.8)	5 (6.3)	16 (11.9)	9 (12.2)
≥ 2	21 (13.2)	13 (15.5)	12 (8.2)	3 (3.8)	6 (4.4)	4 (5.4)
p-value	0.40		0.05		0.96	

New or Enlarging T1w Hypointense Lesions

Treatment with Dronabinol did not lead to a significant difference in the likelihood of developing new or enlarging T1w hypointensities over the course of the entire study, compared to placebo; estimated Odds Ratio 0.89, 95% CI 0.50-1.58; p=0.70. A further breakdown by number of lesions at each of the timepoints is shown in Table 3.8.

Table 3.8: New or newly enlarging T1w hypointense lesions, n (%); p-value calculated using Fisher's exact test.

	Year 1		Year 2		Year 3	
New Lesions	Active	Placebo	Active	Placebo	Active	Placebo
0	123 (77.4)	64 (76.2)	122 (83.6)	74 (93.7)	118 (87.4)	62 (83.8)
1	20 (12.6)	12 (14.3)	16 (11.0)	3 (3.8)	13 (9.6)	10 (13.5)
≥ 2	16 (10.1)	8 (9.5)	8 (5.5)	2 (2.5)	4 (3.0)	2 (2.7)
p-value	0.90		0.10		0.70	

3.5 DISCUSSION

As with the main clinical outcomes of the larger CUPID study (Zajicek *et al.*, 2013), the MRI substudy suggested that Dronabinol was no better than placebo at reducing the number of new T1w or T2w lesions or brain atrophy in patients with progressive MS. The evident conclusion from the CUPID trial would be that that Dronabinol has no demonstrable role in reducing radiological (or clinical, as derived from the main study) progression in MS. However, methodological issues may also have affected the study's ability to detect a true treatment effect.

Generally, MRI measures have utility above and beyond the use of clinical end-points alone, as they may provide *in vivo* evidence of disease progression, which may not be significant enough to manifest clinically in the time-period being examined. That is, they are potentially sensitive to smaller treatment effects, and can thus be performed on a smaller sample size. For example, in the CUPID study, sample size calculations for the clinical arm were calculated at 492 patients, using a power in excess of 90%, to detect a difference of 7 points in the MSIS-29 measure, based on previous SD calculations from initial data from 210 patients (Zajicek *et al.*, 2013). For the MRI arm, allowing for a 5% annual loss to follow-up rate, it was estimated that 261 patients allocated to active treatment and placebo in a 2:1 ratio would give 90% power to detect 40% slowing in atrophy rate, with scans performed pre-treatment, and at years 1, 2 and 3.

As a contrast to the 273 participants in this MRI substudy (and 493 in the main study), the ORATORIO study (Ocrelizumab) included 732 patients (Montalban *et al.*,

2017), the ASCEND study (Natalizumab) included 889 patients (Kapoor *et al.*, 2018), and the EXPAND study (Siponimod) included 1651 patients (Kappos *et al.*, 2018).

It is also possible that the potential to detect a genuine treatment effect might have been reduced in this work by the rates of loss to follow-up, as well as loss of data points due to technical issues and missed scans.

It is also not known whether Dronabinol, if given while patients had not yet developed evidence of secondary progression, might perhaps demonstrate some effect in delaying the onset of progressive disease (Cerqueira *et al.*, 2018). In RRMS, CNS inflammatory/demyelinating lesion formation exceeds neuro-axonal loss and atrophy, but the longer the disease progresses, the greater the amount of neurodegeneration and atrophy seen (Chard *et al.*, 2003). The preceding chapter (voxel-based analysis) examined some of these relationships in the GM between atrophy and demyelination of the various MS subtypes, and suggested that the two processes are probably not linked in the GM. Overall, it is still unclear whether atrophy and demyelination represent unrelated pathophysiological processes, or whether they are somehow linked by as yet unknown factors.

However, while the exact pathophysiological mechanisms underlying secondary progression is not clear, it likely suggests a change in the balance between inflammatory activity and neurodegeneration, with the latter showing a significant increase, relative to the former, with the onset of progression.

Another point to note is that the cohort studied in CUPID had significant disability from the outset (mean EDSS 6.0), and higher EDSS scores have been shown to be associated with greater neuronal loss and atrophy (Ge *et al.*, 2000; Popescu *et al.*, 2013). It could thus be argued that such patients may not show as much potential for demonstrating a true neuroprotective effect (due to both relative biological insensitivity, as well as relative measurement insensitivity), whilst specifically selecting patients with less pre-existing disability, and therefore, less underlying neuronal loss and atrophy, might be preferable in further similar studies of putative neuroprotective agents, thereby giving said agents the best chance to demonstrate any true protective effect.

4. INDIVIDUAL LESION MTR – MSCIMS SUBSTUDY

4.1 BACKGROUND

Stem Cells as a therapeutic option in MS

Stem cells are progenitor cells capable of asymmetric division, allowing production of specialised cell progeny, their "potency" being determined by the number of types of specialised progeny they are able to produce.

Haematopoietic stem cells are multipotent stem cells, derived from the bone marrow, and have been studied for many years as a possible therapeutic option in MS. Autologous Haematopoeitic Stem Cell Transplant (AHSCT) utilizes chemotherapy (either myeloablative or non-myeloablative) to remove causative immune cells from a person's body, and repopulates the immune system with haematopoietic stem cells previously derived and cultured from the patient's bone marrow. It offers the potential of immune system "reset", and has been demonstrated to result in significant and prolonged cessation of CNS inflammatory activity (Atkins *et al.*, 2016), as well as having an effectiveness in reducing relapses (Burt *et al.*, 2018), managing fatigue symptoms (Bose *et al.*, 2018), and possibly improving previously impaired neurological function (Nash *et al.*, 2015).

AHSCT however carries a significant potential side effect profile, including an increased risk of infection, autoimmune disease, and malignancy, and has an up to

2% chance of death. At present, in the UK at least, it is recommended for patients with active disease, and treatment failure on two prior DMDs (with at least one having been a "highly effective" DMD such as Natalizumab or Alemtuzumab). Although progressive patients, and patients with long-standing MS might be considered to AHSCT, in practice patients with RRMS and shorter disease durations are often more likely to be eligible.

Mesenchymal Stem Cells as a potentially Remyelinating or Reparative therapy in MS

Mesenchymal stem cells (MSC) are multipotent non-haematopoietic stromal cells that reside in adult bone marrow, and have the ability to self-renew, and differentiate into tissues of mesodermal origin. MSCs can be expanded *ex-vivo* with minimal manipulation, and this, in concert with their noted immunomodulatory effects, has made them a potential candidate for use in regenerative medicine, and in the treatment of autoimmune disease.

MSCs infused intravenously in experimental autoimmune encephalomyelitis (EAE), an experimental model of MS, ameliorated EAE, and reduced infiltration of the CNS by T cells, B cells and macrophages (Zappia *et al.*, 2005), and reduced demyelination, and axonal loss (Gerdoni *et al.*, 2007). MSCs are thought to exert their therapeutic activity on the inflamed CNS through the peripheral control of immune cells, and a protective effect *in situ* (Uccelli *et al.*, 2007), as well as

promoting endogenous repair by recruiting local neural precursor cells, thus fostering endogenous neurogenesis and remyelination (Bai *et al.*, 2009).

Autologous MSC (AMSC) from MS patients exhibit the same properties as those derived from healthy donors with regard to phenotype, proliferation, in vitro differentiation, and immunosuppressive ability (Mazzanti *et al.*, 2008; Mallam *et al.*, 2010). AMSC have been used in a number of patients with no reports of significant complications such as induction of immunodeficiency, or other associated complications of infection and malignancy.

Prior Studies of AMSC in MS

A small study with 10 patients demonstrated the feasibility of AMSC as an intervention, and reported no significant adverse events (Mohyeddin Bonab *et al.*, 2007). The Mesenchymal Stem Cells in Multiple Sclerosis (MSCIMS) study (Connick *et al.*, 2012), was a phase IIa proof-of-concept study in which 10 patients with secondary progressive MS and visual pathway involvement received (AMSC). This study mainly looked at a number of clinical (visual and physical) markers of disease activity in response to intervention, and demonstrated significant improvement in visual acuity, Visual Evoked Potential (VEP) latency, and optic nerve area. It also looked at mean, patient-level lesional MTR change as a whole, pre- and post-treatment, in addition to other radiological markers such as brain atrophy and lesion volume. There was not noted to be a significant change in lesional MTR with

this technique, or with the other radiological measures. A randomised, double-blind, placebo-controlled trial, utilizing a cross-over design in 9 patients detected a (non-statistically significant) trend to lower mean cumulative number of enhancing GELs in those treated with AMSC, with no serious adverse events (Llufriu *et al.*, 2014).

Rationale for Individual Lesion MTR approach

As noted in the previous chapter, conventional MR imaging methods, such as T2w sequences, are very sensitive for the detection of the WM lesions of MS, but are unable to differentiate between demyelination, axonal loss, gliosis, inflammation, and oedema. A number of imaging methods are more specific for myelin in vivo, and of these, MT imaging is arguably the most promising, as it is relatively straightforward to acquire, calculate and interpret, and acquisition times are short enough to be practical for use in clinical trials of potentially remyelination agents (see chapter on imaging remyelination for further details).

A number of studies have utilised MTR as an outcome measure, and there are a number of different ways of analysing this metric, including histogram, region-of-interest, and voxel-based measurements. More novel ways of utilising MTR data have also recently been described.

A commonly used technique in MS clinical trials has been the use of region-of-interest measurements to follow the mean lesional MTR values per patient per time-point over the course of the study. This is useful to give an indication of how, on average, the myelination of lesions changes over time, and in response to an intervention. This is the method used in MSCIMS study (Connick *et al.*, 2012), which did not detect any significant change in lesional MTR.

However, it is known that not all MS lesions within the same patient necessarily demyelinate, or indeed remyelinate, to the same extent, and mean lesional methods of MTR analysis may not be able to detect more subtle changes occurring with individual lesions, or groups or lesions, at each time point. A more sensitive indicator myelination over time would be to attempt to track individual lesions for their MTR change over time.

4.2 AIMS

I aimed to develop a lesion analysis pathway allowing MTR values of individual lesions to be measured serially over multiple time-points, and investigate the potential of serial individual lesion area MTR measurement to serve as a sensitive indicator of myelination before and after a treatment intervention, and, secondarily, before and after lesion appearance.

4.3 METHODS

This is a *post-hoc* analysis of the MT data acquired from the MSCIMS study (Connick *et al.*, 2012).

Study Design

The study was designed with a 6-month pre-treatment phase, and a 6-month post-treatment phase. During the course of the study, patients had 3 MR scans pre-treatment: 6 months before (baseline), 3 months before (-3m), 0 months (0m); and 2 scans post-treatment: 3 months after (+3m), and 6 months after (+6m).

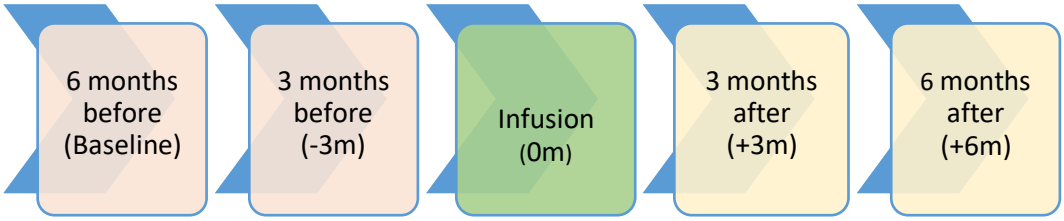

Figure 4.1: MSCIMS MRI timepoints

MR Image Acquisition

MR images were acquired with a Magnetom 3·0 T Tim Trio scanner (Siemens, Erlangen, Germany) with a 12-element receiver head coil, and included Proton Density T2-weighted (PDT2w) images, T1w Spin Echo (SE), and whole brain MT sequences.

PDT2w:

Axial PDT2w Dual Echo, Turbo Spin Echo imaging was acquired on all patients: Axial, TR: 3 Seconds; TE 1 and 2: 11ms and 101ms; Matrix: 192 x 256; field of view: 24cm x 18cm; flip angle: 150; In plane resolution 0.9mm x 0.9mm; 48 x 3mm contiguous slices for each echo, to give 96 slices in total.

T1w Spin Echo:

T1w Spin Echo images were acquired on all patients: Axial, TR: 710ms; TE: 8.5ms, 2 averages; Matrix: 233 x 256; field of view: 22cm x 22cm; In plane resolution: 0.9mm x 0.9mm, 48 x 3mm slices.

Magnetisation Transfer (MT):

3D Gradient Echo was used to acquire 2 sets of images, with and without MT pulse ("MT-on" and "MT-off"): Coronal 3D, TR: 26ms; TE: 3.0ms, flip angle: 10; Matrix: 256 x 160; field of view: 26cm x 16.25cm; In plane resolution 0.7 x 0.7mm; 208 x 1.0mm contiguous slices.

Image Processing

Lesion Marking

The Irregular ROI feature of Jim 6.0 (Xinapse Systems, UK, http://www.xinapse.com) was used to mark lesions appearing on the baseline (6 months pre-treatment) PDT2w and T1w scans ("baseline lesions"), as well as new lesions appearing at each subsequent time point on the PDT2w scans ("new lesions"). Lesions were marked and saved as region-of-interest (ROI) files by myself. Quality Assurance (QA) for an initial group of patient's scans was undertaken by visual inspection with David H. Miller (DHM), and any discrepancies were discussed, and any necessary amendments were made.

Image Registration

NiftyReg (Modat, 2010) was used to create a "PDT2w-average" space (averaged across all timepoints) for each patient, and register, scans from each PDT2w, T1w and MT-on, and MT-off timepoint to that space. Registrations were visually checked by myself, DT and DHM.

MT Ratio (MTR) Map

MTR maps, measured in percentage units (pcu), were created using the registered MT-on and MT-off images, using the formula [MTR = (MToff – MTon) / MToff].

Lesion Mask MTR calculation

Baseline and new lesion ROI files were converted to lesion masks using JIM 6.0. These lesion masks were then registered using NiftyReg to the PDT2w-average space. The registered lesion masks were split such that each lesion area, per MRI slice, was saved as a separate image mask file. Fslmaths (Jenkinson *et al.*, 2012) was used to mask each MTR map file with the individual lesion area masks, and calculate the MTR value for that lesion area.

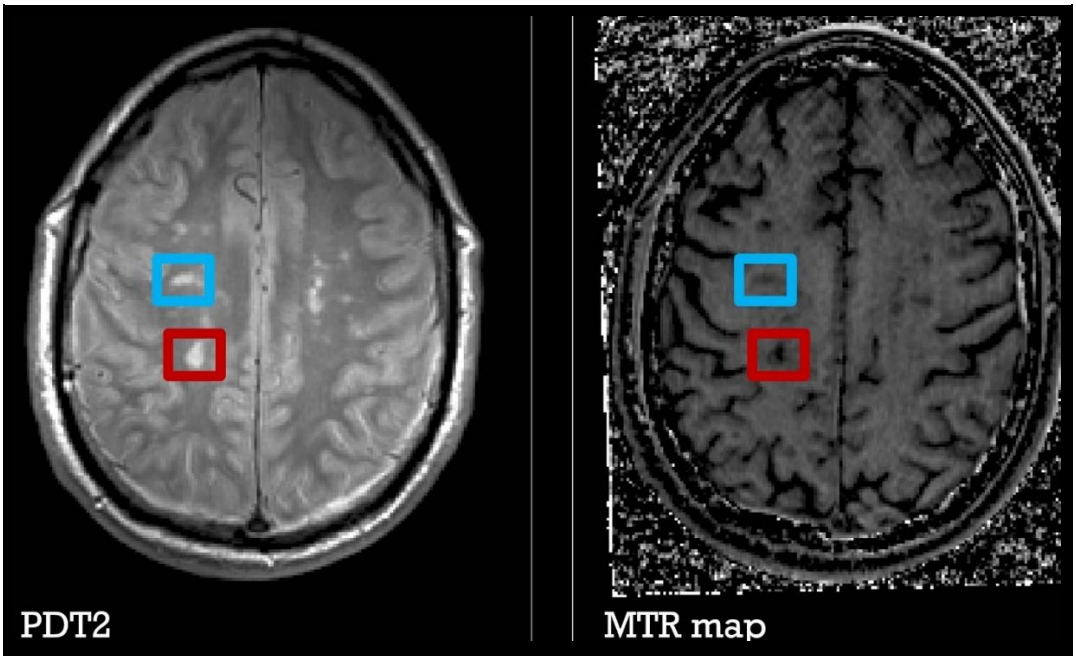

Figure 4.2: Registered Axial a) PDT2w and b) MTR map slices from the same patient at the same timepoint. Coloured squares demonstrate the appearance of the lesions in both images.

Individual Lesion Area MTR forward and backward tracking

- Baseline lesions: The individual baseline PDT2w and T1w lesion area maps were used to follow the baseline lesion area MTR over the time course of the study, effectively allowing us to see how pre-existing or "chronic" lesions changed over time, and in response to the intervention.

- New Lesions: For new lesions appearing subsequent to baseline ("acute" lesions), individual new PDT2w lesion area maps were used to track backwards, as well as forwards, in time, which allowed MTR to be measured pre- and post-lesion appearance, as well as pre- and post-intervention.

Statistical Analysis

Statistical analysis was performed by Dr Daniel Altmann. Piecewise linear mixed models were used, with fixed effects for patient and random lesion intercepts on time, to model the MTR gradients of individual lesions, before and after infusion, and before and after lesion appearance; a similar model was used in the previous analysis of per-patient (average lesional MTR) level gradients.

4.4 RESULTS

Patients

In total 10 patients with SPMS and optic nerve disease were included in this study. Table 4.1 shows the baseline characteristics of each of the patients.

Table 4.1: MSCIMS Patient characteristics at baseline

	Gender	Age (years)	Duration (years)	EDSS
Patient 1	M	44	19	6.5
Patient 2	M	51	26	6.0
Patient 3	F	40	9	6.5
Patient 4	M	48	14	6.0
Patient 5	M	48	11	6.5
Patient 6	M	52	18	6.0
Patient 7	F	54	8	6.5
Patient 8	M	41	6	5.5
Patient 9	F	46	11	6.5
Patient 10	M	50	6	6.5

EDSS: Expanded Disability Status Scale

In all, there were 7 males, and 3 females. The mean age was 47.4 years, with a mean MS duration of 12.8 years (range 6 to 26 years). The median EDSS at baseline was 6.5 (range 5.5 to 6.5, only 1 of the 10 patients had an EDSS score of less than 6.0).

Baseline Lesion Areas

Table 4.2 summarises the number of PDT2w and T1w lesion areas present at baseline.

It is important to note that these are not the same as “lesions”, as the technique used in this study separated lesions spanning multiple contiguous slices into separate lesion areas. For instance, if a lesion was spread over 3 slices, this would lead to the creation to 3 separate lesion areas.

The mean number of baseline PDT2w lesion areas per patient was 253.6 (range 80 – 400). The mean number of baseline T1w lesions areas per patient was 65.1 (range 0 – 151). Medians were very similar to means, suggesting that spread was according to a normal distribution.

Table 4.2: MSCIMS Baseline Lesion Areas		
	PDT2w	**T1w**
Patient 1	328	95
Patient 2	255	151
Patient 3	177	68
Patient 4	240	14
Patient 5	80	0
Patient 6	210	23
Patient 7	212	81
Patient 8	373	60
Patient 9	400	96
Patient 10	261	63
Total	2563	651
Mean (SD)	**253.6 (94.9)**	**65.1 (44.9)**
Median	247.5	65.5

The original MSCIMS study utilised per-patient mean lesional MTR values, shown as percentage units (pcu), and these are shown in Table 4.3 and Table 4.4 (Connick *et al.*, 2012), prior to demonstrating the individual lesion area results.

Table 4.3: Per-Patient Mean Lesional MTR (pcu)		
	PDT2w	**T1w**
Mean Lesional MTR (SD)	32.566 (7.13)	24.187 (7.487)
Range	21.5 – 43.64	17.26 – 35.15

Table 4.4: Per-Patient Mean Lesional MTR gradients, before and after treatment (pcu/month)		
	PDT2w	**T1w**
Before Treatment	-0.174	-0.187
After Treatment	+0.386	+0.579
Change in Gradient	**+0.560**	**+0.766**
95% CI	-0.270 to +1.390	-0.139 to +1.671
p value	**0.186**	**0.097**
CI = Confidence Interval		

Using the individual lesion area technique, MTR values (pcu) of each of the lesion areas present at baseline (both PDT2w and T1w) were followed over time, and the mean gradient (rate of change) before and after treatment was calculated, and these are shown in Table 4.5.

Table 4.5: Individual Lesional MTR rates of change, before and after treatment (pcu/month)			
		PDT2w	**T1w**
Before Treatment	Mean Gradient	-0.053	-0.063
	95% CI	-0.064 to -0.041	-0.087 to -0.039
	p value	0.001	0.001
After Treatment	Mean Gradient	+0.045	-0.017
	95% CI	+0.026 to +0.065	-0.061 to +0.026
	p value	0.001	0.437
Change in Gradient		**+0.098**	**+0.046**
95% CI		+0.072 to +0.124	+0.011 to +0.103
p value		**0.001**	**0.112**
CI = Confidence Interval			

In summary, PDT2w lesion areas present at baseline, with the suggestion that these may represent old or “chronic” lesions, demonstrated a significant change in MTR gradient after treatment with mesenchymal stem cells. There was noted to be a mean MTR gradient change of +0.098 pcu/month (95% CI +0.072 to +0.124) associated with the intervention (p=0.001). Significant difference was not seen with old or “chronic” T1w lesion areas at baseline, with mean MTR gradient change approximately 50% of the magnitude of the PDT2w baseline lesion areas (+0.046 pcu/month; p=0.112).

New Lesion Areas

4 patients developed new PDT2w lesions after the baseline scan. The corresponding lesion areas were examined for their serial MTR, and comparison was made between mean gradient before and after infusion, as well as before and after lesion appearance (with some modification for lesions appearing at the final timepoint, as discussed below). The number of new lesion areas at each timepoint after baseline are summarised in table 4.6.

Table 4.6: New PDT2 lesion areas in 4 patients

	-3 months	0 months	+3 months	+6 months
Total New lesion areas	24	15	2	7
Mean (per patient)	6	3.75	0.5	1.75

In these patients, there were a total of 39 new lesion areas prior to treatment (-3 months and 0 months), and 9 new lesion areas after treatment (+3 months and +6 months); p=0.04 (1 tailed, paired student t-test). There were no new T1w lesions appearing at subsequent timepoints after baseline for any of the patients in the analysis. Tables 4.7 to 4.10 summarise the findings.

Table 4.7: New PDT2w Lesions at -3 months, MTR rates of change (pcu/month)		
Before Treatment	Mean Gradient	-0.043
	95% CI	-0.183 to +0.097
	p value	0.547
After Treatment	Mean Gradient	+0.107
	95% CI	0.148 to +0.363
	p value	0.410
Change in Gradient		**+0.151**
	95% CI	-0.179 to +0.480
	p value	**0.370**
Before Lesion Appearance	Mean Gradient	-0.454
	95% CI	1.076 to +0.169
	p value	0.153
After Lesion Appearance	Mean Gradient	+0.067
	95% CI	0.071 to +0.203
	p value	0.95
Change in Gradient		**+0.520**
	95% CI	-0.183 to +1.223
	p value	**0.147**
CI = Confidence Interval		

Table 4.8: New PDT2w Lesions at 0 months, MTR rates of change (pcu/month)		
Before Lesion Appearance	Mean Gradient	-0.842
	95% CI	-1.087 to -0.596
	p value	p=0.001
After Lesion Appearance	Mean Gradient	+0.191
	95% CI	-0.013 to +0.395
	p value	p=0.066
Change in Gradient		**+1.033**
95% CI		+0.676 to +1.389
p value		**0.001**
CI = Confidence Interval		

Table 4.9: New PDT2w Lesions at +3 months, MTR rates of change (pcu/month)		
Before Treatment	Mean Gradient	-0.216
	95% CI	-0.768 to +0.336
	p value	p=0.443
After Treatment	Mean Gradient	-0.795
	95% CI	-1.478 to -0.113
	p value	p=0.022
Change in Gradient		**-0.579**
	95% CI	-1.361 to +0.202
	p value	**0.146**
Before Lesion Appearance	Mean Gradient	-0.455
	95% CI	-0.934 to +0.024
	p value	0.063
After Lesion Appearance	Mean Gradient	-0.220
	95% CI	-1.804 to +1.364
	p value	0.785
Change in Gradient		**+0.520**
	95% CI	-1.494 to +1.964
	p value	**0.790**
CI = Confidence Interval		

Table 4.10: New PDT2w Lesions at +6 months, MTR rates of change (pcu/month)		
Before Treatment	Mean Gradient	+0.058
	95% CI	-0.150 to +0.267
	p value	p=0.584
After Treatment	Mean Gradient	-0.477
	95% CI	-0.803 to -0.151
	p value	0.004
Change in Gradient		**-0.535**
	95% CI	-0.961 to -0.109
	p value	**0.014**
Before +3 months	Mean Gradient	+0.062
	95% CI	-0.101 to +0.226
	p value	0.456
After + 3 months	Mean Gradient	-1.447
	95% CI	-2.032 to -0.861
	p value	0.001
Change in Gradient		**-1.509**
	95% CI	-2.152 to -0.866
	p value	**0.001**
CI = Confidence Interval		

In summary, for new lesions appearing around the time of infusion (0 months) there appeared to be a significant change in MTR gradient of +1.033 pcu/month (P=0.001) pre- and post-treatment. However, for new lesions occurring at -3 months and +3 months timepoints, there was no significant change in MTR gradient pre- and post-infusion, or pre-and post-appearance. For new lesions appearing at the +3 months and +6 months timepoints, the MTR gradient steeply declined prior to lesion appearance, as would be expected.

4.5 DISCUSSION

For baseline PDT2w lesions there appeared to be a significant change in MTR gradient pre- and post-treatment using the individual lesion area method of this *post-hoc* analysis, but not with the mean patient-level MTR technique used in the original MSCIMS analysis. This significant effect is not seen in T1w lesions at baseline ("black holes") with either method. T1w lesions, as mentioned in previous chapters, are likely to be radiological surrogates of significant neuro-axonal loss, and would thus be potentially less likely to respond to remyelination therapy.

The magnitude of effect appears to be smaller with the individual lesion area method vs the mean lesional method reported in the original published study (~0.1 pcu/month change vs ~0.5 pcu/month). This might simply represent measurement noise, but likely also reflects the increased power of the individual lesion area method to detect smaller changes, most likely due to the presence of an increased

number of observations to compare. It could also suggest that autologous MSC may have some genuine, albeit small, effect on remyelinating pre-existing lesions, which have not demonstrated significant neuro-axonal loss.

For newly appearing lesions, while the numbers are small overall, and only 4 of the 10 patients demonstrated new PDT2w lesions appearing after baseline, there was a significant reduction in new lesion area numbers pre- and post-treatment. In addition, lesions areas that appeared newly at the infusion timepoint (0 months) appeared to demonstrate a significant increase in MTR gradient post-treatment, with a magnitude of effect greater than 1 pcu/month. This was not seen in lesions appearing at other timepoints. One possible interpretation of this observation is that AMSC may have some temporary effect on the capacity to remyelinate new lesions occurring temporally close to the time of treatment.

Methodological considerations

The population in this study were all SPMS, with high EDSS (mean >6.0) at baseline, with relatively long disease durations (mean >12 years), and were not a radiologically “active” group. One might envisage more meaningful assessment of the capacity of AMSC to affect remyelination in a more “active” group of patients, with less disability at baseline, and earlier on in the course of the disease. More clinically progressive and disabled patients are likely demonstrate higher neurodegenerative features and fewer neuroinflammatory features pathologically,

along with less neurological reparative capacity or reserve, and it could thus be posited that less progressive and disabled patients might have more favourable balance between inflammation and neurodegeneration, and better neurological reserve, with which to more optimally test putative remyelinating agents.

The technique used in this study was unable to consider lesions as a whole, and this technical limitation meant "lesion areas" had to be considered instead. This increased the number of observations, which will have had some effect on, somewhat artificially, increasing the statistical significance of any effects noted. In addition, this potentially also meant that individual lesion areas could not all be necessary considered "independent", as areas from one lesion would be expected to demonstrate changes in myelination, and hence MTR, in keeping with the whole lesion. The technique, as described, also did not account for lesion volume, which might have some effect on overall MTR calculations in the presence of significant outliers in terms of lesion size.

A further issue with the technique used was relatively difficulty with scan registration. This method used in this study was to use the "PDT2w-average" space for each patient, and then each PDT2w, T1w and MT-on, and MT-off scan was then registered to that space. While most registrations were straightforward, some difficulty was encountered at certain timepoints for some patients, and registrations needed to be re-run and rechecked on a number of occasions for certain timepoints. It is likely that the relatively low contrast intrinsic to PDT2w

scans might have contributed to this. While multiple assessors made visual checks to confirm that registrations were acceptable for all scans and timepoints, it is possible that some small registration errors may have gone unnoticed. As a key component to such a study is forward (and backward) tracking of small regions of interest for quantifiable data, even small inaccuracies with registration might have some effect on data collected (in this case tissue MT signal).

Overall, this proof-of-concept *post-hoc* analysis of the MSCIMS study has demonstrated the potential usefulness of the individual lesion area method in increasing the sensitivity of studies of potentially remyelinating agents in detecting MTR change, as a surrogate for change in myelination.

In the next chapter, I will look at an attempt at a more refined technique for individual lesion MTR analysis, which aims to address a number of the limitations of this study.

5. INDIVIDUAL LESION MTR – STREAMS SUBSTUDY

5.1 BACKGROUND

The MESEMS and STREAMS study

The International Mesenchymal Stem Cells Transplantation (MSCT) Study Group, formed by a panel of international Neurologists, Immunologists, and Stem Cell experts, published a consensus on the utilisation of mesenchymal stem cells (MSC) in Multiple Sclerosis (MS) (Freedman *et al.*, 2010). Under the name "MESEMS" (Mesenchymal Stem Cells for Multiple Sclerosis), a number of parallel, independent, international phase II studies were devised, utilising identical protocols, inclusion and exclusion criteria, and primary and secondary outcomes. This allowed a number of studies to be carried out in various countries around the world, with the practical benefits provided by running smaller scale studies, but as all the results would be pooled, this also allowed enough statistical power to draw conclusions on the safety and efficacy of MSC in MS.

Overall, 160 patients were planned to be included into the MESEMS study, using power calculations based on the primary radiological outcome of that study, specifically gadolinium enhancing lesions (GEL). A sample size of 160 patients was estimated to give an 80% power, at a significance level of 5%, to detect a 50% reduction in the number of GEL over 6 months. This estimate assumed that the average number of total GEL on 3 MRI scans would be 7.4 (SD=11.4), half of the

number of total number of GEL counted over 6 monthly scans in the phase 2 study of oral fingolimod for MS (Kappos *et al.*, 2006).

STREAMS (Stem Cells in Rapidly Evolving Active Multiple Sclerosis), a Phase II, randomized, double-blind crossover trial, is the UK arm of MESEMS. In its scope, STREAMS aims to assess the safety and efficacy of IV MSC therapy in patients with MS. This includes clinical and radiological markers of efficacy, including incidence of relapses and disability progression, as well as number of new T2-weighted (T2w) lesions, new Gadolinium-enhancing lesions (GEL), and other markers.

STREAMS differs from a previous trial of intravenous mesenchymal stem cells, MSCIMS (Connick *et al.*, 2012), in its active vs placebo comparison, in its cross-over study, as well as its inclusion only of patients with clinically and radiologically active MS.

5.2 AIMS

In this chapter, I will look at a subsection of the imaging results from the STREAMS study, specifically the MTR analysis. As the larger MESEMS study is still underway, we cannot report on the other radiological outcome measures, but I have permission to report the MTR results from STREAMS in this thesis.

I specifically aimed to further develop the lesion MTR analysis pathway as initially described in the MSCIMS *post-hoc* MTR analysis study (previous chapter), with the intention of addressing some of the methodological considerations of that study, and the technical limitations of the lesion analysis method it used. A primary technical consideration was to look at MTR at an individual lesion level (rather than across lesion areas, as in MSCIMS), as well as undertake analysis taking into account individual lesion volume. In addition, I aimed to utilise a more accurate registration process, to reduce some of the registration issues that were initially noted in MSCISM.

5.3 METHODS

Study design

STREAMS utilised a crossover design. Patients were randomised into each arm, either receiving MSC or placebo at week 0, with crossover at week 24. No additional "wash-out" period was designed into the study, as the presence of grafted AMSC would most likely have diminished to almost zero after 12 weeks (Himes *et al.*, 2006).

Patient Selection Criteria

The inclusion criteria (see Table 5.1) specified patients with active MS, defined clinically by relapses or disability progression in the preceding 18 months, and radiologically by the presence of one or gadolinium enhancing lesions (GEL) on

brain MRI in the preceding 6 months. Age was restricted to between 18-50 years (inclusive), and EDSS between 2.0 and 6.5.

Table 5.1: STREAMS Inclusion Criteria

- Clinically and radiologically active RRMS, SPMS and PPMS
- Age 18 - 50 years
- Disease duration 0-10 years (inc) from diagnosis
- EDSS 2.0 - 6.5
- ≥ 1Gd+ lesion on MRI within 6 months prior to harvesting
- Adequate culture and release of MSCs; target dose 1-2 million cells/kg

Figure 5.1 shows the study design.

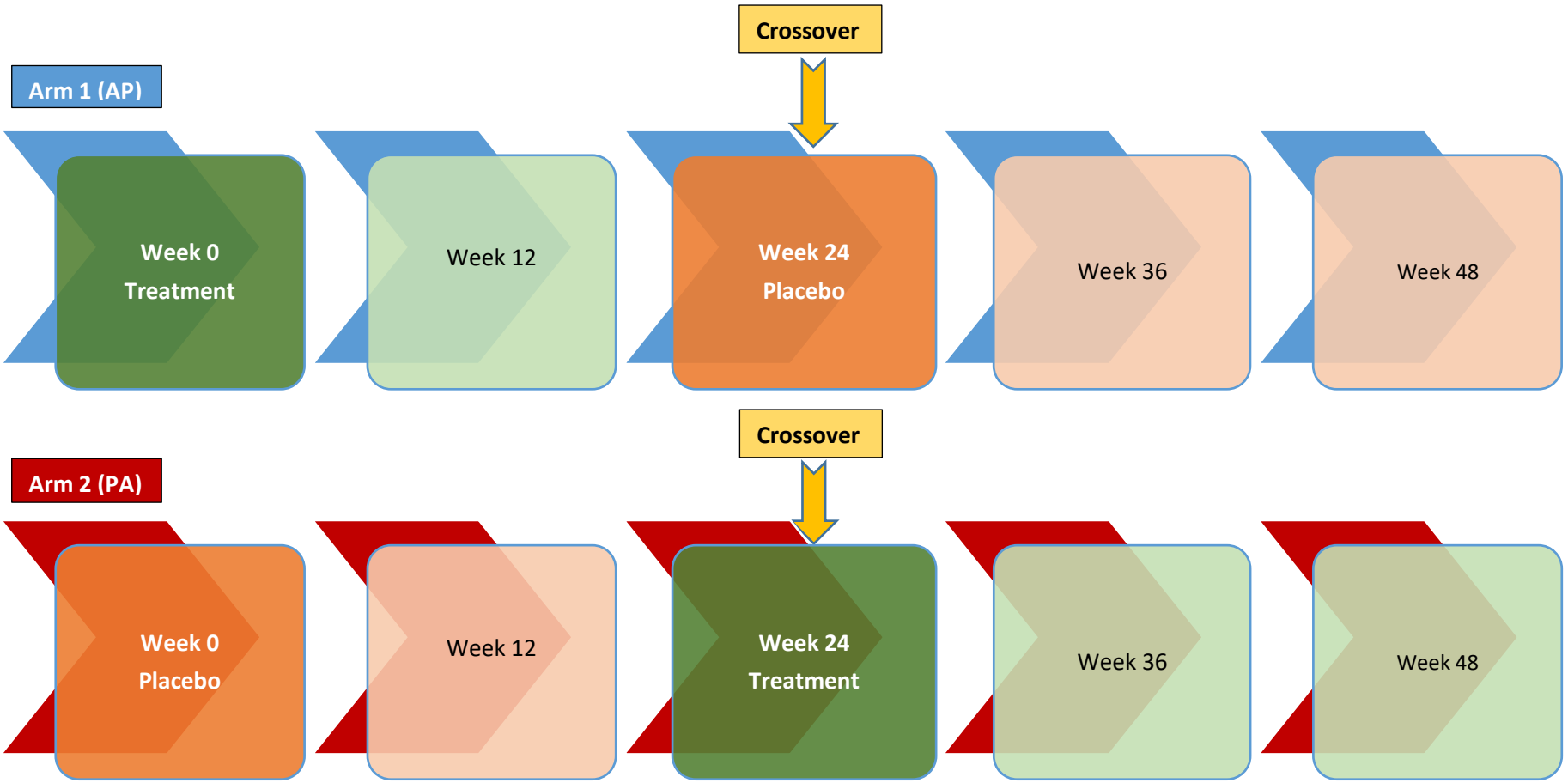

Figure 5.1: STREAMS Study Design, with crossover at Week 24

MRI acquisition

All patients were scanned on a Philips 3T Achieva scanner at the Institute of Neurology, Queen Square, London. There were no hardware or firmware changes to the scanner during the time course of the study. MR images acquired included PDT2w, T1w SE, 3DT1w, and whole brain MT sequences.

PDT2w:

Axial PDT2w Dual Echo, TSE imaging was acquired on all patients: Axial, TR: 3000ms; TE 1 and 2: 20ms and 185ms; Matrix: 192 x 256; flip angle: 90; plane resolution: 1mm x 1mm, 46 x 3mm contiguous slices for each echo, to give 92 slices in total.

T1w Spin Echo:

T1w SE images were acquired on all patients: Axial, TR: 250ms; TE: 2.5ms, 2 averages; Matrix: 192 x 256; flip angle: 75; plane resolution: 1mm x 1mm, 46 x 3mm slices.

Magnetisation Transfer (MT):

3D Gradient Echo was used to acquire 2 sets of images on all patients, with and without MT pulse ("MT-on" and "MT-off"): Axial 3D, TR: 49ms; TE: 5ms, flip angle: 10; Matrix: 256 x 191; In plane resolution 1mm x 1mm; 60 x 3mm contiguous slices.

3DT1w

3D Gradient Echo ("Fast Field Echo" or FFE) T1w images were acquired was used to acquire images on all patients: Saggital 3D, TR: 7ms, TE: 3.2ms, flip angle: 8, Matrix: 256x256; In plane resolution 1mm x 1mm, 180 x 1mm contiguous slices.

Image Processing

NiftyReg was used to create a 3DT1-average space (averaged across all timepoints) for each patient, and register scans from each PDT2w, T1w and MT-on , and MT-off to that space. Registrations were checked visually by myself and Dr Ferran Prados Carrasco (FPC). MTR maps, measured in percentage units (pcu), were created using the registered MT-on and MT-off images, using the formula [MTR = (MToff – MTon) / MToff].

Lesion Marking

The Irregular ROI feature of Jim 6.0 (Xinapse Systems UK, http://www.xinapse.com) was used to mark lesions on the PDT2w and T1w scans, at all timepoints. Lesions were marked and saved as binary region-of-interest masks. Unlike with the MSCIMS study, the lesion masks were split such that each lesion (including those spanning multiple contiguous slices) was saved as a separate mask. Fslmaths (Jenkinson *et al.*, 2012) was used to calculate the volume of each lesion, as well as to mask each MTR map file with the individual lesion masks, and calculate the MTR value for that lesion. This was done over every timepoint.

Statistical Analysis

Statistical Analysis was carried out by Dr Daniel Altmann. The two crossover periods had two follow-up time points each, an early (12-week) and late (24-week follow-up); separate analyses were carried out for each of these follow-up times. The first comparisons, early and late follow-up just in period one, used a linear mixed model with each lesion as the unit of analysis, but with a random effect on patient, thus allowing for within-patient correlation of lesions. The lesion MTR was the response (outcome/"dependent") variable of this model, and the explanatory (predictor/"independent") variables were a binary treatment indicator (active vs placebo), and the baseline lesion MTR. The coefficient on the treatment indicator estimated the active vs placebo mean difference. The estimation method was restricted maximum likelihood (REML). The two full crossover analyses, using early and late follow-up over both periods, used REML-estimated linear mixed models with each lesion as analysis unit. A binary treatment indicator was used to estimate the active vs placebo mean within-lesion difference, and any difference due to period, independent of treatment

5.4 RESULTS

Patients

In total 12 patients with active MS were included in this study. There were 8 females and 4 males. Table 5.2 shows the baseline characteristics of each of the patients. Mean age was 37.4 years. Mean EDSS was 4.0.

Table 5.2: STREAMS Patient characteristics at baseline

	Patient Number											
	1	**2**	**3**	**4**	**5**	**6**	**7**	**8**	**9**	**10**	**11**	**12**
Gender	F	M	F	F	F	F	M	F	M	F	M	F
Age	44	46	50	41	34	25	43	30	36	29	31	40
EDSS	3.5	3	3.5	4.5	6	6	3.5	3.5	4	2.5	4	4

EDSS = Expanded Disability Status Scale

Figure 5.2 shows patient flow-chart of patients through the study.

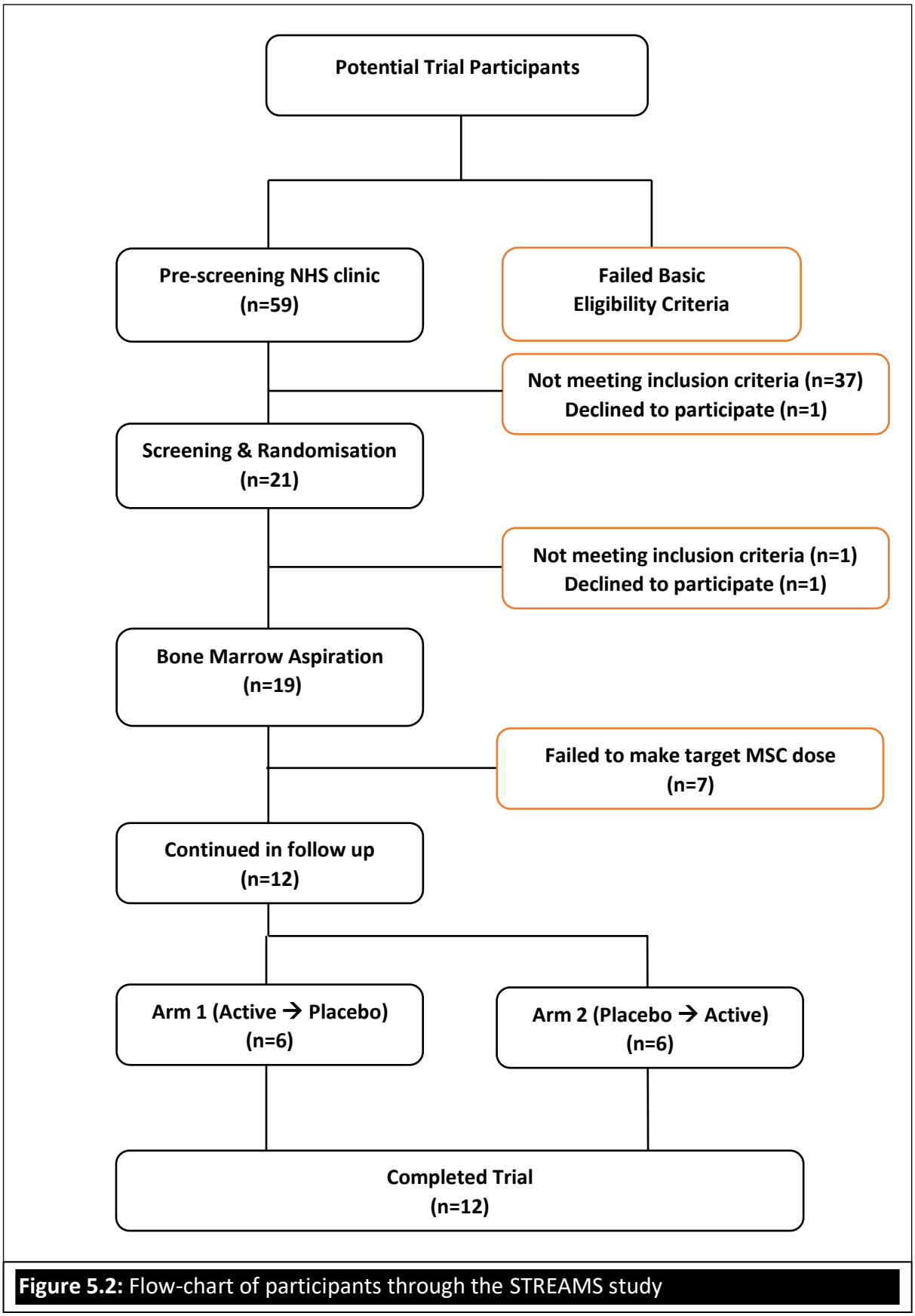

Figure 5.2: Flow-chart of participants through the STREAMS study

Baseline Lesions

Table 5.3: Brain Characteristics at Week 0 (Baseline)	
Mean Brain Volume BV (ml)	1671.51
SD	49.93
Range	1599.56 – 1779.87

Table 5.4: Lesion characteristics at Week 0 (Baseline)		
Mean lesion Volume (ml)	0.11	0.09
SD	0.25	0.16
Range	0.05 – 3.98	0.05 – 1.90
Mean lesion load volume (ml)	6.64	3.21
Range	0.72 – 14.611	0.26 – 10.95
Mean lesion load as % of BV	0.40%	0.19%
Range	0.04% – 0.87%	0.02% – 0.65%
Mean MTR (SD) (pcu)	43.97 (4.40)	41.95 (4.90)
Range	27.26 to 54.39	26.08 to 52.50

Tables 5.3 and 5.4 show the brain and lesion MTR characteristics, respectively, at week 0. At week 24 (crossover point), the mean lesion MTR was 44.39, SD 4.38, with a range between 21.55 to 54.20.

There was no significant difference between mean lesional MTR at Week 0 vs Week 24 (p=0.325). Median MTR values were very close to mean MTR, suggesting that the MTR values were spread according to a Normal distribution.

Table 5.5: Mean PDT2w lesion MTR (SD) in percent units (pcu) by group and timepoint

Timepoint	Arm 1 (AP)	Arm 2 (PA)	Total Cohort
Week 0	44.54 (4.46)	43.36 (4.27)	43.97 (4.40)
Week 12	44.60 (4.23)	42.95 (4.36)	43.80 (4.37)
Week 24	44.95 (4.42)	43.37 (4.30)	44.19 (4.43)
Week 36	44.82 (4.33)	42.94 (4.39)	43.91 (4.4.6)
Week 48	44.87 (4.25)	43.29 (4.43)	44.11 (4.41)

Table 5.6: Mean T1w lesion MTR (SD) in percent units (pcu) by group and timepoint

Timepoint	Arm 1 (AP)	Arm 2 (PA)	Total Cohort
Week 0	41.94 (4.78)	40.93 (4.98)	41.44 (4.90)
Week 12	42.22 (4.81)	40.40 (5.15)	41.33 (5.05)
Week 24	42.41 (4.93)	40.83 (4.99)	41.63 (5.01)
Week 36	42.28 (4.91)	40.37 (5.02)	41.34 (5.05)
Week 48	42.40 (4.80)	40.65 (4.98)	41.54 (4.96)

Tables 5.5 and 5.6 show the mean lesion MTR at each timepoint for both arms, as well as over the entire cohort, for PDT2w lesions as well as T1w lesions. T1w lesions

demonstrated lower MTR by a few percent units (pcu) overall compared to PDT2w lesions, with is likely an indication of chronicity and severity (T1w lesions or “black holes” are thought to represent significant neuroaxonal loss). At entry into study (week 0), Arm 1 (AP) has a significantly higher mean PDT2w lesion MTR than Arm 2 (PA): 1.83 pcu, p=0.037, and a higher mean T1w lesion MTR than Arm 2 (PA), but this was not statistically significant: 1.51 pcu, p=0.215. Adjustments were made for this for the Week 0-24 comparisons, but did not affect the Crossover results. Period effects, as a consequence of the cross-over design, were calculated, and accounted for in the analysis.

Figure 5.3: Baseline Lesion MTR over time

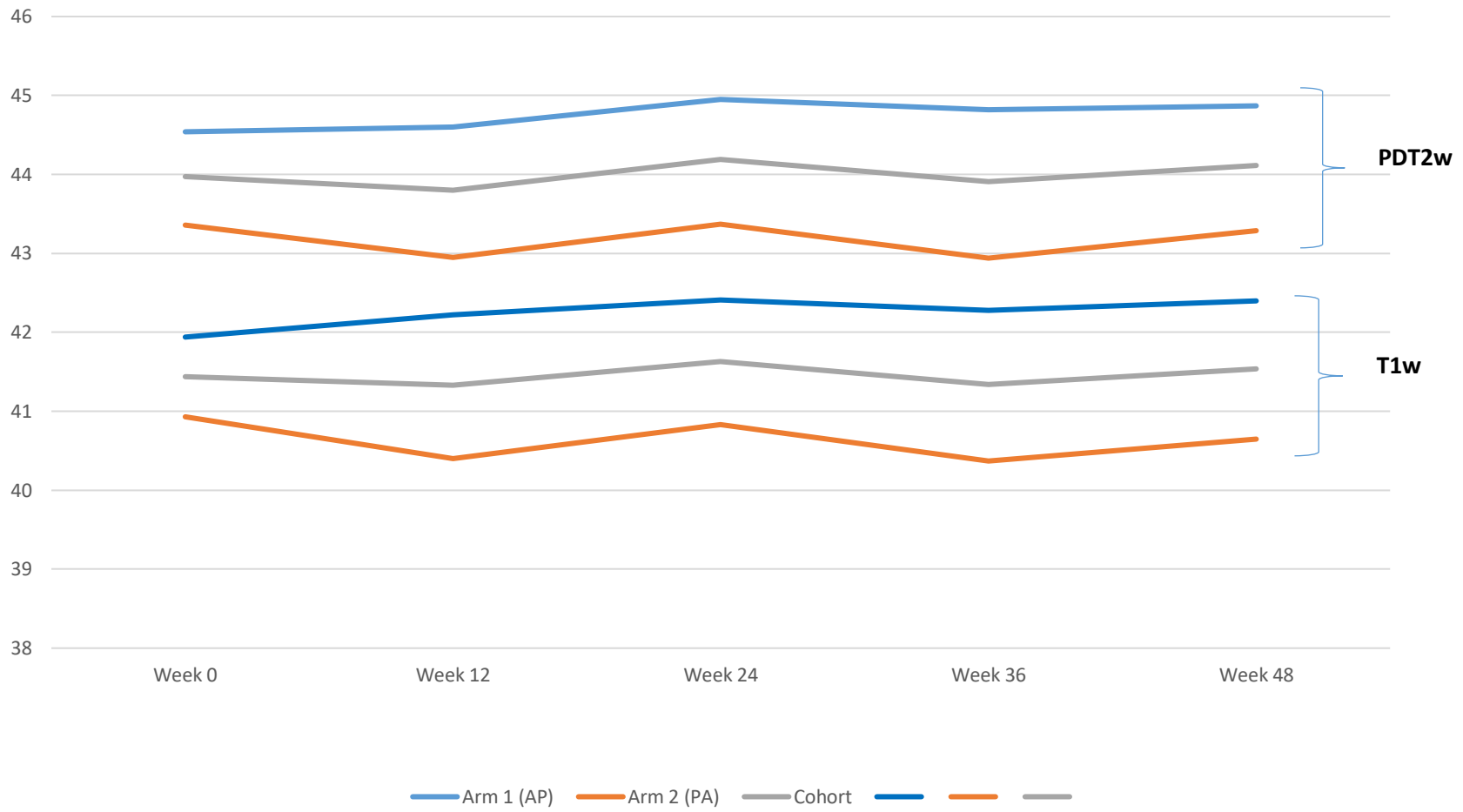

Post-treatment differences between Active and Placebo

Table 5.7: Week 0 lesions, Difference between Active and Placebo MTR (pcu), prior to cross-over (adjusted for baseline MTR difference)

Weeks		MTR (Active vs Placebo)	PDT2w	T1w
0 - 24	0 - 12	**Difference**	**0.24**	**0.48**
		95% CI	-0.57 to 1.05	-0.40 to 1.36
		p value	**0.564**	**0.284**
	12 - 24	**Difference**	**0.10**	**0.37**
		95% CI	-0.58 to 0.79	0.36 to 1.11
		p value	**0.765**	**0.321**

CI = Confidence Interval

Table 5.8: Week 0 lesions, Difference between Active and Placebo MTR (pcu), full cross-over			
Weeks	**MTR (pcu)**	**PDT2w**	**T1w**
Early	**Difference**	**-0.12**	**-0.05**
Arm 1 (AP): 0-12	95% CI	-0.23 to -0.01	-0.20 to -0.10
Arm 2 (PA): 24-36	**p value**	**0.038**	**0.524**
Late	**Difference**	**-0.004**	**-0.09**
Arm 1 (AP): 12-24	95% CI	-0.10 to 0.10	-0.23 to 0.05
Arm 2 (PA): 36-48	**p value**	**0.945**	**0.228**
CI = Confidence Interval			

Table 5.7 shows the differences in MTR between Active and Placebo groups, for both PDT2w and T1w lesions, for the first half of the study, prior to cross-over. This essentially represents a standard parallel group, non-cross over, study. For both 0-12 weeks and 12-24 weeks, the results were non-significant.

Table 5.8 in contrast shows the full cross-over data, again comparing MTR between Active and Placebo groups, for both PDT2w and T1w lesions. For both pre- and post-cross-over periods, the early and late phases of each showed no significant

improvement. In fact, the PDT2w lesion MTR for the early phase showed a net reduction in MTR with the Active treatment.

Overall, there was no evidence of an Active vs Placebo treatment effect on baseline PDT2w or T1w lesion MTR.

New PDT2 Lesions

New PDT2w lesions were noted, appearing subsequent to the first timepoint (week 0). For these new lesions, the MTR was calculated before and after appearance. Figures 4-7 plot the MTR changes of these new lesions over time. The crossover analysis of the difference in MTR between active and placebo is summarised in Table 5.9.

Table 5.9: New PDT2w lesions - Difference between Active and Placebo MTR					
	MTR (pcu)	*Week 12*	*Week 24*	*Week 36*	*Week 48*
Early	**Difference**	**-0.41**	**-0.92**	**-0.50**	**0.01**
Arm 1 (AP): 0-12	95% CI	-1.09 to 0.27	-1.68 to -0.16	-1.31 to -0.31	-0.32 to 0.34
Arm 2 (PA): 24-36	**p value**	**0.233**	**0.017**	**0.227**	**0.953**
Late	**Difference**	**0.37**	**0.53**	**-0.29**	**-0.51**
Arm 1 (AP): 0-12	95% CI	-0.21 to 0.96	-0.27 to 1.34	-0.96 to 0.37	-1.43 to 0.40
Arm 2 (PA): 24-36	**p value**	**0.212**	**0.195**	**0.390**	**0.273**
CI = Confidence Interval					

There was no evidence of any beneficial treatment effect for any new PDT2 lesions appearing at any point after Week 0.

Figure 5.4: MTR (pcu) of New PDT2w lesions occuring at Week 12

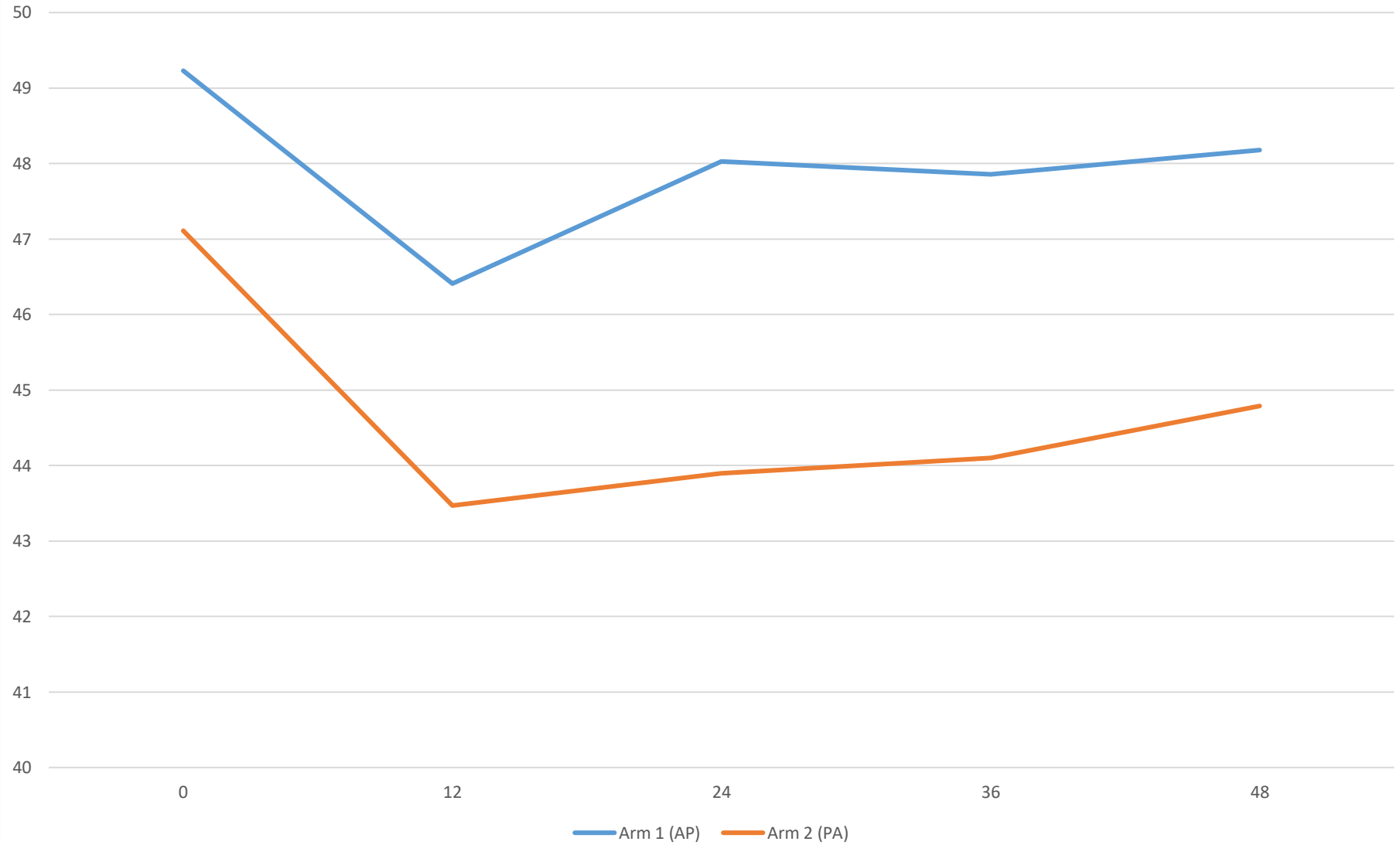

Figure 5.5: MTR (pcu) of New PDT2w lesions occuring at Week 24

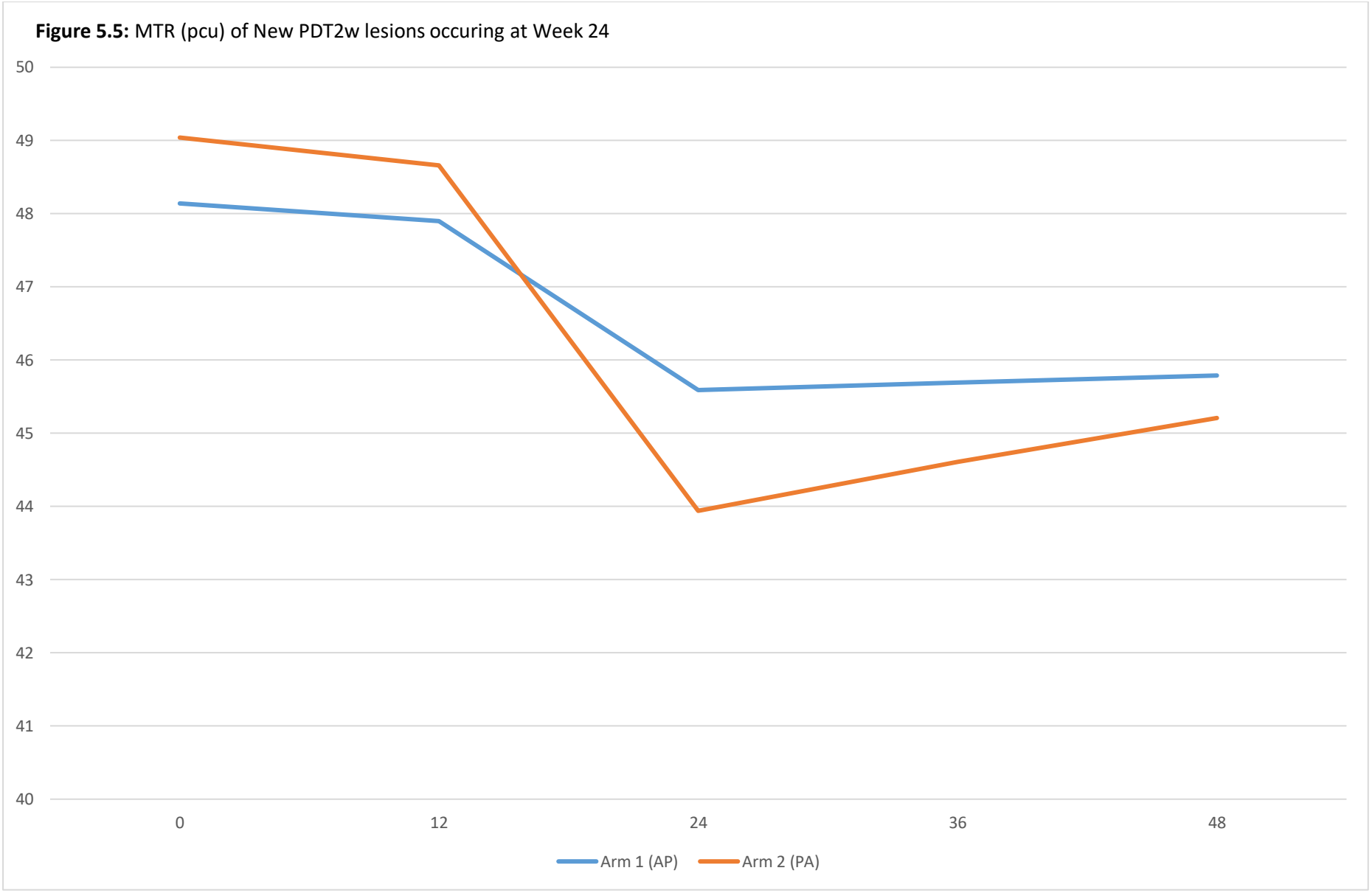

Figure 5.6: MTR (pcu) of New PDT2w lesions occuring at Week 36

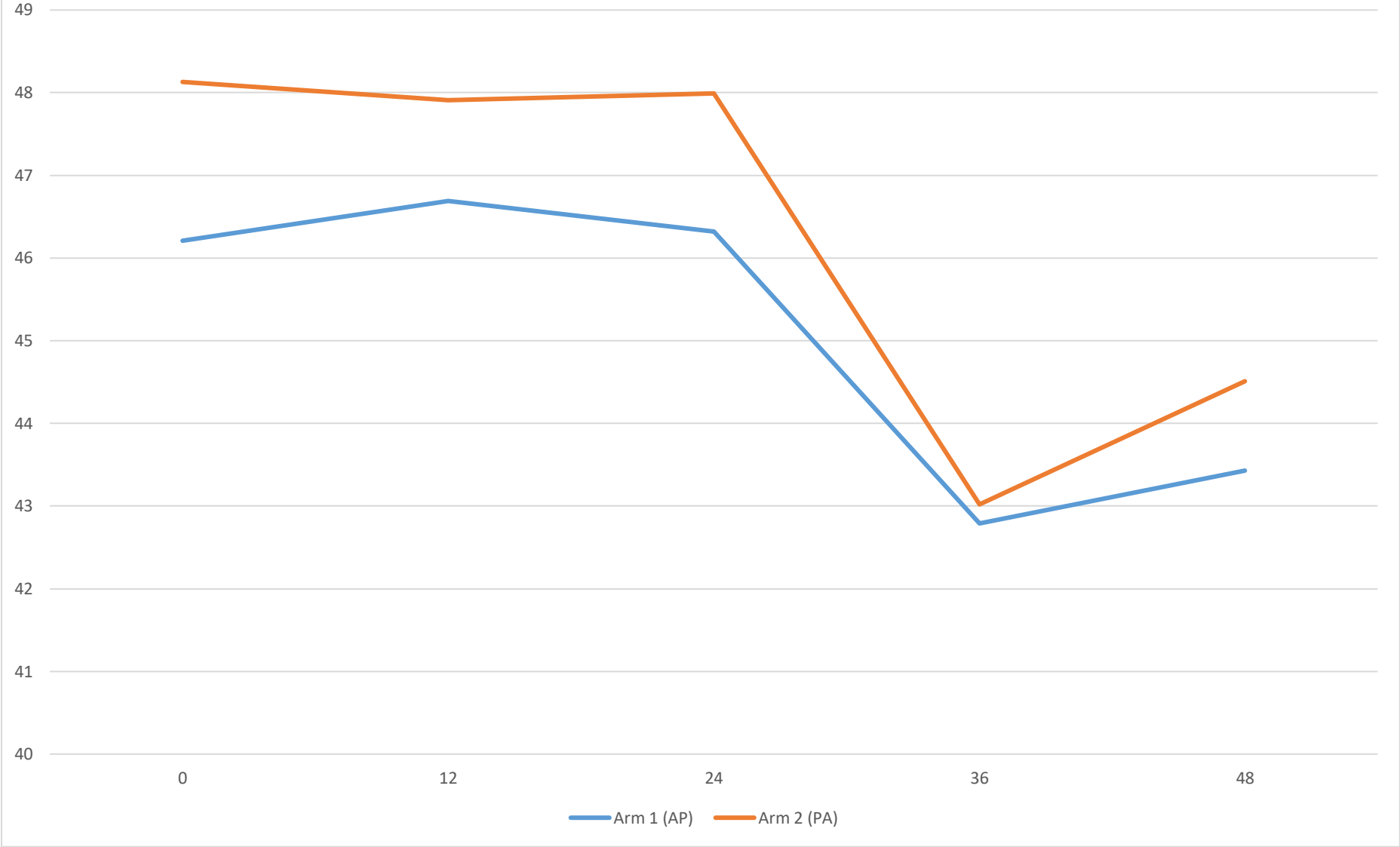

Figure 5.7: MTR (pcu) of New PDT2w lesions occuring at Week 48

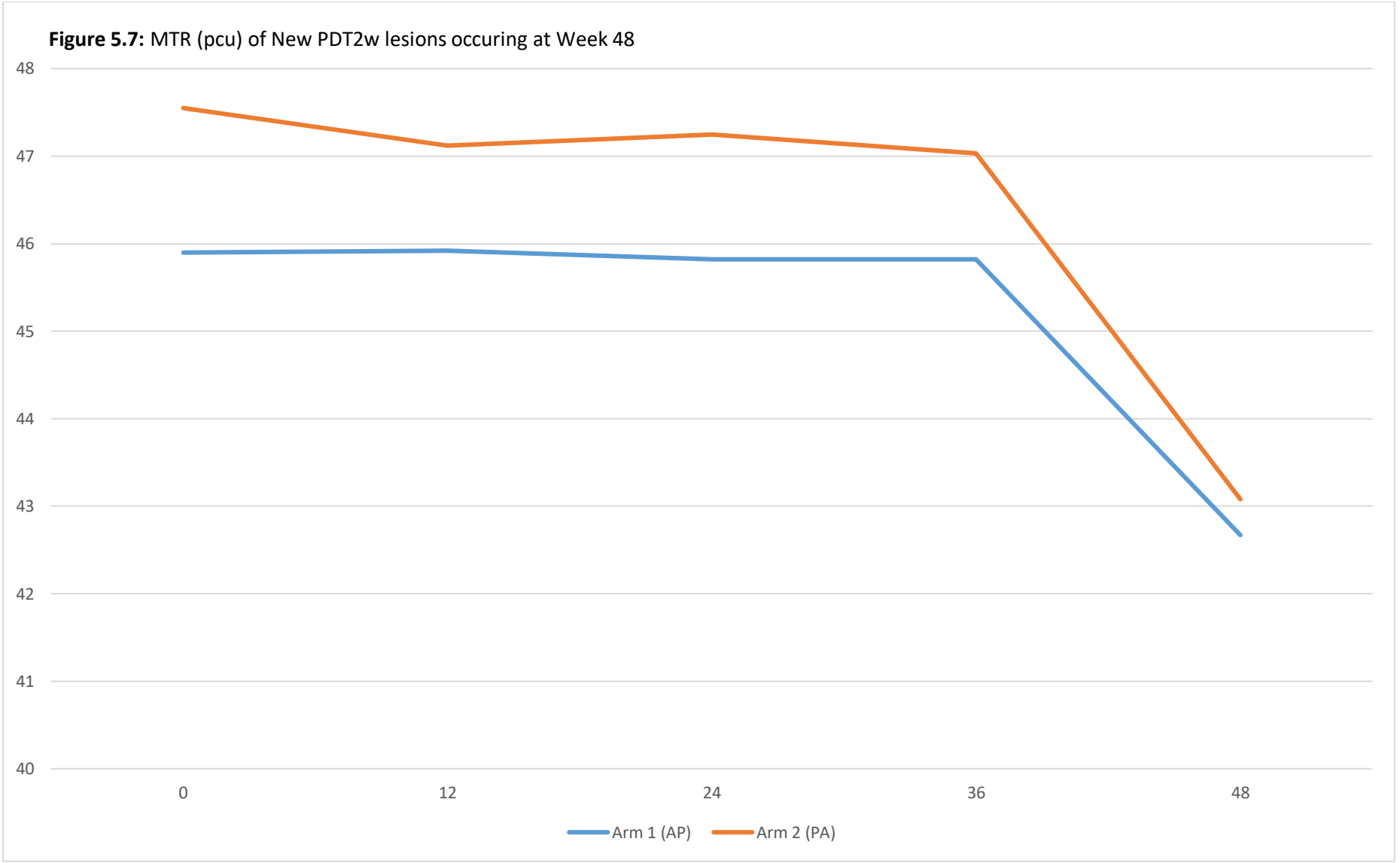

5.5 DISCUSSION

Overall there was not noted to be any significant effect of intravenous AMSC on the MTR of either lesions already present at baseline ("chronic" or "old" lesions), or on lesions appearing subsequent to baseline ("acute" or "new" lesions).

Methodological considerations

The study employed a crossover design, which has a number of inherent advantages, but also some particular methodological considerations. In general, crossover studies are better powered with smaller sample sizes. In addition, because the effects of the intervention being investigated are evaluated within the same patient, this eliminates the confounding effects of inter-patient variability.

Crossover trials may be at risk of carryover across intervention periods. Even though the timing of crossover in this study did not necessitate building in extra wash-out period, based on the understanding that AMSC grafted are no longer detectable after 12 weeks, it is known that neurological effects might persist beyond that time (Himes *et al.*, 2006). Indeed, if remyelination were to occur, this would have a significant impact on the likelihood of crossover effect, and this might be of some relevance in the AP group who received the AMSC in the first period. This did not appear to affect the MTR analysis results in our cohort, but needs to be borne in mind for the larger analysis, which will include other MRI markers as well as clinical outcomes. As such,

although the assumption is that there were no carry-over effects, this is difficult to test accurately.

Period effects might also have been a potential issue, especially if there is a change in the MS disease process over the time of the study (for instance if a patient was transitioning from RRMS to SPMS).

Also, given the crossover nature, specific statistical considerations were needed to analyse the data. Two active vs placebo comparisons were carried out: the first comparison was cross-sectional, using just the first period data, in effect handling the data as though it were a simple parallel group study, comparing active vs placebo lesion MTR just in the first period. The disadvantage of this first-period comparison is lack of power compared to the full crossover analysis, which compares the active vs placebo MTR for each lesion, between the two periods.

Compared to the MSCIMS substudy, the patients included in STREAMS had clinically and radiologically active MS, were younger (mean age 37.4 vs 47.4 years), and had a lower EDSS (mean EDSS at baseline of 4.0 vs 6.0). These were important differences and addressed some of the core limitations of the MSCISMS study in choice of patients, and the study's overall ability to assess the effects of intervention (autologous MSC) in MS disease activity.

In addition, this substudy addressed some key technological limitations of the MSCIMS substudy, namely accounting for lesions as a whole (rather than lesion areas), a better registration pathway (by utilising the superior contrast of the 3DT1 scans to create an average scan to which other scans were registered), and accounting for lesion volume in the statistical analysis to help minimise any potential skewing of results by lesions of sizes lying outside the “normal” distribution curve.

The STREAMS study was not necessarily powered to be able to detect MTR change over the period of time being investigated. The larger MESEMS study will have 160 patients, and while its sample size calculations were based on detecting change in GEL, many other sites are also collecting MTR data, and a larger MTR analysis using this individual lesion analysis pathway is planned.

It remains to be seen whether autologous MSCs given intravenously have any clinical or other radiological effect (such as reduction in number of new T2w or GEL) on active MS. However, purely from the point of view of change in MTR, taken as a radiological marker for myelination, this substudy of STREAMS does not demonstrate an effect of MSC given intravenously on myelination of lesions.

6. CONCLUSIONS

Research focus in MS has evolved over the last few decades, from chiefly exploratory and pathological work attempting to understand and describe the condition, to investigations into mainly immune-based disease-modifying agents. We now have a better understanding of the pathological processes at work in MS, and there are now numerous potential DMD therapies available to patients with RRMS, which have recently also been demonstrated to potentially have some effect in delaying onset of secondary progression. In addition, trials of neuroprotection in MS have come of age, and we now have several pharmacological directions, and innovative study designs, with which to detect and measure neuroprotection.

A key area of MS as yet remaining to be fully understood however is how relapsing and progressive forms of MS differ in their basic underlying pathology, and whether they represent intrinsically different disease processes. It has, however, recently become somewhat clearer that underlying immune-mediated inflammatory disease in the CNS drives demyelination, and that neurodegeneration is the main driver of neuroaxonal loss. How the two processes interrelate is not yet clearly explained.

This thesis looked at a number of areas of current and future interest in MS, including current imaging analysis techniques for a study of a potentially neuroprotective agent, an exploratory look at the relationships between demyelination and atrophy in the GM in MS, a forward look at how best to

potentially image remyelination, and proof-of-concept work in developing, and then improving upon, an individual lesion analysis pathway using MTR.

The voxel-based study of MTR (Chapter 2) has helped provide some understanding of how the demyelination and atrophy potentially correlate in the GM. The differing location and extent of regional MTR and volumetric abnormalities in MS subgroups argues against a single mechanism for demyelination and neuronal loss in the GM of MS patients, and further supports the concept of there being two separate pathological processes underlying MS, namely immune-driven inflammation, and neurodegeneration. It follows that, while the exact pathophysiological mechanisms underlying progression is not clear, it may suggest a change in the balance between inflammatory activity and neurodegeneration, with the latter showing a significant increase, relative to the former, with the onset of progression.

This explains, at least partially, why chiefly immune-based therapies help reduce inflammation and relapses, and why AHSCT, offering an immune “reset”, demonstrates near complete cessation of CNS inflammatory activity, but also why these therapies appear to be less effective in progressive disease.

Understanding these fundamental differences in pathological process can be helpful in designing studies aimed with various interventions and desired effects in mind. For

instance, with the CUPID study (Chapter 3), despite a negative clinical and MRI outcome, useful lessons can still be learnt for future studies, including:

- optimising patient inclusion criteria, as per the discussion above, possibly favouring those with RRMS and early SPMS, and lower measures of pre-existing disability.
- larger study sizes (in practice necessitating large, possibly international, multi-centre trials).

In addition, future studies of neuroprotection and repair could also consider:

- study designs with multiple parallel groups (rather than just 2), such as the MS-SMART trial (Chataway, 2013), which compared 3 separate putative neurotherapeutic agents against placebo (4 arms).
- other study designs, including retrospective studies, which can by their nature allow for larger comparison groups, especially for investigating the potential neuroprotective effects of already established therapies in MS.

In addition, trials of potentially remyelinating agents are becoming more important in the overall spectrum of MS research, and should be designed in order to maximise their sensitivity to true treatment effects (Chapter 1). As well as selecting patient groups with the most potential to show a response, and generating sound sample size calculations that give a trial sufficient power to detect a true effect on the

chosen primary outcome measure, imaging outcomes are needed that are feasible from a time and practicality point of view, as well as being sensitive and specific to myelin, whilst also being reproducible, and clinically meaningful.

MTR has demonstrated a number of favourable characteristics which would warrant its consideration as an outcome measure in future trials of potentially neuroprotective agent, chief amongst these is its sensitivity to detecting changes in myelin in vivo. With this in mind, a proof-of-concept individual lesion MTR analysis pipeline was designed, and implemented in data from the MSCIMS substudy (Chapter 4), and this technique was further improved upon with the subsequent STREAMS substudy (Chapter 5). Although the actual results from the MTR analysis of the STREAMS data were negative, individual lesion MTR analysis represents a potentially useful method of assessing myelination of lesions over time. The MT sequences are quick and easy to acquire using most commercially available MR scanners, and image processing and analysis is relatively straightforward. The technique as described might be an important metric to consider for inclusion in future trials of potentially remyelinating therapies in MS.

Looking forward, future studies of neuroprotection, repair and remyelination will need to consider including not only brain measures, but also optic nerve and spinal cord measures as imaging outcomes. MTR, as well as other metrics such as DTI, are practical and feasible in the CNS regions, as they are in the brain.

7. REFERENCES

- Altmann, D. R. *et al.* (2013) 'Sample sizes for lesion magnetisation transfer ratio outcomes in remyelination trials for multiple sclerosis', *Multiple Sclerosis and Related Disorders*. Elsevier, pp. 1–7. doi: 10.1016/j.msard.2013.09.007.
- Ashburner, J. (2007) 'A fast diffeomorphic image registration algorithm.', *NeuroImage*, 38(1), pp. 95–113. doi: 10.1016/j.neuroimage.2007.07.007.
- Ashburner, J. and Friston, K. J. (2000) 'Voxel-based morphometry--the methods.', *NeuroImage*, 11(6 Pt 1), pp. 805–21. doi: 10.1006/nimg.2000.0582.
- Atkins, H. L. *et al.* (2016) 'Immunoablation and autologous haemopoietic stem-cell transplantation for aggressive multiple sclerosis: a multicentre single-group phase 2 trial', *The Lancet*. Elsevier Ltd, 388(10044), pp. 576–585. doi: 10.1016/S0140-6736(16)30169-6.
- Audoin, B. *et al.* (2004) 'Voxel-based analysis of MTR images: a method to locate gray matter abnormalities in patients at the earliest stage of multiple sclerosis.', *Journal of magnetic resonance imaging : JMRI*, 20(5), pp. 765–71. doi: 10.1002/jmri.20178.
- Audoin, B. *et al.* (2006) 'Localization of grey matter atrophy in early RRMS : A longitudinal study.', *Journal of neurology*, 253(11), pp. 1495–501. doi: 10.1007/s00415-006-0264-2.
- Audoin, B. *et al.* (2007) 'Voxel-based analysis of grey matter magnetization transfer ratio maps in early relapsing remitting multiple sclerosis.', *Multiple sclerosis (Houndmills, Basingstoke, England)*, 13(4), pp. 483–9. doi: 10.1177/1352458506070450.

- Audoin, B. *et al.* (2010) 'Atrophy mainly affects the limbic system and the deep grey matter at the first stage of multiple sclerosis.', *Journal of neurology, neurosurgery, and psychiatry*, 81(6), pp. 690–5. doi: 10.1136/jnnp.2009.188748.
- Bai, L. *et al.* (2009) 'Human bone marrow-derived mesenchymal stem cells induce Th2-polarized immune response and promote endogenous repair in animal models of multiple sclerosis', *Glia*, 57(11), pp. 1192–1203. doi: 10.1002/glia.20841.
- Balcer, L. J. (2006) 'Optic Neuritis', *The New England journal of medicine*, 354(12), pp. 1273–1280.
- Barker, G. J. (2000) 'Technical issues for the study of the optic nerve with MRI.', *Journal of the neurological sciences*, 172 Suppl, pp. S13-6.
- Barker, G. J. (2001) 'Diffusion-weighted imaging of the spinal cord and optic nerve', *Journal of the neurological sciences*, 186, pp. S45-9.
- Barkhof, F. *et al.* (2009) 'Imaging outcomes for neuroprotection and repair in multiple sclerosis trials.', *Nature reviews. Neurology*, 5(5), pp. 256–66. doi: 10.1038/nrneurol.2009.41.
- Barnett, M. H. and Prineas, J. W. (2004) 'Relapsing and remitting multiple sclerosis: pathology of the newly forming lesion.', *Annals of neurology*, 55(4), pp. 458–68. doi: 10.1002/ana.20016.
- Bieber, A. J., Ure, D. R. and Rodriguez, M. (2005) 'Genetically dominant spinal cord repair in a murine model of chronic progressive multiple sclerosis.', *Journal of neuropathology and experimental neurology*, 64(1), pp. 46–57.
- Bitsch, A. *et al.* (2001) 'A Longitudinal MRI Study of Histopathologically Defined

Hypointense Multiple Sclerosis Lesions', *Annals of neurology*, 49(6), pp. 793–796.

- Bjartmar, C. and Trapp, B. D. (2003) 'Axonal degeneration and progressive neurologic disability in multiple sclerosis', *Neurotoxicity Research*, 5(1–2), pp. 157–164. doi: 10.1007/BF03033380.
- Bjartmar, C., Wujek, J. R. and Trapp, B. D. (2003) 'Axonal loss in the pathology of MS: consequences for understanding the progressive phase of the disease.', *Journal of the neurological sciences*, 206(2), pp. 165–71.
- Bø, L. *et al.* (2003) 'Intracortical multiple sclerosis lesions are not associated with increased lymphocyte infiltration', *Multiple Sclerosis*, 9(4), pp. 323–331. doi: 10.1191/1352458503ms917oa.
- Bonati, U. *et al.* (2011) 'Cervical cord and brain grey matter atrophy independently associate with long-term MS disability.', *Journal of neurology, neurosurgery, and psychiatry*, 82(4), pp. 471–2. doi: 10.1136/jnnp.2009.194480.
- Bordet, T. *et al.* (2007) 'Identification and Characterization of Cholest-4-en-3-one , Oxime (TRO19622), a Novel Drug Candidate for Amyotrophic Lateral Sclerosis.', *The Journal ff Pharmacology And Experimental Therapeutics*, 322(2), pp. 709–20. doi: 10.1124/jpet.107.123000.
- Bose, G. *et al.* (2018) 'Autologous hematopoietic stem cell transplantation improves fatigue in multiple sclerosis', *Multiple Sclerosis Journal*, p. 135245851880254. doi: 10.1177/1352458518802544.
- Breij, E. C. W. *et al.* (2008) 'Homogeneity of Active Demyelinating Lesions in Established Multiple Sclerosis', *Annals of neurology*, 63, pp. 16–25. doi: 10.1002/ana.21311.

- Brink, B. P. *et al.* (2005) 'The pathology of multiple sclerosis is location-dependent: no significant complement activation is detected in purely cortical lesions.', *Journal of neuropathology and experimental neurology*, 64(2), pp. 147–55.
- Brown, J. W. L. *et al.* (2019) 'Association of Initial Disease-Modifying Therapy With Later Conversion to Secondary Progressive Multiple Sclerosis', *Jama*, 321(2), p. 175. doi: 10.1001/jama.2018.20588.
- Brown, R. a, Narayanan, S. and Arnold, D. L. (2013) 'Segmentation of magnetization transfer ratio lesions for longitudinal analysis of demyelination and remyelination in multiple sclerosis.', *NeuroImage*. Elsevier Inc., 66C, pp. 103–109. doi: 10.1016/j.neuroimage.2012.10.059.
- Burt, R. K. *et al.* (2018) 'Non-myeloablative hematopoietic stem cell transplantation (HSCT) is superior to disease modifying drug (DMD) treatment in highly active Relapsing Remitting Multiple Sclerosis (RRMS): interim results of the Multiple Sclerosis International Stem cell Transp', *Neurology*, 90(15 Supplement), p. S36.004.
- Calabrese, M. *et al.* (2007) 'Detection of Cortical Inflammatory Lesions by Double Inversion Recovery Magnetic Resonance Imaging in Patients With Multiple Sclerosis', *Archives of Neurology*, 64(10), pp. 1416–1422.
- Calabrese, M. *et al.* (2009) 'Cortical lesions and atrophy associated with cognitive impairment in relapsing-remitting multiple sclerosis.', *Archives of neurology*, 66(9), pp. 1144–50. doi: 10.1001/archneurol.2009.174.
- Ceccarelli, a *et al.* (2012) 'The impact of lesion in-painting and registration

methods on voxel-based morphometry in detecting regional cerebral gray matter atrophy in multiple sclerosis.', *AJNR. American journal of neuroradiology*, 33(8), pp. 1579–85. doi: 10.3174/ajnr.A3083.

- Ceccarelli, A. *et al.* (2008) 'A voxel-based morphometry study of grey matter loss in MS patients with different clinical phenotypes.', *NeuroImage*, 42(1), pp. 315–22. doi: 10.1016/j.neuroimage.2008.04.173.
- Cercignani, M. *et al.* (2005) 'Three-dimensional quantitative magnetisation transfer imaging of the human brain.', *NeuroImage*, 27(2), pp. 436–41. doi: 10.1016/j.neuroimage.2005.04.031.
- Cerqueira, J. J. *et al.* (2018) 'Time matters in multiple sclerosis: Can early treatment and long-term follow-up ensure everyone benefits from the latest advances in multiple sclerosis?', *Journal of Neurology, Neurosurgery and Psychiatry*, 89(8), pp. 844–850. doi: 10.1136/jnnp-2017-317509.
- Chard, D. *et al.* (2003) 'The longitudinal relation between brain lesion load and atrophy in multiple sclerosis: a 14 year follow up study', *Journal of neurology, neurosurgery, and psychiatry*, 74(11), pp. 1551–1554.
- Chard, D. and Miller, D. (2009) 'Is multiple sclerosis a generalized disease of the central nervous system? An MRI perspective', *Current Opinion in Neurology*, 22(3), pp. 214–218. doi: 10.1097/WCO.0b013e32832b4c62.
- Chard, D. T. *et al.* (2002) 'Brain atrophy in clinically early relapsing-remitting multiple sclerosis', *Brain*, 125(2), pp. 327–337. doi: 10.1093/brain/awf025.
- Chard, D. T. *et al.* (2010) 'Reducing the impact of white matter lesions on automated measures of brain gray and white matter volumes.', *Journal of*

magnetic resonance imaging : JMRI, 32(1), pp. 223–8. doi: 10.1002/jmri.22214.

- Chataway, J. *et al.* (2012) 'The MS-STAT trial: High dose simvastatin demonstrates neuroprotection without immune-modulation in secondary progressive multiple sclerosis (SPMS) – a phase II trial.', in *ECTRIMS 2012 Abstract*.
- Chataway, J. (2013) 'MS-SMART:A Multi-arm Phase IIB Randomised, Double Blind Placebo-controlled Clinical Trial Comparing the Efficacy of Three Neuroprotective Drugs in Secondary Progressive Multiple Sclerosis.', *ClinicalTrials.Gov; Identifier: NCT01910259*.
- Chataway, J. (2017) 'MS-STAT2 : Multiple Sclerosis - Simvastatin Trial 2', *ISRCTN*. doi: https://doi.org/10.1186/ISRCTN82598726.
- Chen, J. *et al.* (2012) 'Clinically feasible MTR is sensitive to cortical demyelination in MS.', *Neurology*. doi: 10.1212/WNL.0b013e31827deb99.
- Chen, J. T. *et al.* (2008) 'Magnetization transfer ratio evolution with demyelination and remyelination in multiple sclerosis lesions.', *Annals of neurology*, 63(2), pp. 254–62. doi: 10.1002/ana.21302.
- Choi, S. R. *et al.* (2012) 'Meningeal inflammation plays a role in the pathology of primary progressive multiple sclerosis', *Brain*, pp. 1–13. doi: 10.1093/brain/aws189.
- Ciccarelli, O. and Miller, D. H. (2002) 'Magnetic resonance imaging in multiple sclerosis', *Practical Neurology*, (April), pp. 103–112.
- Clarke, C. *et al.* (eds) (2016) *Neurology: A Queen Square Textbook*. Oxford: Wiley-Blackwell.
- Compston, A. and Coles, A. (2008) 'Multiple sclerosis.', *Lancet*. Elsevier Ltd,

372(9648), pp. 1502–17. doi: 10.1016/S0140-6736(08)61620-7.

- Compston, D. (2005) *McAlpine's multiple sclerosis. 4th edn.* London: Elsevier.
- Connick, P. *et al.* (2012) 'Autologous mesenchymal stem cells for the treatment of secondary progressive multiple sclerosis: an open-label phase 2a proof-of-concept study.', *Lancet neurology*. Elsevier Ltd, 11(2), pp. 150–6. doi: 10.1016/S1474-4422(11)70305-2.
- Correale, J. *et al.* (2017) 'Progressive multiple sclerosis: from pathogenic mechanisms to treatment', *Brain*, 140(3), pp. 527–546. doi: 10.1093/brain/aww258.
- Davies, G. R. *et al.* (2005) 'Increasing normal-appearing grey and white matter magnetisation transfer ratio abnormality in early relapsing-remitting multiple sclerosis.', *Journal of neurology*, 252(9), pp. 1037–44. doi: 10.1007/s00415-005-0808-x.
- Dehmeshki, J. *et al.* (2003) 'The normal appearing grey matter in primary progressive multiple sclerosis: a magnetisation transfer imaging study.', *Journal of neurology*, 250(1), pp. 67–74. doi: 10.1007/s00415-003-0955-x.
- DeLuca, G. C. *et al.* (2006) 'The contribution of demyelination to axonal loss in multiple sclerosis.', *Brain : a journal of neurology*, 129(Pt 6), pp. 1507–16. doi: 10.1093/brain/awl074.
- Deoni, S. C. L. *et al.* (2008) 'Gleaning multicomponent T1 and T2 information from steady-state imaging data.', *Magnetic resonance in medicine : official journal of the Society of Magnetic Resonance in Medicine / Society of Magnetic Resonance in Medicine*, 60(6), pp. 1372–87. doi: 10.1002/mrm.21704.

- Dobson, R., Giovannoni, G. and Ramagopalan, S. (2013) 'The month of birth effect in multiple sclerosis: systematic review, meta-analysis and effect of latitude.', *Journal of neurology, neurosurgery, and psychiatry*, 84(4), pp. 427–32. doi: 10.1136/jnnp-2012-303934.
- Dousset, V. *et al.* (1998) 'Early structural changes in acute MS lesions assessed by serial magnetization transfer studies', *Neurology*, 51(4), pp. 1150–1155. doi: 10.1212/WNL.51.4.1150.
- van den Elskamp, I. J. *et al.* (2008) 'Persistent T1 hypointensity as an MRI marker for treatment efficacy in multiple sclerosis.', *Multiple sclerosis (Houndmills, Basingstoke, England)*, 14(6), pp. 764–9. doi: 10.1177/1352458507087842.
- van den Elskamp, I. J. *et al.* (2010) 'Lesional magnetization transfer ratio: a feasible outcome for remyelinating treatment trials in multiple sclerosis.', *Multiple sclerosis (Houndmills, Basingstoke, England)*, 16(6), pp. 660–9. doi: 10.1177/1352458510364630.
- Fancy, S. P. J. *et al.* (2009) 'Dysregulation of the Wnt pathway inhibits timely myelination and remyelination in the mammalian CNS.', *Genes & development*, 23(13), pp. 1571–85. doi: 10.1101/gad.1806309.
- Filippi, M. *et al.* (1995) 'A magnetization transfer imaging study of normal-appearing white matter in multiple sclerosis.', *Neurology*, 45(3 Pt 1), pp. 478–82.
- Filippi, M. *et al.* (2000) 'A conventional and magnetization transfer MRI study of the cervical cord in patients with MS.', *Neurology*, 54(1), pp. 207–13.
- Filippi M De Stefano N, et al, R. M. A. (2011) 'Magnetic resonance techniques in multiple sclerosis: The present and the future', *Archives of Neurology*, 68(12), pp.

1514–1520.

- Fisher, E. *et al.* (2008) 'Gray matter atrophy in multiple sclerosis: a longitudinal study.', *Annals of neurology*, 64(3), pp. 255–65. doi: 10.1002/ana.21436.
- Fisher, J. B. *et al.* (2006) 'Relation of visual function to retinal nerve fiber layer thickness in multiple sclerosis.', *Ophthalmology*, 113(2), pp. 324–32. doi: 10.1016/j.ophtha.2005.10.040.
- Fisniku, L. K. *et al.* (2008) 'Gray matter atrophy is related to long-term disability in multiple sclerosis.', *Annals of neurology*, 64(3), pp. 247–54. doi: 10.1002/ana.21423.
- Fox, R. J. *et al.* (2011) 'Measuring myelin repair and axonal loss with diffusion tensor imaging.', *AJNR. American journal of neuroradiology*, 32(1), pp. 85–91. doi: 10.3174/ajnr.A2238.
- Franklin, R. J. M. *et al.* (2012) 'Neuroprotection and repair in multiple sclerosis.', *Nature reviews. Neurology*. Nature Publishing Group, 8(11), pp. 624–34. doi: 10.1038/nrneurol.2012.200.
- Franklin, R. J. M. and Ffrench-Constant, C. (2008) 'Remyelination in the CNS: from biology to therapy.', *Nature reviews. Neuroscience*, 9(11), pp. 839–55. doi: 10.1038/nrn2480.
- Freedman, M. S. *et al.* (2010) 'The therapeutic potential of mesenchymal stem cell transplantation as a treatment for multiple sclerosis: Consensus report of the international MSCT study group', *Multiple Sclerosis*, 16(4), pp. 503–510. doi: 10.1177/1352458509359727.
- Frohman, E. M. *et al.* (2008) 'Optical coherence tomography: a window into the

mechanisms of multiple sclerosis.', *Nature clinical practice. Neurology*, 4(12), pp. 664–75. doi: 10.1038/ncpneuro0950.

- Gareau, P. J. *et al.* (2000) 'Magnetization transfer and multicomponent T2 relaxation measurements with histopathologic correlation in an experimental model of MS.', *Journal of magnetic resonance imaging : JMRI*, 11(6), pp. 586–95.
- Ge, Y. *et al.* (2000) 'Brain Atrophy in Relapsing-Remitting Multiple Sclerosis and Secondary Progressive Multiple Sclerosis: Longitudinal Quantitative Analysis', *Radiology*, 214(3), pp. 665–670. doi: 10.1148/radiology.214.3.r00mr30665.
- Gerdoni, E. *et al.* (2007) 'Mesenchymal stem cells effectively modulate pathogenic immune response in experimental autoimmune encephalomyelitis', *Annals of Neurology*, 61(3), pp. 219–227. doi: 10.1002/ana.21076.
- Geurts, J. J. G. *et al.* (2005) 'Cortical lesions in multiple sclerosis: Combined postmortem MR imaging and histopathology', *American Journal of Neuroradiology*, 26(3), pp. 572–577.
- Geurts, J. J. G. *et al.* (2012) 'Measurement and clinical effect of grey matter pathology in multiple sclerosis.', *Lancet neurology*. Elsevier Ltd, 11(12), pp. 1082–92. doi: 10.1016/S1474-4422(12)70230-2.
- Geurts, J. J. G. and Barkhof, F. (2008) 'Grey matter pathology in multiple sclerosis.', *Lancet neurology*, 7(9), pp. 841–51. doi: 10.1016/S1474-4422(08)70191-1.
- Gilmore, C. P. *et al.* (2009) 'Regional variations in the extent and pattern of grey matter demyelination in multiple sclerosis: a comparison between the cerebral cortex, cerebellar cortex, deep grey matter nuclei and the spinal cord.', *Journal of*

neurology, neurosurgery, and psychiatry, 80(2), pp. 182–7. doi: 10.1136/jnnp.2008.148767.

- Giuliani, N. R. *et al.* (2005) 'Voxel-based morphometry versus region of interest: a comparison of two methods for analyzing gray matter differences in schizophrenia.', *Schizophrenia research*, 74(2–3), pp. 135–47. doi: 10.1016/j.schres.2004.08.019.
- Goldschmidt, T. *et al.* (2009) 'Remyelination capacity of the MS brain decreases with disease chronicity.', *Neurology*, 72(22), pp. 1914–21. doi: 10.1212/WNL.0b013e3181a8260a.
- Gourraud, P.-A. *et al.* (2012) 'The genetics of multiple sclerosis: an up-to-date review.', *Immunological reviews*, 248(1), pp. 87–103. doi: 10.1111/j.1600-065X.2012.01134.x.
- Gouw, A. A. *et al.* (2008) 'Heterogeneity of white matter hyperintensities in Alzheimer's disease: post-mortem quantitative MRI and neuropathology.', *Brain : a journal of neurology*, 131(Pt 12), pp. 3286–98. doi: 10.1093/brain/awn265.
- Grossman, R. I., Barkhof, F. and Filippi, M. (2000) 'Assessment of spinal cord damage in MS using MRI.', *Journal of the neurological sciences*, 172, pp. S36–S39.
- Grussu, F. *et al.* (2013) 'Towards Spinal Cord Microstructure Mapping with the Neurite Orientation Dispersion and Density Imaging.', in *21st Annual Meeting of the International Society for Magnetic Resonance in Medicine*, p. 2095.
- Henderson, A. P. D. *et al.* (2011) 'Early factors associated with axonal loss after optic neuritis.', *Annals of neurology*, 70(6), pp. 955–63. doi: 10.1002/ana.22554.
- Hickman, S. J., Hadjiprocopis, a, *et al.* (2004) 'Cervical spinal cord MTR histogram

analysis in multiple sclerosis using a 3D acquisition and a B-spline active surface segmentation technique.', *Magnetic resonance imaging*, 22(6), pp. 891–5. doi: 10.1016/j.mri.2004.01.056.

- Hickman, S. J., Toosy, a T., *et al.* (2004) 'Serial magnetization transfer imaging in acute optic neuritis.', *Brain*, 127(3), pp. 692–700. doi: 10.1093/brain/awh076.
- Hickman, S. J. *et al.* (2005) 'Optic Nerve Diffusion Measurement from Diffusion-Weighted Imaging in Optic Neuritis', *American Journal of Neuroradiology*, 26, pp. 951–956.
- Himes, B. T. *et al.* (2006) 'Recovery of function following grafting of human bone marrow-derived stromal cells into the injured spinal cord', *Neurorehabilitation and Neural Repair*, 20(2), pp. 278–296. doi: 10.1177/1545968306286976.
- Hornabrook, R. *et al.* (1992) 'Frequent involvement of the optic radiation in patients with acute isolated optic neuritis.', *Neurology*, 42(1), pp. 77–9.
- van Horssen, J. *et al.* (2007) 'The blood-brain barrier in cortical multiple sclerosis lesions.', *Journal of neuropathology and experimental neurology*, 66(4), pp. 321–8. doi: 10.1097/nen.0b013e318040b2de.
- Howell, O. W. *et al.* (2011) 'Meningeal inflammation is widespread and linked to cortical pathology in multiple sclerosis.', *Brain : a journal of neurology*, 134(Pt 9), pp. 2755–71. doi: 10.1093/brain/awr182.
- Huang, J. K. *et al.* (2011) 'Retinoid X receptor gamma signaling accelerates CNS remyelination.', *Nature neuroscience*. Nature Publishing Group, 14(1), pp. 45–53. doi: 10.1038/nn.2702.
- Hulst, H. E. and Geurts, J. J. G. (2011) 'Gray matter imaging in multiple sclerosis:

what have we learned?', *BMC neurology*. BioMed Central Ltd, 11(1), p. 153. doi: 10.1186/1471-2377-11-153.

- Hyppönen, E. and Power, C. (2007) 'Hypovitaminosis D in British adults at age 45 y: nationwide cohort study of dietary and lifestyle predictors.', *The American journal of clinical nutrition*, 85(3), pp. 860–8.
- Inglese, M. *et al.* (2002) 'Irreversible Disability and Tissue Loss in Multiple Sclerosis: A Conventional and Magnetization Transfer Magnetic Resonance Imaging Study of the Optic Nerves.', *Archives of neurology*, 59(2), pp. 250–55.
- Irvine, K. a and Blakemore, W. F. (2008) 'Remyelination protects axons from demyelination-associated axon degeneration.', *Brain : a journal of neurology*, 131(Pt 6), pp. 1464–77. doi: 10.1093/brain/awn080.
- Jenkinson, M. *et al.* (2012) 'Fsl.', *NeuroImage*, 62(2), pp. 782–90. doi: 10.1016/j.neuroimage.2011.09.015.
- Jespersen, S. N. *et al.* (2010) 'Neurite density from magnetic resonance diffusion measurements at ultrahigh field: comparison with light microscopy and electron microscopy.', *NeuroImage*. Elsevier Inc., 49(1), pp. 205–16. doi: 10.1016/j.neuroimage.2009.08.053.
- Johnson, G. *et al.* (1987) 'STIR sequences in NMR imaging of the optic nerve.', *Neuroradiology*, 29, pp. 238–245.
- Kapoor, R. *et al.* (2010) 'Lamotrigine for neuroprotection in secondary progressive multiple sclerosis: a randomised, double-blind, placebo-controlled, parallel-group trial.', *Lancet neurology*. Elsevier Ltd, 9(7), pp. 681–8. doi: 10.1016/S1474-4422(10)70131-9.

- Kapoor, R. *et al.* (2018) 'Effect of natalizumab on disease progression in secondary progressive multiple sclerosis (ASCEND): a phase 3, randomised, double-blind, placebo-controlled trial with an open-label extension', *The Lancet Neurology*, 17(5), pp. 405–415. doi: 10.1016/S1474-4422(18)30069-3.
- Kappos, L. *et al.* (2006) 'Oral Fingolimod (FTY720) for Relapsing Multiple Sclerosis', *New England Journal of Medicine*, 355(11), pp. 1124–1140. doi: 10.1056/NEJMoa052643.
- Kappos, L. *et al.* (2018) 'Siponimod versus placebo in secondary progressive multiple sclerosis (EXPAND): a double-blind, randomised, phase 3 study', *The Lancet*, 391(10127), pp. 1263–1273. doi: 10.1016/S0140-6736(18)30475-6.
- Khaleeli, Z. *et al.* (2007) 'Localized grey matter damage in early primary progressive multiple sclerosis contributes to disability.', *NeuroImage*, 37(1), pp. 253–61. doi: 10.1016/j.neuroimage.2007.04.056.
- Klaver, R. *et al.* (2013) 'Grey matter damage in multiple sclerosis: a pathology perspective.', *Prion*, 7(1), pp. 66–75. doi: 10.4161/pri.23499.
- Klawiter, E. C. *et al.* (2011) 'Radial diffusivity predicts demyelination in ex vivo multiple sclerosis spinal cords.', *NeuroImage*. Elsevier Inc., 55(4), pp. 1454–60. doi: 10.1016/j.neuroimage.2011.01.007.
- Klistorner, A. *et al.* (2011) 'Magnetisation transfer ratio in optic neuritis is associated with axonal loss, but not with demyelination.', *NeuroImage*. Elsevier B.V., 56(1), pp. 21–6. doi: 10.1016/j.neuroimage.2011.02.041.
- Klistorner, A. *et al.* (2013) 'Axonal loss in non-optic neuritis eyes of patients with multiple sclerosis linked to delayed visual evoked potential.', *Neurology*, 80(3),

pp. 242–5. doi: 10.1212/WNL.0b013e31827deb39.

- Kolasinski, J. *et al.* (2012) 'A combined post-mortem magnetic resonance imaging and quantitative histological study of multiple sclerosis pathology.', *Brain : a journal of neurology*, 135(Pt 10), pp. 2938–51. doi: 10.1093/brain/aws242.
- Kolind, S. *et al.* (2012) 'Myelin water imaging reflects clinical variability in multiple sclerosis.', *NeuroImage*. Elsevier Inc., 60(1), pp. 263–70. doi: 10.1016/j.neuroimage.2011.11.070.
- Kolind, S. H. and Deoni, S. C. (2011) 'Rapid three-dimensional multicomponent relaxation imaging of the cervical spinal cord.', *Magnetic resonance in medicine : official journal of the Society of Magnetic Resonance in Medicine / Society of Magnetic Resonance in Medicine*, 65(2), pp. 551–6. doi: 10.1002/mrm.22634.
- Kurtzke, J. F. (1983) 'Rating neurologic impairment in multiple sclerosis: An expanded disability status scale (EDSS)', *Neurology*, 33(11), pp. 1444–1444. doi: 10.1212/WNL.33.11.1444.
- Kutzelnigg, A. *et al.* (2005) 'Cortical demyelination and diffuse white matter injury in multiple sclerosis.', *Brain : a journal of neurology*, 128(Pt 11), pp. 2705–12. doi: 10.1093/brain/awh641.
- Lafaye, G. *et al.* (2017) 'Cannabis, cannabinoids, and health', *Dialogues Clin Neurosci*, 19(3), pp. 309–316. doi: 10.1201/b10936-40.
- Lankford, C. L. and Does, M. D. (2013) 'On the inherent precision of mcDESPOT.', *Magnetic resonance in medicine : official journal of the Society of Magnetic Resonance in Medicine / Society of Magnetic Resonance in Medicine*, 69(1), pp. 127–36. doi: 10.1002/mrm.24241.

- Lassmann, H., Van Horssen, J. and Mahad, D. (2012) 'Progressive multiple sclerosis: Pathology and pathogenesis', *Nature Reviews Neurology*. Nature Publishing Group, 8(11), pp. 647–656. doi: 10.1038/nrneurol.2012.168.
- Laule, C. *et al.* (2007) 'Magnetic resonance imaging of myelin.', *Neurotherapeutics : the journal of the American Society for Experimental NeuroTherapeutics*, 4(3), pp. 460–84. doi: 10.1016/j.nurt.2007.05.004.
- Laule, C. *et al.* (2008) 'Myelin water imaging of multiple sclerosis at 7 T: correlations with histopathology.', *NeuroImage*, 40(4), pp. 1575–80. doi: 10.1016/j.neuroimage.2007.12.008.
- Levesque, I. R., Giacomini, P. S., *et al.* (2010) 'Quantitative magnetization transfer and myelin water imaging of the evolution of acute multiple sclerosis lesions.', *Magnetic resonance in medicine : official journal of the Society of Magnetic Resonance in Medicine / Society of Magnetic Resonance in Medicine*, 63(3), pp. 633–40. doi: 10.1002/mrm.22244.
- Levesque, I. R., Sled, J. G., *et al.* (2010) 'Reproducibility of quantitative magnetization-transfer imaging parameters from repeated measurements.', *Magnetic resonance in medicine : official journal of the Society of Magnetic Resonance in Medicine / Society of Magnetic Resonance in Medicine*, 64(2), pp. 391–400. doi: 10.1002/mrm.22350.
- Li, W.-W. *et al.* (2006) 'Females remyelinate more efficiently than males following demyelination in the aged but not young adult CNS.', *Experimental neurology*, 202(1), pp. 250–4. doi: 10.1016/j.expneurol.2006.05.012.
- Llufriu, S. *et al.* (2014) 'Randomized placebo-controlled phase II trial of

autologous mesenchymal stem cells in multiple sclerosis', *PLoS ONE*, 9(12), pp. 1–15. doi: 10.1371/journal.pone.0113936.

- Lovas, G. *et al.* (2000) 'Axonal changes in chronic demyelinated cervical spinal cord plaques.', *Brain*, 123, pp. 308–317.
- Lublin, F. *et al.* (2016) 'Oral fingolimod in primary progressive multiple sclerosis (INFORMS): A phase 3, randomised, double-blind, placebo-controlled trial', *The Lancet*, 387(10023), pp. 1075–1084. doi: 10.1016/S0140-6736(15)01314-8.
- Lucchinetti, C. *et al.* (2000) 'Heterogeneity of multiple sclerosis lesions: implications for the pathogenesis of demyelination.', *Annals of neurology*, 47(6), pp. 707–17.
- Lucchinetti, C. F. *et al.* (2011) 'Inflammatory cortical demyelination in early multiple sclerosis.', *The New England journal of medicine*, 365(23), pp. 2188–97. doi: 10.1056/NEJMoa1100648.
- MacKay, A. *et al.* (1994) 'In vivo visualization of myelin water in brain by magnetic resonance.', *Magnetic resonance in medicine : official journal of the Society of Magnetic Resonance in Medicine / Society of Magnetic Resonance in Medicine*, 31(6), pp. 673–7.
- Mackenzie, I. S. *et al.* (2014) 'Incidence and prevalence of multiple sclerosis in the UK 1990-2010: a descriptive study in the General Practice Research Database.', *Journal of neurology, neurosurgery, and psychiatry*, 85(1), pp. 76–84. doi: 10.1136/jnnp-2013-305450.
- Magalon, K. *et al.* (2012) 'Olesoxime accelerates myelination and promotes repair in models of demyelination.', *Annals of neurology*, 71(2), pp. 213–26. doi:

10.1002/ana.22593.

- Magliozzi, R. *et al.* (2007) 'Meningeal B-cell follicles in secondary progressive multiple sclerosis associate with early onset of disease and severe cortical pathology.', *Brain : a journal of neurology*, 130(Pt 4), pp. 1089–104. doi: 10.1093/brain/awm038.
- Magliozzi, R. *et al.* (2010) 'A Gradient of neuronal loss and meningeal inflammation in multiple sclerosis.', *Annals of neurology*, 68(4), pp. 477–93. doi: 10.1002/ana.22230.
- Mallam, E. *et al.* (2010) 'Characterization of in vitro expanded bone marrow-derived mesenchymal stem cells from patients with multiple sclerosis', *Multiple Sclerosis*, 16(8), pp. 909–918. doi: 10.1177/1352458510371959.
- La Mantia, L. *et al.* (2013) 'Interferon β for secondary progressive multiple sclerosis: A systematic review', *Journal of Neurology, Neurosurgery and Psychiatry*, 84(4), pp. 420–426. doi: 10.1136/jnnp-2012-303291.
- Mazzanti, B. *et al.* (2008) 'Differences in mesenchymal stem cell cytokine profiles between MS patients and healthy donors: Implication for assessment of disease activity and treatment', *Journal of Neuroimmunology*, 199(1–2), pp. 142–150. doi: 10.1016/j.jneuroim.2008.05.006.
- Mcdonald, W. *et al.* (2001) 'Recommended diagnostic criteria for multiple scle ... [Ann Neurol . 2001] - PubMed - ... Recommended diagnostic criteria for multiple sclerosis : guidelines from the International Panel on the diagnosis of multiple sclerosis . Publication Types , MeSH T', *Annals of Neurology*, 59(April), p. 11456302. doi: 10.1002/ana.1032.

- Mellion, M. *et al.* (2017) 'Efficacy Results from the Phase 2b SYNERGY Study: Treatment of Disabling Multiple Sclerosis with the Anti-LINGO-1 Monoclonal Antibody Opicinumab (S33.004)', *Neurology*, 88(16 Supplement), p. S33.004.
- Mi, S. *et al.* (2005) 'LINGO-1 negatively regulates myelination by oligodendrocytes.', *Nature neuroscience*, 8(6), pp. 745–51. doi: 10.1038/nn1460.
- Mi, S. *et al.* (2007) 'LINGO-1 antagonist promotes spinal cord remyelination and axonal integrity in MOG-induced experimental autoimmune encephalomyelitis.', *Nature medicine*, 13(10), pp. 1228–33. doi: 10.1038/nm1664.
- Miller, D. *et al.* (2005) 'Clinically isolated syndromes suggestive of multiple sclerosis, part I: natural history, pathogenesis, diagnosis, and prognosis.', *Lancet neurology*, 4(5), pp. 281–8. doi: 10.1016/S1474-4422(05)70071-5.
- Miller, D. H. *et al.* (2002) 'Measurement of atrophy in multiple sclerosis: pathological basis, methodological aspects and clinical relevance.', *Brain : a journal of neurology*, 125(Pt 8), pp. 1676–95.
- Minagar, A. *et al.* (2013) 'The thalamus and multiple sclerosis: Modern views on pathologic, imaging, and clinical aspects.', *Neurology*, 80(2), pp. 210–219. doi: 10.1212/WNL.0b013e31827b910b.
- Miron, V. E. *et al.* (2010) 'Fingolimod (FTY720) enhances remyelination following demyelination of organotypic cerebellar slices.', *The American journal of pathology*. American Society for Investigative Pathology, 176(6), pp. 2682–94. doi: 10.2353/ajpath.2010.091234.
- Moccia, M., de Stefano, N. and Barkhof, F. (2017) 'Imaging outcome measures for progressive multiple sclerosis trials', *Multiple Sclerosis*, 23(12), pp. 1614–1626.

doi: 10.1177/1352458517729456.

- Modat, M. (2010) 'Niftyreg. Available from: https://sourceforge.net/projects/niftyreg/develop'.
- Mohyeddin Bonab, M. *et al.* (2007) 'Does mesenchymal stem cell therapy help multiple sclerosis patients? Report of a pilot study', *Iranian Journal of Immunology*, 4(1), pp. 50–57. doi: IJIv4i1A7.
- Montalban, X. *et al.* (2017) 'Ocrelizumab versus placebo in primary progressive multiple sclerosis', *New England Journal of Medicine*, 376(3), pp. 209–220. doi: 10.1056/NEJMoa1606468.
- Mottershead, J. P. *et al.* (2003) 'High field MRI correlates of myelin content and axonal density in multiple sclerosis--a post-mortem study of the spinal cord.', *Journal of neurology*, 250(11), pp. 1293–301. doi: 10.1007/s00415-003-0192-3.
- Munger, K. L. *et al.* (2004) 'Vitamin D intake and incidence of multiple sclerosis', *Neurology*, 62(1), pp. 60–65. doi: 10.1212/01.WNL.0000101723.79681.38.
- Munger, K. L. *et al.* (2006) 'Serum 25-hydroxyvitamin D levels and risk of multiple sclerosis.', *JAMA : the journal of the American Medical Association*, 296(23), pp. 2832–8. doi: 10.1001/jama.296.23.2832.
- Naismith, R. T. *et al.* (2010) 'Radial diffusivity in remote optic neuritis discriminates visual outcomes.', *Neurology*, 74(21), pp. 1702–10. doi: 10.1212/WNL.0b013e3181e0434d.
- Naismith, R. T. *et al.* (2012) 'Diffusion tensor imaging in acute optic neuropathies: predictor of clinical outcomes.', *Archives of neurology*, 69(1), pp. 65–71. doi: 10.1001/archneurol.2011.243.

- Naismith, R. T. *et al.* (2013) 'Spinal cord tract diffusion tensor imaging reveals disability substrate in demyelinating disease.', *Neurology*, 80(24), pp. 2201–9. doi: 10.1212/WNL.0b013e318296e8f1.
- Nash, R. A. *et al.* (2015) 'High-dose immunosuppressive therapy and autologous hematopoietic cell transplantation for relapsing-remitting multiple sclerosis (HALT-MS): A 3-year interim report', *JAMA Neurology*, 72(2), pp. 159–169. doi: 10.1001/jamaneurol.2014.3780.
- Nguyen, T. D. *et al.* (2012) 'T2 prep three-dimensional spiral imaging with efficient whole brain coverage for myelin water quantification at 1.5 tesla.', *Magnetic resonance in medicine : official journal of the Society of Magnetic Resonance in Medicine / Society of Magnetic Resonance in Medicine*, 67(3), pp. 614–21. doi: 10.1002/mrm.24128.
- Ou, X. *et al.* (2009) 'Quantitative magnetization transfer measured pool-size ratio reflects optic nerve myelin content in ex vivo mice.', *Magnetic resonance in medicine : official journal of the Society of Magnetic Resonance in Medicine / Society of Magnetic Resonance in Medicine*, 61(2), pp. 364–71. doi: 10.1002/mrm.21850.
- Patrikios, P. *et al.* (2006) 'Remyelination is extensive in a subset of multiple sclerosis patients.', *Brain : a journal of neurology*, 129(Pt 12), pp. 3165–72. doi: 10.1093/brain/awl217.
- Pertwee, R. G. *et al.* (2010) 'Cannabinoid Receptors and Their Ligands : Beyond CB 1 and CB 2', *Pharmacological reviews*, 62(4), pp. 588–631. doi: 10.1124/pr.110.003004.588.

- Petzold, A. *et al.* (2010) 'Optical coherence tomography in multiple sclerosis: a systematic review and meta-analysis.', *Lancet neurology*. Elsevier Ltd, 9(9), pp. 921–32. doi: 10.1016/S1474-4422(10)70168-X.
- Pierpaoli, C. *et al.* (2001) 'Water diffusion changes in Wallerian degeneration and their dependence on white matter architecture.', *NeuroImage*, 13(6 Pt 1), pp. 1174–85. doi: 10.1006/nimg.2001.0765.
- Plant, G. *et al.* (1992) 'Symptomatic retrochiasmal lesions in multiple sclerosis: clinical features, visual evoked potentials, and magnetic resonance imaging.', *Neurology*, 42(1), pp. 68–76.
- Polman, C. H. *et al.* (2011) 'Diagnostic criteria for multiple sclerosis: 2010 revisions to the McDonald criteria.', *Annals of neurology*, 69(2), pp. 292–302. doi: 10.1002/ana.22366.
- Popescu, B. F. G. and Lucchinetti, C. F. (2012) 'Meningeal and cortical grey matter pathology in multiple sclerosis.', *BMC neurology*. BioMed Central Ltd, 12(1), p. 11. doi: 10.1186/1471-2377-12-11.
- Popescu, V. *et al.* (2013) 'Brain atrophy and lesion load predict long term disability in multiple sclerosis', *Journal of Neurology, Neurosurgery and Psychiatry*, 84(10), pp. 1082–1091. doi: 10.1136/jnnp-2012-304094.
- Prasloski, T. *et al.* (2012) 'Rapid whole cerebrum myelin water imaging using a 3D GRASE sequence.', *NeuroImage*. Elsevier Inc., 63(1), pp. 533–9. doi: 10.1016/j.neuroimage.2012.06.064.
- Prineas, J. W. *et al.* (1993) 'Multiple Sclerosis : Remyelination of Nascent Lesions', *Annals of neurology*, 33(127), pp. 137–151.

- Pryce, G. *et al.* (2003) 'Cannabinoids inhibit neurodegeneration in models of multiple sclerosis', *Brain*, 126(10), pp. 2191–2202. doi: 10.1093/brain/awg224.
- Ranjeva, J.-P. *et al.* (2005) 'Local tissue damage assessed with statistical mapping analysis of brain magnetization transfer ratio: relationship with functional status of patients in the earliest stage of multiple sclerosis.', *AJNR. American journal of neuroradiology*, 26(1), pp. 119–27.
- Redford, E. J., Kapoor, R. and Smith, K. J. (1997) 'Nitric oxide donors reversibly block axonal conduction: demyelinated axons are especially susceptible.', *Brain : a journal of neurology*, 120 (Pt 1, pp. 2149–57.
- Reynolds, R. *et al.* (2011) 'The neuropathological basis of clinical progression in multiple sclerosis.', *Acta neuropathologica*, 122(2), pp. 155–70. doi: 10.1007/s00401-011-0840-0.
- Richert, N. D. *et al.* (2001) 'Interferon beta-1b and intravenous methylprednisolone promote lesion recovery in multiple sclerosis', *Multiple Sclerosis*, 7(1), pp. 49–58. doi: 10.1177/135245850100700109.
- Riva, M. *et al.* (2009) 'Tissue-specific imaging is a robust methodology to differentiate in vivo T1 black holes with advanced multiple sclerosis-induced damage', *American Journal of Neuroradiology*, 30(7), pp. 1394–1401. doi: 10.3174/ajnr.A1573.
- Rorden, C., Karnath, H.-O. and Bonilha, L. (2007) 'Improving lesion-symptom mapping.', *Journal of cognitive neuroscience*, 19(7), pp. 1081–8. doi: 10.1162/jocn.2007.19.7.1081.
- Rovaris, M. and Filippi, M. (2000) 'MRI correlates of cognitive dysfunction in

multiple sclerosis patients.', *Journal of neurovirology*, 6 Suppl 2, pp. S172-5.

- Rudick, R. A. *et al.* (2009) 'Gray Matter Atrophy Correlates With MS Disability Progression Measured with MSFC But Not EDSS', *J Neurol Sci*, 282, pp. 106–111. doi: 10.1016/j.dcn.2011.01.002.The.
- Rudick, R. a, Mi, S. and Sandrock, A. W. (2008) 'LINGO-1 antagonists as therapy for multiple sclerosis: in vitro and in vivo evidence.', *Expert opinion on biological therapy*, 8(10), pp. 1561–70. doi: 10.1517/14712598.8.10.1561.
- S.M. Smith, Y. Zhang, M. Jenkinson, J. Chen, P.M. Matthews, A. Federico, and N. D. S. (2002) 'Accurate, robust and automated longitudinal and cross-sectional brain change analysis.', *NeuroImage*, 17, pp. 479–489.
- Saidha, S. *et al.* (2011) 'Visual dysfunction in multiple sclerosis correlates better with optical coherence tomography derived estimates of macular ganglion cell layer thickness than peripapillary retinal nerve fiber layer thickness.', *Multiple sclerosis (Houndmills, Basingstoke, England)*, 17(12), pp. 1449–63. doi: 10.1177/1352458511418630.
- Samson, R. S. *et al.* (2013) 'Development of a high-resolution fat and CSF-suppressed optic nerve DTI protocol at 3T : application in multiple sclerosis', *Functional Neurology*, 28(2), pp. 93–100.
- Schmierer, K. *et al.* (2004) 'Magnetization transfer ratio and myelin in postmortem multiple sclerosis brain.', *Annals of neurology*, 56(3), pp. 407–15. doi: 10.1002/ana.20202.
- Schmierer, K., Wheeler-Kingshott, C. a M., *et al.* (2007) 'Diffusion tensor imaging of post mortem multiple sclerosis brain.', *NeuroImage*, 35(2), pp. 467–77. doi:

10.1016/j.neuroimage.2006.12.010.

- Schmierer, K., Tozer, D. J., *et al.* (2007) 'Quantitative magnetization transfer imaging in postmortem multiple sclerosis brain.', *Journal of magnetic resonance imaging : JMRI*, 26(1), pp. 41–51. doi: 10.1002/jmri.20984.
- Schmierer, K. *et al.* (2008) 'Quantitative Magnetic Resonance of Post Mortem Multiple Sclerosis Brain before and after Fixation', *Magnetic resonance in medicine*, 59(2), pp. 268–277. doi: 10.1002/mrm.21487.Quantitative.
- Schumacher, M. *et al.* (2012) 'Progesterone synthesis in the nervous system: implications for myelination and myelin repair.', *Frontiers in neuroscience*, 6(February), p. 10. doi: 10.3389/fnins.2012.00010.
- Sepulcre, J. *et al.* (2006) 'Regional Gray Matter Atrophy in Early Primary Progressive Multiple Sclerosis: A Voxel-Based Morphometry Study', *Archives of neurology*, 63, pp. 1175–80.
- Simpson, S. *et al.* (2010) 'Higher 25-hydroxyvitamin D is associated with lower relapse risk in multiple sclerosis.', *Annals of neurology*, 68(2), pp. 193–203. doi: 10.1002/ana.22043.
- Simpson, S. *et al.* (2011) 'Latitude is significantly associated with the prevalence of multiple sclerosis: a meta-analysis.', *Journal of neurology, neurosurgery, and psychiatry*, 82(10), pp. 1132–41. doi: 10.1136/jnnp.2011.240432.
- Smith, S. a *et al.* (2005) 'Magnetization transfer weighted imaging in the upper cervical spinal cord using cerebrospinal fluid as interpatient normalization reference (MTCSF imaging).', *Magnetic resonance in medicine*, 54, pp. 201–6. doi: 10.1002/mrm.20553.

- Smith, S. M. *et al.* (2001) 'Normalized accurate measurement of longitudinal brain change', *Journal of Computer Assisted Tomography*, 25(3), pp. 466–475. doi: 10.1097/00004728-200105000-00022.
- Smith, S. M. *et al.* (2002) 'Accurate, robust, and automated longitudinal and cross-sectional brain change analysis', *NeuroImage*, 17(1), pp. 479–489. doi: 10.1006/nimg.2002.1040.
- Smith, S. M. (2002) 'Fast robust automated brain extraction', *Human Brain Mapping*, 17(3), pp. 143–155. doi: 10.1002/hbm.10062.
- Smith, S. M. *et al.* (2004) 'Advances in functional and structural MR image analysis and implementation as FSL', *NeuroImage*, 23(SUPPL. 1), pp. 208–220. doi: 10.1016/j.neuroimage.2004.07.051.
- Song, S.-K. *et al.* (2002) 'Dysmyelination Revealed through MRI as Increased Radial (but Unchanged Axial) Diffusion of Water', *NeuroImage*, 17(3), pp. 1429–1436. doi: 10.1006/nimg.2002.1267.
- Song, S.-K. *et al.* (2005) 'Demyelination increases radial diffusivity in corpus callosum of mouse brain.', *NeuroImage*, 26(1), pp. 132–40. doi: 10.1016/j.neuroimage.2005.01.028.
- Stankoff, B. *et al.* (2006) 'Imaging of CNS myelin by positron-emission tomography.', *Proceedings of the National Academy of Sciences of the United States of America*, 103(24), pp. 9304–9. doi: 10.1073/pnas.0600769103.
- Stankoff, B. *et al.* (2011) 'Imaging central nervous system myelin by positron emission tomography in multiple sclerosis using [methyl-^{11}C]-2-(4'-methylaminophenyl)- 6-hydroxybenzothiazole.', *Annals of neurology*, 69(4), pp.

673–80. doi: 10.1002/ana.22320.

- Stys, P. K. (2004) ‘Axonal degeneration in multiple sclerosis: is it time for neuroprotective strategies?’, *Annals of neurology*, 55(5), pp. 601–3. doi: 10.1002/ana.20082.
- The Optic Neuritis Study Group (2008) ‘Multiple Sclerosis Risk After Optic Neuritis’, *Archives of neurology*, 65(6), pp. 727–732.
- Thompson, A. J., Banwell, B. L., *et al.* (2018) ‘Diagnosis of multiple sclerosis: revision of the McDonald criteria 2017’, *Lancet Neurology*, 17, pp. 162–73. doi: 10.1007/s00115-018-0550-0.
- Thompson, A. J., Baranzini, S. E., *et al.* (2018) ‘Multiple sclerosis’, *Neuromethods*. Elsevier Ltd, 138(10130), pp. 263–295. doi: 10.1007/978-1-4939-7880-9_8.
- Thorpe, J. W. *et al.* (1995) ‘Magnetisation transfer ratios and transverse magnetisation decay curves in optic neuritis: correlation with clinical findings and electrophysiology.’, *Journal of neurology, neurosurgery, and psychiatry*, 59(5), pp. 487–92.
- Toussaint, D. *et al.* (1983) ‘Toussaint 1983.pdf’, *Journal of Clinical Neuro-Ophthalmology*, 3(3), pp. 211–20.
- Trapp, B. D. *et al.* (1998) ‘Axonal transection in the lesions of multiple sclerosis.’, *The New England journal of medicine*, 338(5), pp. 278–85. doi: 10.1056/NEJM199801293380502.
- Trip, S. *et al.* (2007) ‘Optic nerve magnetization transfer imaging and measures of axonal loss and demyelination in optic neuritis.’, *Multiple sclerosis (Houndmills, Basingstoke, England)*, 13(7), pp. 875–9. doi: 10.1177/1352458507076952.

- Trip, S. A. *et al.* (2006) 'Optic nerve diffusion tensor imaging in optic neuritis.', *NeuroImage*, 30, pp. 498–505. doi: 10.1016/j.neuroimage.2005.09.024.
- Tzourio-Mazoyer, N. *et al.* (2002) 'Automated anatomical labeling of activations in SPM using a macroscopic anatomical parcellation of the MNI MRI single-patient brain.', *NeuroImage*, 15(1), pp. 273–89. doi: 10.1006/nimg.2001.0978.
- Uccelli, A. *et al.* (2007) 'Mesenchymal stem cells: a new strategy for immunosuppression?', *Trends in immunology*, 28(5), pp. 219–26. doi: 10.1016/j.it.2007.03.001.
- Uccelli, A., Laroni, A. and Freedman, M. S. (2011) 'Mesenchymal stem cells for the treatment of multiple sclerosis and other neurological diseases.', *Lancet neurology*. Elsevier Ltd, 10(7), pp. 649–56. doi: 10.1016/S1474-4422(11)70121-1.
- Vavasour, I. M. *et al.* (2000) 'Different magnetization transfer effects exhibited by the short and long T(2) components in human brain.', *Magnetic resonance in medicine : official journal of the Society of Magnetic Resonance in Medicine / Society of Magnetic Resonance in Medicine*, 44(6), pp. 860–6.
- Vavasour, I. M. *et al.* (2009) 'Longitudinal changes in myelin water fraction in two MS patients with active disease.', *Journal of the neurological sciences*. Elsevier B.V., 276(1–2), pp. 49–53. doi: 10.1016/j.jns.2008.08.022.
- Vavasour, I. M. *et al.* (2011) 'Is the magnetization transfer ratio a marker for myelin in multiple sclerosis?', *Journal of magnetic resonance imaging : JMRI*, 33(3), pp. 713–8. doi: 10.1002/jmri.22441.
- Vercellino, M. *et al.* (2005) 'Grey matter pathology in multiple sclerosis.', *Journal of neuropathology and experimental neurology*, 64(12), pp. 1101–7.

- Vercellino, M. *et al.* (2009) 'Demyelination, inflammation, and neurodegeneration in multiple sclerosis deep gray matter.', *Journal of neuropathology and experimental neurology*, 68(5), pp. 489–502. doi: 10.1097/NEN.0b013e3181a19a5a.
- Villoslada, P. (2016) 'Neuroprotective therapies for multiple sclerosis', *Multiple Sclerosis and Demyelinating Disorders*. Multiple Sclerosis and Demyelinating Disorders, 1(1), pp. 1–11. doi: 10.1186/s40893-016-0004-0.
- Visser, E. M. *et al.* (2012) 'A new prevalence study of multiple sclerosis in Orkney, Shetland and Aberdeen city.', *Journal of neurology, neurosurgery, and psychiatry*, 83(7), pp. 719–24. doi: 10.1136/jnnp-2011-301546.
- Walderveen, M. A. A. van *et al.* (1998) 'Histopathologic correlate of hypointense lesions on T1-weighted spin-echo MRI in multiple sclerosis', *Neurology*, 50(5), pp. 1282–1288. doi: 10.1212/wnl.50.5.1282.
- van Walderveen, M. a *et al.* (1998) 'Histopathologic correlate of hypointense lesions on T1-weighted spin-echo MRI in multiple sclerosis.', *Neurology*, 50(5), pp. 1282–8.
- Wegner, C., Esiri, M. and Chance, S. (2006) 'Neocortical neuronal, synaptic, and glial loss in multiple sclerosis', *Neurology*, 67(6), pp. 960–967.
- Wheeler-kingshott, C. A. M. *et al.* (2002) 'ADC Mapping of the Human Optic Nerve : Increased Resolution , Coverage , and Reliability With CSF-Suppressed ZOOM-EPI', *Magnetic resonance in medicine*, 47, pp. 24–31. doi: 10.1002/mrm.10016.
- Wheeler-kingshott, C. A. M. *et al.* (2012) 'A new approach to structural integrity

assessment baesd on axial and radial diffusivities', *Functional Neurology*, 27(2), pp. 85–90.

- Wheeler-Kingshott, C. a *et al.* (2013) 'The current state-of-the-art of spinal cord imaging: Methods.', *NeuroImage*. Elsevier Inc., pp. 1–12. doi: 10.1016/j.neuroimage.2013.04.124.
- Wheeler-Kingshott, C. a M. and Cercignani, M. (2009) 'About "axial" and "radial" diffusivities.', *Magnetic resonance in medicine : official journal of the Society of Magnetic Resonance in Medicine / Society of Magnetic Resonance in Medicine*, 61(5), pp. 1255–60. doi: 10.1002/mrm.21965.
- Willer, C. J. *et al.* (2003) 'Twin concordance and sibling recurrence rates in multiple sclerosis.', *Proceedings of the National Academy of Sciences of the United States of America*, 100(22), pp. 12877–82.
- Woodruff, R. H. and Franklin, R. J. (1999) 'Demyelination and remyelination of the caudal cerebellar peduncle of adult rats following stereotaxic injections of lysolecithin, ethidium bromide, and complement/anti-galactocerebroside: a comparative study.', *Glia*, 25(3), pp. 216–28.
- Wu, C. *et al.* (2010) 'A novel PET marker for in vivo quantification of myelination.', *Bioorganic & medicinal chemistry*. Elsevier Ltd, 18(24), pp. 8592–9. doi: 10.1016/j.bmc.2010.10.018.
- Wu, C. *et al.* (2013) 'Longitudinal PET imaging for monitoring myelin repair in the spinal cord.', *Annals of neurology*, 9, pp. 1–32. doi: 10.1002/ana.23965.
- Xu, J. *et al.* (2008) 'Assessing optic nerve pathology with diffusion MRI : from mouse to human.', *NMR in Biomedicine*, 186(August), pp. 928–940. doi:

10.1002/nbm.

- Youl, B. *et al.* (1991) 'The Pathophysiology of Acute Optic Neuritis.', *Brain*, 114, pp. 2437–2450.
- Zackowski, K. M. *et al.* (2009) 'Sensorimotor dysfunction in multiple sclerosis and column-specific magnetization transfer-imaging abnormalities in the spinal cord.', *Brain : a journal of neurology*, 132(Pt 5), pp. 1200–9. doi: 10.1093/brain/awp032.
- Zajicek, J. *et al.* (2013) 'Effect of dronabinol on progression in progressive multiple sclerosis (CUPID): a randomised, placebo-controlled trial.', *Lancet neurology*. Elsevier Ltd, 12, pp. 857–65. doi: 10.1016/S1474-4422(13)70159-5.
- Zajicek, J. P. *et al.* (2005) 'Cannabinoids in multiple sclerosis (CAMS) study: Safety and efficacy data for 12 months follow up', *Journal of Neurology, Neurosurgery and Psychiatry*, 76(12), pp. 1664–1669. doi: 10.1136/jnnp.2005.070136.
- Zajicek, J. P. and Apostu, V. I. (2011) 'Role of cannabinoids in multiple sclerosis', *CNS Drugs*, 25(3), pp. 187–201. doi: 10.2165/11539000-000000000-00000.
- Zappia, E. *et al.* (2005) 'Mesenchymal stem cells ameliorate experimental autoimmune encephalomyelitis inducing T-cell anergy', *Blood*, 106(5), pp. 1755–1761. doi: 10.1182/blood-2005-04-1496.
- Zhang, H. *et al.* (2012) 'NODDI: practical in vivo neurite orientation dispersion and density imaging of the human brain.', *NeuroImage*. Elsevier Inc., 61(4), pp. 1000–16. doi: 10.1016/j.neuroimage.2012.03.072.
- Zou, S. and Kumar, U. (2018) 'Cannabinoid receptors and the endocannabinoid system: Signaling and function in the central nervous system', *International Journal of Molecular Sciences*, 19(3), p. 833. doi: 10.3390/ijms19030833.

8. APPENDICES

Appendix 1: Cortical MTR reduction (FWE 0.05)													
RRMS					***SPMS***					***PPMS***			
Area	*Voxels*	*X*	*Y*	*Z*	*Area*	*Voxels*	*X*	*Y*	*Z*	*Area*	*Voxels*	*X*	*Y*	*Z*
Heschl L	90	-41	-22	8	Precentral L	1795	-31	-19	66	Heschl R	85	48	-15	5
Temporal Sup L	58	-42	-23	8	Postcentral L	1411	-49	-10	39	Temporal Sup R	76	48	-15	4
Precentral R	45	37	-15	49	Temporal Sup L	1275	-41	-25	13	Precentral R	59	41	-10	37
Postcentral L	38	-40	-17	43	Postcentral R	1019	45	-11	3	Temporal Sup L	45	-44	-23	7
Lingual R	37	9	-32	1	Precentral R	781	43	-11	7	Postcentral R	26	41	-10	36
Heschl R	33	46	-20	7	Heschl L	649	-39	-26	1	Lingual R	10	15	-35	0
Hippocampus L	28	-13	-32	9	Calcarine R	579	13	-91	7	Precuneus R	10	13	-35	3
Temporal Sup R	28	47	-20	7	Heschl R	459	41	-24	-6	Hippocampus R	7	17	-34	1
Hippocampus R	18	11	-32	9	Temporal Sup R	280	43	-24	-2					
Lingual L	8	-9	-34	3	Lingual L	174	-10	-33	0					
Precuneus R	8	13	-34	4	Lingual R	165	10	-33	1					
Postcentral R	6	43	-9	36	Paracentral Lobule L	142	-6	-18	-4					
Cingulum Post R	2	11	-34	7	Occipital Inf R	124	31	-95	-4					
					Rolandic Oper L	91	-39	-28	-6					
					Occipital Mid L	89	-29	-96	36					
					Hippocampus L	87	-13	-34	38					
					Hippocampus R	71	13	-34	2					
					Precuneus R	51	13	-34	3					
					ParaHippocampal L	33	-18	-32	73					
					Precuneus L	18	-12	-36	11					
					Occipital Inf L	12	-29	-95	11					
					Insula L	10	-46	-12	10					
					Cingulum Post R	5	11	-34	11					

Appendix 2: Deep GM MTR reduction (FWE 0.05)													
RRMS					***SPMS***					***PPMS***			
Area	*Voxels*	*X*	*Y*	*Z*	*Area*	*Voxels*	*X*	*Y*	*Z*	*Area*	*Voxels*	*X*	*Y*	*Z*
Thalamus L	1631	-10	-28	10	Thalamus L	1327	-10	-31	5					
Thalamus R	1411	2	-21	4	Caudate R	1021	12	1	17					
Caudate R	95	12	4	17	Thalamus R	998	10	-31	4					
Caudate L	79	-20	-24	21	Caudate L	443	-14	1	19					

Appendix 3: Cortical Atrophy (FWE 0.05)													
RRMS					***SPMS***					***PPMS***			
Area	*Voxels*	*X*	*Y*	*Z*	*Area*	*Voxels*	*X*	*Y*	*Z*	*Area*	*Voxels*	*X*	*Y*	*Z*
Precentral L	162	-33	-21	60	Precentral L	111	-36	-21	65					
Hippocampus L	24	-13	-34	3	Occipital Mid L	6	-30	-97	-3					
Lingual L	20	-9	-34	3										

Appendix 4: Deep GM Atrophy (FWE 0.05)													
RRMS					***SPMS***					***PPMS***			
Area	*Voxels*	*X*	*Y*	*Z*	*Area*	*Voxels*	*X*	*Y*	*Z*	*Area*	*Voxels*	*X*	*Y*	*Z*
Thalamus R	2714	3	-10	7	Thalamus L	807	-14	-26	3					
Thalamus L	2033	-12	-28	5	Thalamus R	614	9	-12	7					
Putamen L	71	-29	-12	0										
Pallidum L	2	-27	-9	-2										

Appendix 5: Cortical MTR reduction and Atrophy Co-localisation (FWE 0.05)													
RRMS					***SPMS***					***PPMS***			
Area	*Voxels*	*X*	*Y*	*Z*	*Area*	*Voxels*	*X*	*Y*	*Z*	*Area*	*Voxels*	*X*	*Y*	*Z*
Hippocampus L	15	-13	-34	5	Precentral L	103	-33	-19	65					
Lingual L	6	-9	-34	3	Occipital Mid L	6	-30	-97	-3					

Appendix 6: Deep GM MTR reduction and Atrophy Co-localisation (FWE 0.05)													
RRMS					***SPMS***					***PPMS***			
Area	*Voxels*	*X*	*Y*	*Z*	*Area*	*Voxels*	*X*	*Y*	*Z*	*Area*	*Voxels*	*X*	*Y*	*Z*
Thalamus L	1143	-10	-28	10	Thalamus L	500	-10	-31	5					
Thalamus R	993	1	-20	5	Thalamus R	1	13	-28	2					

Appendix 7: RRMS MTR reduction subgroup comparisons (0.001, uncorrected)									
RRMS vs PPMS					***RRMS vs SPMS***				
Area	*Voxels*	*X*	*Y*	*Z*	*Area*	*Voxels*	*X*	*Y*	*Z*
	Cortical GM					*Cortical GM*			
Cingulum Mid R	2351	1	-26	36	Precuneus R	2386	2	-42	56
Cingulum Mid L	1176	0	-26	36	Cingulum Mid L	869	-5	-43	53
Precuneus R	198	6	-50	29	Precuneus L	691	-5	-44	54
Cingulum Post R	129	6	-49	30	Cingulum Mid R	429	5	-41	52
Supp Motor Area R	119	7	-21	49	Frontal Mid R	100	30	9	55
Paracentral Lobule L	119	-3	-32	52	Frontal Mid L	79	-31	29	36
Occipital Mid R	118	38	-82	7	Cingulum Post L	56	0	-52	34
Temporal Inf R	92	55	-55	-8	Occipital Sup R	56	26	-62	41
Temporal Inf L	87	-41	-4	-39	Frontal Sup R	36	27	1	65
Precentral R	79	40	-1	47	Cingulum Post R	32	1	-51	32
ParaHippocampal L	39	-24	-6	-34	Paracentral Lobule R	25	4	-43	61
Fusiform L	26	-25	-7	-34	Angular R	13	28	-62	42
Lingual R	9	16	-89	-11	Frontal Sup L	12	-17	27	52
SupraMarginal L	8	-56	-42	36	Parietal Inf R	9	42	-45	45
Frontal Inf Orb L	7	-46	27	-10	Parietal Sup R	6	24	-52	63
Cingulum Post L	6	-1	-31	34	Supp Motor Area L	3	0	-1	65
Paracentral Lobule R	6	6	-31	52	Supp Motor Area R	3	1	0	65
Lingual L	4	-21	-79	-12	Paracentral Lobule L	3	-1	-37	55
Parietal Inf R	3	38	-46	43					
Parietal Inf L	2	-56	-42	37					
Occipital Inf L	1	-48	-59	-15					
Temporal Sup L	1	-57	-5	-2					
	Deep GM					*Deep GM*			
Putamen L	1	-29	3	9	No significant differences detected				

Appendix 8: PPMS MTR reduction subgroup comparisons (0.001, uncorrected)									
PPMS vs SPMS					***PPMS vs RRMS***				
Area	*Voxels*	*X*	*Y*	*Z*	*Area*	*Voxels*	*X*	*Y*	*Z*
	Cortical GM					*Cortical GM*			
Frontal Mid L	212	-32	29	34	Frontal Inf Oper R	336	52	19	39
Frontal Mid R	136	35	23	41	Frontal Mid R	45	53	19	41
SupraMarginal R	61	53	-33	39	Frontal Inf Orb R	25	53	21	-2
Precentral L	10	-48	11	50	Temporal Pole Sup R	9	53	19	-4
Frontal Sup L	8	-20	18	62	Cerebelum 8 R	9	17	-67	-50
Frontal Inf Oper L	2	-50	20	34	Frontal Inf Tri R	4	53	21	1
Parietal Inf L	2	-45	-48	50	Cerebelum Crus1 R	2	23	-89	-24
	Deep GM					*Deep GM*			
No significant differences detected					No significant differences detected				

Appendix 9: SPMS MTR reduction subgroup comparisons (0.001, uncorrected)									
SPMS vs PPMS					***SPMS vs RRMS***				
Area	*Voxels*	*X*	*Y*	*Z*	*Area*	*Voxels*	*X*	*Y*	*Z*
	Cortical GM					*Cortical GM*			
Calcarine R	1687	14	-92	-4	Calcarine R	4717	21	-48	8
Occipital Inf R	828	36	-94	-4	Lingual R	1957	10	-78	-1
Precentral R	812	47	-10	41	Precentral L	1904	-28	-19	69
Precentral L	736	-33	-20	65	Temporal Sup L	1377	-56	-14	7
Paracentral Lobule L	456	-4	-16	76	Precentral R	1329	30	-20	71
Lingual R	452	14	-92	-6	Cerebelum 8 L	512	-25	-51	-53
Occipital Mid L	366	-19	-84	18	Hippocampus R	506	18	-35	6
Cingulum Mid R	363	13	-17	45	Postcentral L	432	-53	-4	24
Occipital Mid R	269	24	-94	9	Precuneus R	410	25	-51	3
Postcentral L	261	-47	-7	36	Occipital Mid L	394	-20	-83	15
Postcentral R	236	48	-9	40	Postcentral R	285	47	-9	40
Occipital Sup L	191	-19	-83	18	Temporal Pole Sup L	244	-45	14	-14
Lingual L	151	-19	-80	-7	Heschl L	239	-48	-16	7
Supp Motor Area R	112	10	-19	49	Cerebelum 8 R	197	21	-44	-51
Temporal Pole Sup L	84	-45	22	-16	Occipital Inf L	195	-35	-80	-3
Calcarine L	83	-19	-75	7	Hippocampus L	185	-19	-31	-5
Occipital Inf L	72	-35	-80	-2	ParaHippocampal L	149	-19	-33	-6
Occipital Sup R	54	23	-94	11	Calcarine L	148	4	-83	3
Cerebelum Crus2 L	46	-38	-64	-42	ParaHippocampal R	132	21	-30	-9
Cuneus R	23	15	-92	7	Frontal Inf Orb R	116	52	19	-6
Fusiform L	21	-20	-81	-9	Temporal Mid L	79	-48	-10	-14
Supp Motor Area L	7	-3	-11	76	Occipital Sup L	74	-19	-83	15
Paracentral Lobule R	6	9	-28	53	Insula L	66	-46	-12	3
Temporal Sup L	3	-54	-12	-3	Temporal Pole Sup R	54	53	19	-6
Hippocampus L	2	-21	-30	-6	Occipital Inf R	53	25	-88	-5
					Cerebelum 9 L	51	-20	-49	-52
					Temporal Sup R	36	47	-10	2
					Cerebelum 9 R	30	20	-44	-49
					Lingual L	29	-16	-34	-3
					Frontal Inf Oper R	10	54	22	-1
					Cuneus R	8	7	-82	15
					Frontal Inf Tri R	7	55	22	0
					Fusiform R	7	27	-87	-5
					Frontal Sup Orb R	6	13	48	-24
					Insula R	5	46	-6	-3
					Cerebelum Crus1 R	3	56	-52	-33
					Rolandic Oper L	2	-48	-7	2
					Frontal Inf Orb L	1	-46	17	-12
					Olfactory R	1	4	17	-1
					Cingulum Mid R	1	14	-15	42
	Deep GM					*Deep GM*			
Thalamus L	546	-7	-27	3	Thalamus R	15	16	-33	6
Thalamus R	283	5	-21	0	Caudate L	6	-7	22	-2
					Caudate R	4	4	16	-1

Appendix 10: RRMS Atrophy subgroup comparisons (0.001, uncorrected)									
RRMS vs PPMS					***RRMS vs SPMS***				
Area	*Voxels*	*X*	*Y*	*Z*	*Area*	*Voxels*	*X*	*Y*	*Z*
	Cortical GM					*Cortical GM*			
Cerebelum 8 L	122	-23	-36	-50	No significant differences detected				
Frontal Mid Orb R	91	33	49	-3					
Lingual L	53	-20	-81	-12					
Fusiform L	46	-21	-83	-6					
Occipital Mid L	6	-20	-85	-4					
Frontal Mid R	4	32	49	0					
Insula R	4	28	22	-16					
Cerebelum 9 L	3	-21	-38	-50					
	Deep GM					*Deep GM*			
Thalamus L	17	-15	-12	17	No significant differences detected				
Caudate R	14	11	6	8					
Pallidum R	4	15	6	6					
Caudate L	3	-14	-11	21					

Appendix 11: SPMS Atrophy subgroup comparisons (0.001, uncorrected)									
SPMS vs PPMS					***SPMS vs RRMS***				
Area	*Voxels*	*X*	*Y*	*Z*	*Area*	*Voxels*	*X*	*Y*	*Z*
	Cortical GM					*Cortical GM*			
Frontal Sup R	1490	17	33	44	Occipital Mid L	302	-24	-86	14
Supp Motor Area R	740	10	12	62	Precentral L	254	-36	-21	68
Temporal Inf R	450	53	-49	-24	Postcentral L	199	-63	-8	24
Frontal Mid L	332	-31	27	35	Precentral R	124	33	-18	61
Temporal Mid L	267	-43	3	-29	Precuneus R	32	17	-63	27
SupraMarginal L	192	-52	-51	25	Calcarine L	24	-10	-102	-8
Frontal Sup Medial R	146	12	34	49	Cuneus R	2	19	-63	29
Angular L	92	-51	-51	26	Occipital Inf L	2	-10	-101	-7
ParaHippocampal L	71	-14	5	-26					
Parietal Inf L	42	-44	-49	46					
Temporal Mid R	28	51	-61	1					
Precuneus L	20	-12	-48	50					
Temporal Inf L	12	-43	3	-30					
Parietal Inf R	2	44	-57	47					
Calcarine R	1	15	-84	15					
Cerebelum Crus1 R	1	55	-47	-28					
	Deep GM					*Deep GM*			
Putamen L	1	-29	3	9	No significant differences detected				

Appendix 12: Participating Sites for the Main CUPID Study, and MRI Substudy Sites	
All sites	**MRI**
Aberdeen Royal Infirmary, Aberdeen	Y
Addenbrooke's Hospital, Cambridge)	
Ayrshire Central Hospital, Irvine	
Barts and the Royal London, London	Y
Charing Cross Hospital, London	Y
Derriford Hospital, Plymouth	Y
Frenchay Hospital, Bristol	Y
Gloucestershire Royal Hospital, Gloucester	
Hertford County Hospital, Hertfordshire	
Hope Hospital, Manchester	
John Radcliffe Hospital, Oxford	
Leicester General Hospital, Leicester	Y
Musgrove Park Hospital, Taunton	Y
Norfolk and Norwich University Hospital, Norwich	Y
Poole General Hospital, Dorset	
Queen Elizabeth Hospital, Birmingham	
Royal Berkshire Hospital, Reading	
Royal Cornwall Hospital, Truro	Y
Royal Hallamshire Hospital, Sheffield	Y
Royal Preston Hospital, Preston	
Royal Victoria Infi rmary, Newcastle	Y
University Hospital of North Staff , Stoke on Trent	
University Hospital of Wales, Cardiff	Y
University Hospital, Nottingham	
University Hospitals Coventry and Warwickshire, Coventry	
West Midlands Rehabilitation Centre, Birmingham	
Western General Hospital, Edinburgh	Y

This page left intentionally blank. Except for this text. And the page number at the bottom.